STABILITY OF CONVECTIVE FLOW BETWEEN VERTICAL PLANES

Ahmad Abdulla Al-Ali, BSc, MSc.

Submitted for the degree of PhD.

Department of Mathematics

City University,

London.

January 1993

CONTENT **PAGE**

CONTENT **PAGE**

CONTENT **PAGE**

ACKNOWLEDGMENTS

I wish to express my sincere gratitude to my supervisor, Professor P.G. Daniels, for his assistance and encouragement. I also would like to thank the U.A.E University for financial support.

ABSTRACT

This thesis considers instability of the convective flow between differentially heated vertical planes at infinite and large Prandtl numbers.

For infinite Prandtl number, asymptotic methods are used to describe the solution of the linear stability problem in the limit $A \to \infty$, where A is the Rayleigh number. The solution is expanded in the neighbourhood of γ_0, where γ_0 is the critical value of a convective parameter γ associated with the base flow. The base flow vanishes mid-way between the planes where a thermal critical layer forms. Matching across the critical layer leads to two sets of bridging conditions which allow the critical wavelength of the stationary disturbance to be found.

The effect of large (but not infinite) Prandtl number on the neutral stability equation is considered in Chapter 5, and in Chapter 6 the lower branch of the neutral stability curve for finite and large Prandtl numbers is studied. This leads to a complete picture of the neutrally stable stationary disturbances in the limit $A \to \infty$ for both large and infinite Prandtl numbers.

CHAPTER ONE : INTRODUCTION

1.1 Background Work

The classical problem of natural convection in a cavity, where one of the vertical walls is uniformly heated while the opposing wall is uniformly cooled, has been studied by many investigators experimentally, analytically and numerically. The buoyancy-driven flow is of relevance in a variety of geophysical, astrophysical and industrial areas and thermal properties of the flow are of interest in connection with the insulation of walls and windows, the cooling of nuclear reactors, solar collectors and certain crystal growing techniques.

One of the earliest studies of heat transfer, in air, was performed by Nusselt (1909) and many analytical and experimental studies have followed, notable contributions having been made by Batchelor (1954), Eckert and Carlson (1961), Elder (1965) and Gill (1966). Batchelor (1954), motivated by the application to window insulation, demonstrated that the flow in a two-dimensional cavity is uniquely determined by three parameters: the Rayleigh number A, based on the horizontal temperature difference across the cavity (and defined explicitly below), the Prandtl number of the fluid, σ, and the aspect ratio of the cavity, h (height/width). He discussed the form of the solution in the situation where conduction dominates and also suggested that for large Rayleigh

numbers, where convection dominates, the inner region of the cavity has a constant temperature and a non zero constant vorticity. Detailed observations of the primary temperature distribution in air and measurements of the local heat transfer at the walls were made in experiments by Eckert and Carlson (1961) using interferometer techniques. Their observations did not support Batchelor´s suggestion that the inner region has constant temperature at large values of the Rayleigh number; instead, they observed a region of constant vertical temperature gradient. This was supported by experimental observations by Mordchelles Regnier & Kaplan (1963) and later by Elder (1965) who obtained more extensive velocity and temperature measurements for high Prandtl-number fluids, such as silicon oil, in tall cavities (or slots).

Elder's experiments identified three main flow regimes, known as the conductive, convective and boundary-layer regimes. When the Rayleigh number is small, heat is transferred across the slot primarily by conduction but as the Rayleigh number increases a stable vertical temperature gradient develops in the core of the flow and the buoyancy-driven vertical velocities are progressively diminished. Finally as the Rayleigh number becomes sufficiently large the vertical flow is confined primarily to boundary layers at the side walls. Elder also gave a theoretical description of the flow in which he established that the convective flow in a vertical slot can be approximated by an exact solution of the Boussinesq equations equivalent to flow between infinite parallel vertical planes with a specified vertical temperature gradient, β. The choice

$\beta = 1/2h$ led to good agreement with the experimental results. This exact solution has formed the basis of stability analyses of the convective regime by, for example, Birikh et al (1969), Gill & Kirkham (1970), Hart (1971), Mizushima & Gotoh (1976) and Bergholz (1978). Elder's experiments showed that the main single-cell circulation becomes unstable to stationary multicellular convection when the Rayleigh number reaches a critical level. In a typical experiment stationary convection set in at $A \approx 5 \times 10^5$ in the form of vertically-stacked transverse rolls near the centre of the slot. At higher Rayleigh numbers $A \approx 10^7$ the wall regions became unstable to travelling waves.

A more complete asymptotic structure for the boundary layer regime was developed by Gill (1966). He showed that a consistent solution for the vertical boundary layers and the core led to a horizontal parallel flow across the core and to a core temperature field which is vertically stratified . Further studies of the boundary layer regime and its stability have been made by Gill & Davey (1969), Blythe, Daniels & Simpkins (1983) and Daniels (1985).

There have been many other studies of convection in laterally-heated vertical slots, both by experiment and numerical simulation. Elder (1966) obtained various numerical results to model his experiments. Vest & Arpaci (1969) in their experiments using air convected in a tall cavity, reported the onset of multicellular convection at sufficiently high Rayleigh numbers. Similar motions were observed numerically by de Vahl Davis & Mallinson (1975). Experiments and numerical simulations by Seki, Fukusako & Inaba (1978), using several kinds of fluids

in a tall cavity with insulated upper and lower boundaries, focused on the effect of the Prandtl number of the fluid and the influence of the aspect ratio on the flow pattern. They observed that the primary single-cell circulation gave way to multicellular convection as the Rayleigh number increased, in the form of secondary flow inside the primary flow in the central region of the cavity.

The prediction of the onset of secondary motion by means of stability analysis has concentrated on the theoretical model first introduced by Elder (1965). This model, which consists of a fluid bounded by infinite vertical planes held at different temperatures and with a constant vertical temperature gradient, β, allows an exact solution of the Boussinesq equations which in many respects approximates the primary circulation in a vertical slot. A comprehensive stability analysis of this basic flow was undertaken by Bergholz (1978) covering the whole range of values of the three governing parameters A, σ and β. Here the parameter β replaces the aspect ratio h of the corresponding cavity flow. Bergholz showed that the instability of the convective and boundary layer regimes is generally in the form of travelling waves for low Prandtl number fluids but at high Prandtl numbers the instability sets in as a stationary state, consistent with Elder's (1965) observations. Conversely, earlier studies by Vest & Arpaci (1969) and Korpela, Gozum and Baxi (1973) had demonstrated that for the conductive regime, time-dependent instability is preferred for sufficiently high Prandtl numbers, $\sigma > 12.7$. The stability of the boundary layer regime was discussed by Gill and Davey (1969) and more recently

stationary modes of convection which arise at infinite Prandtl number have been discussed by Daniels (1985).

New analytical insight into the relationship between vertical slot flow and the flow between vertical planes with a specified vertical temperature gradient, was provided by Daniels (1987). Based on a boundary layer approximation to describe the convective regime at large values of both A and h and at infinite Prandtl number, he showed how the vertical temperature gradient develops in the core of the slot as a function of the convective parameter $l=(A/h)^{1/4}$, and that many of the flow properties are well approximated by the exact solution for infinite vertical planes introduced by Elder (1965). Moreover, the solution demonstrated the onset of instability in the form of transverse rolls at $l_{crit} \approx 11$, in good agreement with the experimental work of Elder (1965), Vest and Arpaci (1969), Seki et al (1978) and Simpkins and Dudderar (1981). By analyzing the instability using the aforementioned exact solution of the Boussinesq equations, it became possible to identify the equivalent stability criterion in terms of the imposed vertical temperature gradient, β, this criterion being $\gamma=(\beta A/4)^{1/4} = \gamma_0 = 6.30$. Here γ is a convective parameter for the exact Boussinesq system replacing the parameter $l=(A/h)^{1/4}$ of the vertical slot flow. With $\beta = 1/2h$ the two criteria for instability, $l \approx 11$ and $\gamma = 6.30$, are in reasonable agreement. Further work on the nature of the instability and its development as the convective parameter increases beyond its critical value has also been carried out using the exact Boussinesq formulation for flow between infinite vertical

planes as a basis. Daniels (1987) identified the lower branch of a neutral stability curve stemming from $\gamma = \gamma_0$, valid in the limit of large Rayleigh number, $A \to \infty$, and corresponding to long wavelength disturbances, of order A relative to the gap width between the planes. More recently, the upper branch of the neutral curve has been found (Daniels 1989) and this corresponds to disturbances for which the wavelength is comparable with the gap width. One of the major properties of the solution that still remains to be determined is the critical wavelength at the point of instability and this is one of the key problems addressed in the present thesis.

1.2 Mathematical Model

Here the theoretical model first introduced by Elder (1965), and subsequently used widely in stability analyses of slot flows, is described. Aspects of the stability of the flow are also discussed.

Consider a vertical fluid layer containing fluid of kinematic viscosity ν, thermal diffusivity κ and coefficient of thermal expansion δ, bounded by infinite rigid vertical planes $x^* = \pm l^*/2$, maintained at temperatures

$$T^* = T_0^* + \Delta T^* (\beta z^*/l^* \pm \tfrac{1}{2}) \ . \qquad (1.2.1)$$

Here x^*, z^* are cartesian coordinates with z^* vertically upwards, T_0^* is the average temperature of the two planes at $z^*=0$ and $\beta \Delta T^*/l^*$ is the uniform vertical temperature gradient.

Two-dimensional motion is assumed to be governed by the following system of equations, which follow from considerations of conservation of mass, conservation of momentum, thermal energy and the equation of state of the fluid :

$$\partial\rho^*/\partial t^* + \nabla^* .(\rho^* \underline{u}^*) = 0, \qquad (1.2.2)$$

$$\partial \underline{u}^*/\partial t^* + (\underline{u}^*.\nabla^*)\underline{u}^* = \underline{F} + \nu\nabla^{*2}\underline{u}^* - \nabla^* p^*/\rho^* , \qquad (1.2.3)$$

$$\partial T^*/\partial t^* + (\underline{u}^*.\nabla^*)T^* = \kappa\nabla^{*2} T^* , \qquad (1.2.4)$$

$$\rho^* = \rho_0^*(1 - \delta(T^* - T_0^*)). \qquad (1.2.5)$$

Here $\nabla^* = (\partial/\partial x^*, 0, \partial/\partial z^*)$, t^* is the time, p^* is the pressure, ρ^* is the density, $\underline{F} = (0,0,-g)$ is the external force per unit mass (where g is the acceleration due to gravity), $\underline{u}^*$ is the fluid velocity and ρ_0^* is the density of the fluid at temperature T_0^*.

Applying the Boussinesq approximation, which assumes that variations of density are small and can be neglected except where multiplied by the acceleration due to gravity, the system (1.2.2)-(1.2.5) can be reduced to the non-dimensional form

$$\frac{\partial u}{\partial x} + \frac{\partial w}{\partial z} = 0 , \qquad (1.2.6)$$

$$\sigma^{-1}\left(\frac{\partial u}{\partial t} + u\frac{\partial u}{\partial x} + w\frac{\partial u}{\partial z} \right) = -\frac{\partial p}{\partial x} + \nabla^2 u , \qquad (1.2.7)$$

$$\sigma^{-1}\left(\frac{\partial w}{\partial t} + u\frac{\partial w}{\partial x} + w\frac{\partial w}{\partial z} \right) = -\frac{\partial p}{\partial z} + \nabla^2 w + AT , \qquad (1.2.8)$$

$$\frac{\partial T}{\partial t} + u\frac{\partial T}{\partial x} + w\frac{\partial T}{\partial z} = \nabla^2 T \ . \qquad (1.2.9)$$

Here the coordinates, time and velocity components are non-dimensionalised by writing $x^* = l^* x$, $z^* = l^* z$, $t^* = \kappa t$, $u^* = \kappa u/l^*$, $w^* = \kappa w/l^*$ and the non-dimensional temperature, T, and reduced pressure, p, are defined by

$$T^* = T_0^* + \Delta T^* T \ , \quad p^* = p_0^* - \rho_0^* g z^* + \rho_0^* g \delta \Delta T^* z^* + \rho_0^* \nu \kappa p/l^{*2}. \qquad (1.2.10)$$

The Rayleigh number A is defined by

$$A = \delta g \Delta T^* l^{*3}/\kappa\nu, \qquad (1.2.11)$$

and the Prandtl number σ is defined by

$$\sigma = \nu/\kappa \ . \qquad (1.2.12)$$

From (1.2.6) a stream function ψ can be defined by the relations

$$u = \partial\psi/\partial z, \quad w = -\partial\psi/\partial x \qquad (1.2.13)$$

and the boundary conditions at the vertical planes are

$$\psi = \partial\psi/\partial x = 0, \quad T = \beta z \pm 1/2 \qquad (x = \pm 1/2). \qquad (1.2.14)$$

There is a simple exact solution of the Boussinesq system as defined above, which depends on the single combination of parameters

$$\gamma = (\beta A/4)^{1/4} \qquad (1.2.15)$$

(Elder 1965). This solution is the steady unidirectional flow

$$\psi = A\,\Psi(x), \qquad T = \beta z + \Theta(x). \tag{1.2.16}$$

The functions Ψ and Θ satisfy the following equations and boundary conditions

$$\Psi^{iv} = \Theta', \qquad \Theta'' + 4\gamma^4\Psi' = 0, \tag{1.2.17}$$

$$\Psi = \Psi' = 0, \qquad \Theta = \pm 1/2 \quad (x = \pm 1/2). \tag{1.2.18}$$

The solutions for Θ and Ψ are odd and even functions of x respectively and are given by

$$\Theta = 2(D_- - D_+)\sinh\gamma x\cos\gamma x - 2(D_- + D_+)\cosh\gamma x\sin\gamma x, \tag{1.2.19}$$

$$\Psi = \gamma^{-3}(D + D_+\cosh\gamma x\cos\gamma x + D_-\sinh\gamma x\sin\gamma x), \tag{1.2.20}$$

where the constants $D_\pm$ and D are defined by

$$D_\pm = -(\cosh(\gamma/2)\sin(\gamma/2) \pm \sinh(\gamma/2)\sin(\gamma/2))/8d, \tag{1.2.21}$$

$$D = (\sinh\gamma + \sin\gamma)/16d, \tag{1.2.22}$$

with $d = \sinh^2(\gamma/2) + \sin^2(\gamma/2)$. This solution represents a stratified flow with a lateral temperature variation which, in general, drives the fluid up near the hot plane ($x = 1/2$) and down near the cold plane ($x = -1/2$). The limit $\gamma \to 0$ corresponds to the conductive regime in which the solution is given by

$$\Theta \sim x, \qquad \Psi \sim (x^2 - \tfrac{1}{4})^2/24 \tag{1.2.23}$$

with an ascending motion when $x > 0$ and a descending motion when $x < 0$. Increase in the value of the convective parameter γ results in an inversion of the horizontal temperature gradient which becomes negative near the centre line ($x = 0$) when

$\gamma=\gamma_a=4.73$. Reversal of the flow first occurs near the centre line when $\gamma=\gamma_b=7.85$. The limit $\gamma\to\infty$ corresponds to the boundary layer regime and results in the formation of buoyancy layers near each vertical plane, with the intervening core region left vertically stratified and motionless. The buoyancy layer solution near the cold plane, $x=-1/2$, obtained from (1.2.19) and (1.2.20), is

$$\Theta \sim -(e^{-X}\cos X)/2, \qquad \Psi' \sim (\gamma^2 e^{-X}\sin X)/4, \qquad (1.2.24)$$

where $X=\gamma(x+1/2)$. Profiles of the velocity and temperature for various values of γ are displayed in Figures 1.1-1.4.

The stability of the above exact solution is investigated, in the usual manner, by superimposing a small disturbance upon the basic state, so that

$$\psi = A[\Psi(x) + \varepsilon\bar{\phi}(x,z,t)], \quad T = \beta z + \Theta(x) + \varepsilon\bar{\theta}(x,z,t). \qquad (1.2.25)$$

The linear stability equations are now obtained by substituting (1.2.25) into the Boussinesq system (1.2.6)-(1.2.9), eliminating the pressure p, and neglecting terms of $O(\varepsilon^2)$. The general solution of the stability equations can then be written in normal mode form to give

$$\psi = A(\Psi(x) + \varepsilon\phi(x)e^{i\alpha(z-ct)}), \quad T = \beta z + \Theta(x) + \varepsilon\theta(x)e^{i\alpha(z-ct)} \qquad (1.2.26)$$

where α is the vertical wavenumber, assumed to be real, and c is the wave speed. The functions ϕ and θ satisfy the following equations and boundary conditions:

$$\phi'''' - 2\alpha^2\,\phi'' + \alpha^4\phi = \theta' + i\alpha[A\Psi'''\phi - (c + A\Psi')(\phi'' - \alpha^2\phi)]/\sigma, \quad (1.2.27)$$

$$\theta'' - \alpha^2\theta = i\alpha[A\Theta'\phi - (c + A\Psi')\theta] - 4\gamma^4\phi', \quad (1.2.28)$$

$$\phi = \phi' = \theta = 0 \qquad (x = \pm 1/2). \quad (1.2.29)$$

For neutral stability, so that the disturbance neither grows nor decays in time, the wave speed c must be real and then the disturbance is stationary if $c=0$, or represents a travelling wave if $c \neq 0$. For sufficiently large values of the Rayleigh number A, such solutions exist and have been found numerically by Bergholz (1978) for a range of values of both the convective parameter γ and the Prandtl number σ. The nature of the instability was found to depend on the relative magnitudes of these two parameters. If the value of the Prandtl number is in the low to moderate range, there is a transition from stationary to travelling-wave instability if the convective parameter γ exceeds a certain magnitude. However, if the Prandtl number is large, the transition, with increasing γ, is from travelling-wave to stationary instability. These results are consistent with a stability analysis of the boundary layer regime ($\gamma >> 1$) by Gill and Davey (1969), who considered travelling-wave instabilities at finite Prandtl numbers, and with later results for the limit of infinite Prandtl number ($\sigma = \infty$, $\gamma >> 1$) by Daniels (1985) where stationary convection is the preferred mode of instability.

For the conductive regime ($\gamma << 1$) Bergholz' results confirmed the preference for stationary convection at low and moderate Prandtl numbers ($\sigma < 12.7$) and travelling waves at high

Prandtl numbers ($\sigma > 12.7$) . This was consistent with results by Vest and Arpaci (1969), who showed that stationary convection occurs for $A>7880\sigma$ for virtually the whole range of Prandtl numbers, and Gill and Kirkham (1970) who showed that travelling waves occur for $A>9400\sigma^{1/2}$ when $\sigma >>1$. The critical value of the Prandtl number above which travelling waves are the preferred mechanism was determined by Korpela, Gozum and Baxi (1973) as $\sigma=12.7$.

At infinite Prandtl number, stationary convection is the preferred mode of instability in the convective regime and was shown by Daniels (1987) to occur for values of the convective parameter γ greater than a critical value $\gamma_0 = 6.30$. This result was obtained by considering the limiting case $A\rightarrow\infty$, equivalent to the situation pertaining to the convective regime in a vertical slot where A and h are large with A/h finite. The usual procedure adopted in stability analyses such as those of Bergholz (1978) is to compute neutral curves in the A-α plane for given values of γ. Daniels (1987) argued that the stability properties of the convective flow with infinite Prandtl number are best described by analysis based on large Rayleigh number A, which leads to a universal neutral curve in the (γ,α) plane. The relevant stability equations for infinite Prandtl number are obtained by setting $\sigma=\infty$ in the right-hand side of (1.2.27) and for stationary convection ($c = 0$), the equations

$$\phi'''' - 2\alpha^2 \phi'' + \alpha^4 \phi = \theta', \qquad (1.2.30)$$

$$\theta'' - \alpha^2 \theta = i\alpha A(\Theta'\phi - \Psi'\theta) - 4\gamma^4 \phi', \qquad (1.2.31)$$

must be solved subject to the boundary conditions (1.2.29). For

large Rayleigh numbers A, the neutral stability curve in the (γ,α) plane has a form in which the wavenumber α is either small (of order A^{-1}) or finite, corresponding to lower and upper branches of the curve respectively.

An investigation of the lower branch of the neutral curve was carried out by Daniels (1987). The wavenumber α is assumed to have the form

$$\alpha \sim \bar{\alpha} A^{-1}, \qquad \text{as } A \to \infty, \tag{1.2.32}$$

where $\bar{\alpha}$ is finite, and the leading approximation to the stability equations and boundary conditions is then

$$\phi'''' = \theta', \tag{1.2.33}$$

$$\theta'' = i\bar{\alpha}(\Theta'\phi - \Psi'\theta) - 4\gamma^4\phi' \tag{1.2.34}$$

$$\phi = \phi' = \theta = 0, \qquad (x = \pm 1/2). \tag{1.2.35}$$

It was established that real solutions for $\bar{\alpha}$ exist only when the convective parameter γ is greater than a critical value γ_0, where $\gamma_0 \approx 6.30$, and this lower branch solution is shown in Figure 1.5. The critical position corresponds to the point at which $\bar{\alpha} \to \infty$, when the convective terms on the right-hand side of (1.2.34) dominate and a critical layer of thickness order $\bar{\alpha}^{-1/3}$ forms on the cenre-line x=0. The critical value γ_0 is determined by the requirement that there is a solution of the system

$$f_1''' - \frac{\Theta'}{\Psi'} f_1 = 0; \quad (f_1, f_1', f_1'') = (0, 0, 1) \text{ at } x = -1/2, \tag{1.2.36}$$

in the region $-1/2 \leq x \leq 0$ for which $f_1'(0)=0$. This condition results from consideration of appropriate bridging conditions across the critical layer, to be discussed in detail in Chapter 3. The value of γ_0, based on an accurate numerical solution of the above eigenvalue problem by Daniels & Weinstein (1992) is 6.29829 to six significant figures.

The above scaling of α in (1.2.32) corresponds to the lower branch of the neutral curve and there is another class of solution of (1.2.29)-(1.2.31) in which α remains finite as $A \to \infty$, equivalent to an upper branch (Daniels 1989). This branch also exists in the region $\gamma > \gamma_0$ and is shown in Figure 1.6. As γ increases the curve asymptotes the position $\gamma_b = 7.85$ at which the base flow reverses on the centre-line of the slot. The upper branch equations are dominated by the convective terms on the right-hand side of (1.2.31) except in a critical layer of thickness order $A^{-1/3}$ at the centre-line $x=0$. As $\gamma \to \gamma_0+$ the wavenumber α decreases to zero and the upper and lower branches coalesce in the neighbourhood of $\gamma = \gamma_0$, $\alpha = 0$ in the $(\gamma-\alpha)$ plane. This is shown schematically in Figure 1.7.

The previous analyses of both the upper and lower branch solutions do not determine one of the most important properties of the instability - the critical wavenumber with which disturbances will occur when the convective parameter γ reaches the neighbourhood of the critical value γ_0. The earlier work suggests that the critical wavenumber α will be such that $\alpha = O(A^{-k})$ as $A \to \infty$ where $0<k<1$ and in fact it emerges that $k=1/3$. One of the primary aims of the present work is to determine the precise form of this critical wavenumber, and

more generally, the local form of the neutral stability curve near γ_0. Another aim is to relax the assumption of infinite Prandtl number and to discuss how the neutral stability curve is modified for large but finite Prandtl numbers.

1.3 Plan of Thesis

The plan of the thesis is as follows.

Chapters 2-4 are concerned with the determination of the critical wave number in the limit $A \to \infty$ when the Prandtl number of the fluid is infinite. In Chapter 2, the solution of the linear stability equations (1.2.30)-(1.2.31) is derived in the limit as $A \to \infty$ by use of asymptotic methods, expanding the solution in the neighbourhood of the critical value γ_0. This leads to asymptotic forms of the perturbation functions ϕ and θ in an 'outer' region $-1/2 < x < 0$ and $0 < x < 1/2$ which spans most of the gap between the planes. The solution here breaks down as $|x| \to 0$, due to the vanishing of the base flow on the centre line $x = 0$, and a thermal critical layer forms.

In Chapter 3, the critical layer solutions for ϕ and θ are obtained, and matching with the outer solution leads to two sets of bridging conditions across the critical layer. This in turn leads to the form of the neutral stability curve near γ_0, from which the critical wavenumber α of order $A^{-1/3}$ can be determined. Solutions in the neighbourhood of each vertical plane are also discussed.

Chapter 4 describes the numerical calculations needed to obtain the values of the various coefficients which appear in the equation of the neutral stability curve. These calculations involve the use of a Runge-Kutta scheme to solve both the leading order and the second order problems in the outer region. This allows the precise form of the critical wavenumber α to be determined and a comparison to be made with the results of full numerical simulations, experimental observations and stability analyses for finite values of A, such as that by Bergholz (1978).

In Chapter 5 the earlier results are modified to incorporate the effect of a large, but not infinite, Prandtl number. This is done by assuming the Prandtl number to adopt a scaling proportional to $A^{4/3}$ as $A \to \infty$. The bridging conditions obtained in Chapter 3 are not affected but the second order outer solutions are, leading to a modification to the equation of the neutral stability curve obtained in Chapter 4.

Finally, Chapter 6 considers the lower branch of the neutral stability curve for finite and large Prandtl numbers, including numerical solutions for finite σ and an asymptotic analysis of the solution in the limit as $\sigma \to \infty$. This reveals neutrally stable solutions in the limit $A \to \infty$ over the entire range of the convective parameter $\gamma > 0$ and an interesting transition to the restricted class of solutions in the range $\gamma > \gamma_0$ as $\sigma \to \infty$.

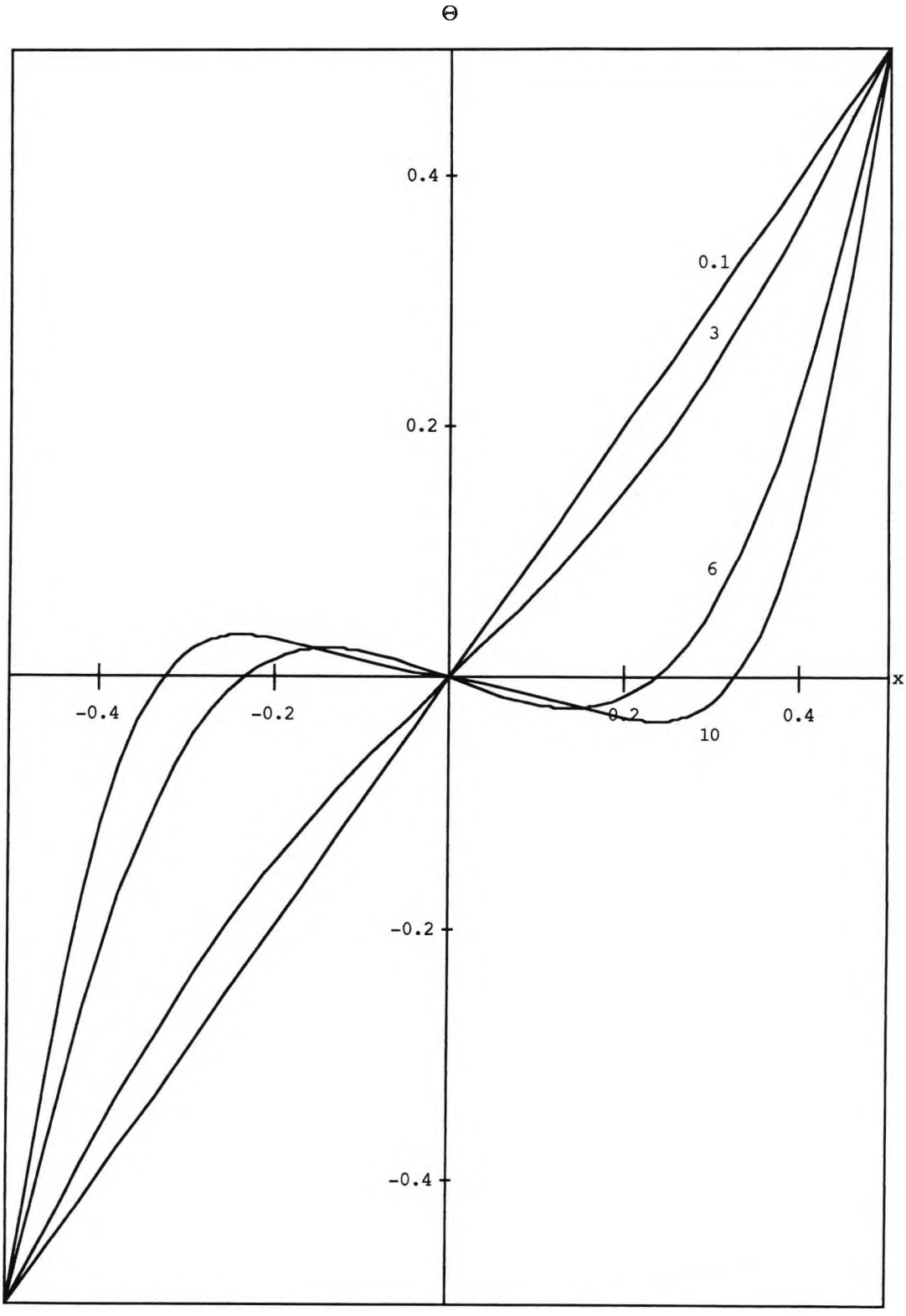

FIGURE 1.1. Base flow temperature profiles Θ for various values of the convective parameter, γ.

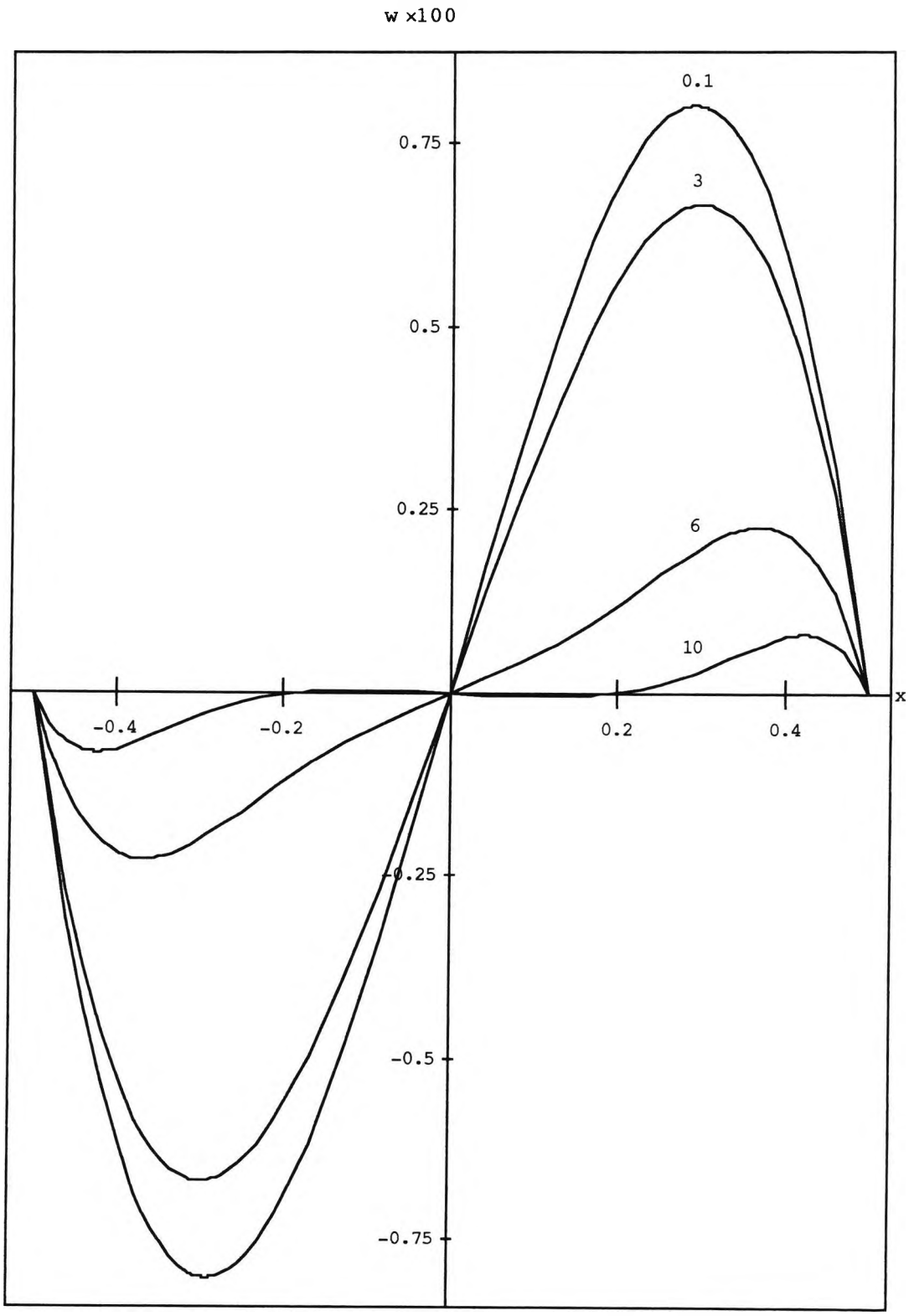

FIGURE 1.2. Base flow velocity profiles $w \times 10^2$ for various values of the convective parameter, γ.

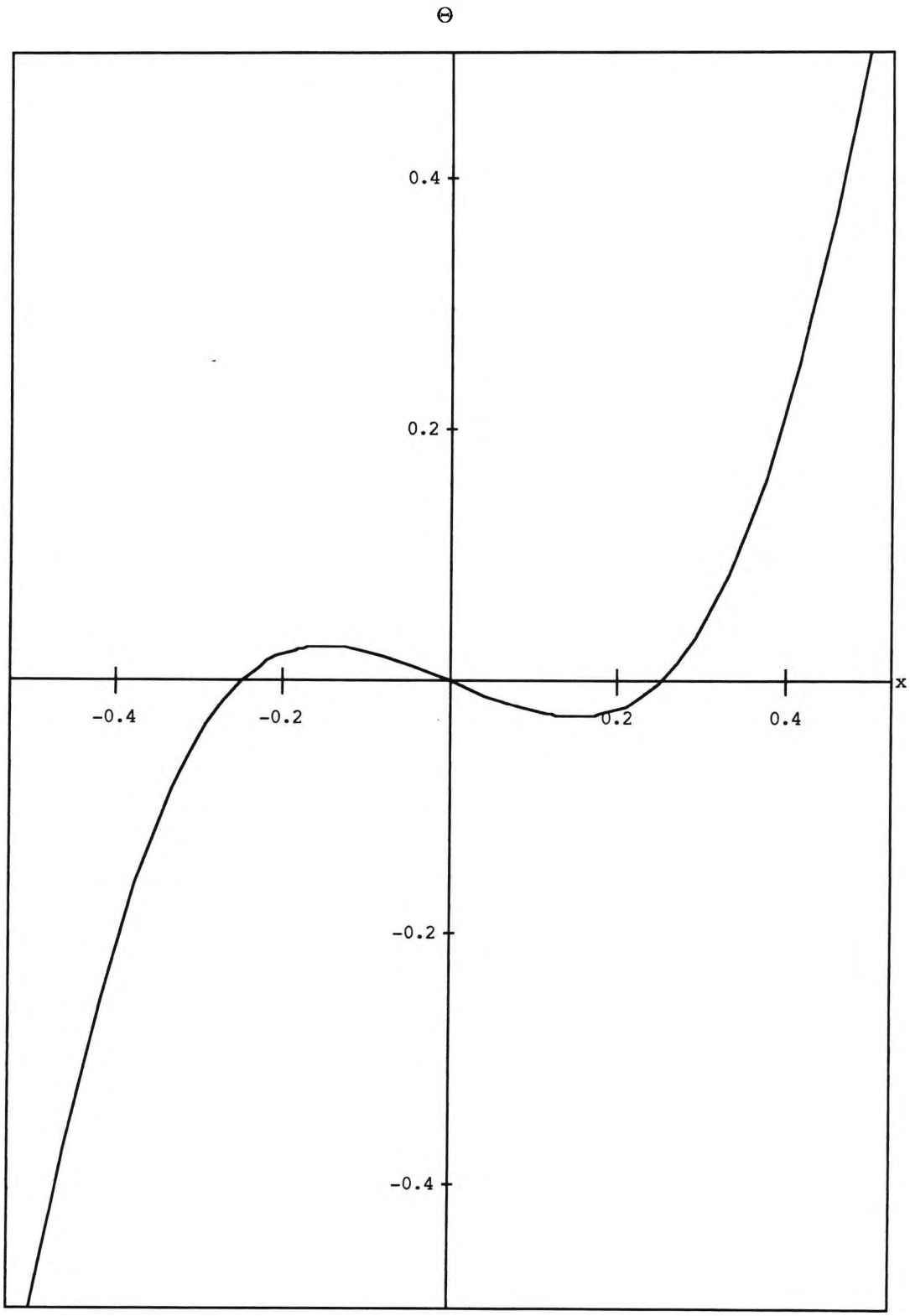

FIGURE 1.3. Base flow temperature profile Θ for the critical value of the convective parameter, γ_0.

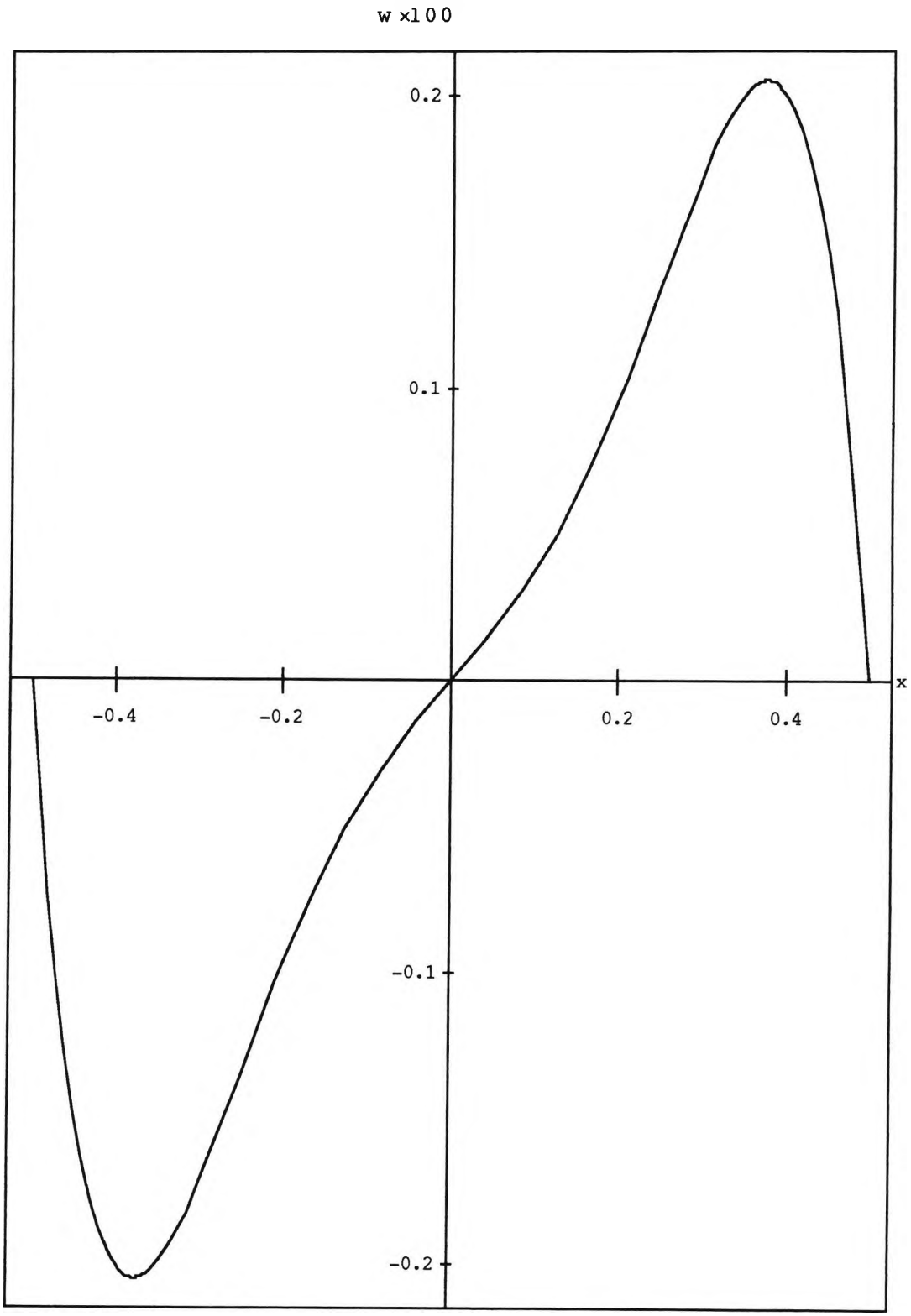

FIGURE 1.4. Base flow velocity profile $w \times 10^2$ for the critical value of the convective parameter, γ_0.

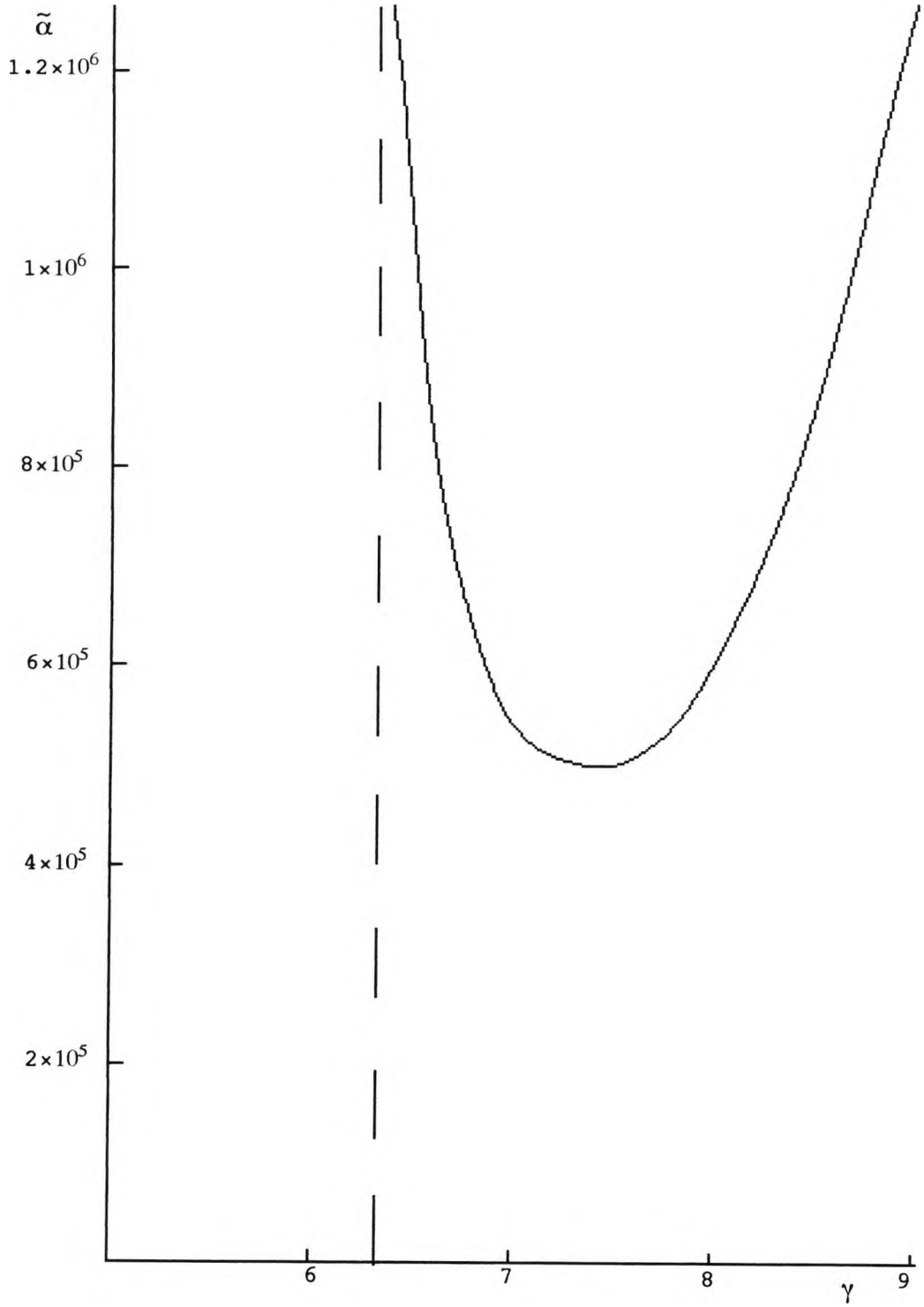

FIGURE 1.5. The lower branch of the neutral curve and the asymptote at γ_0=6.30.

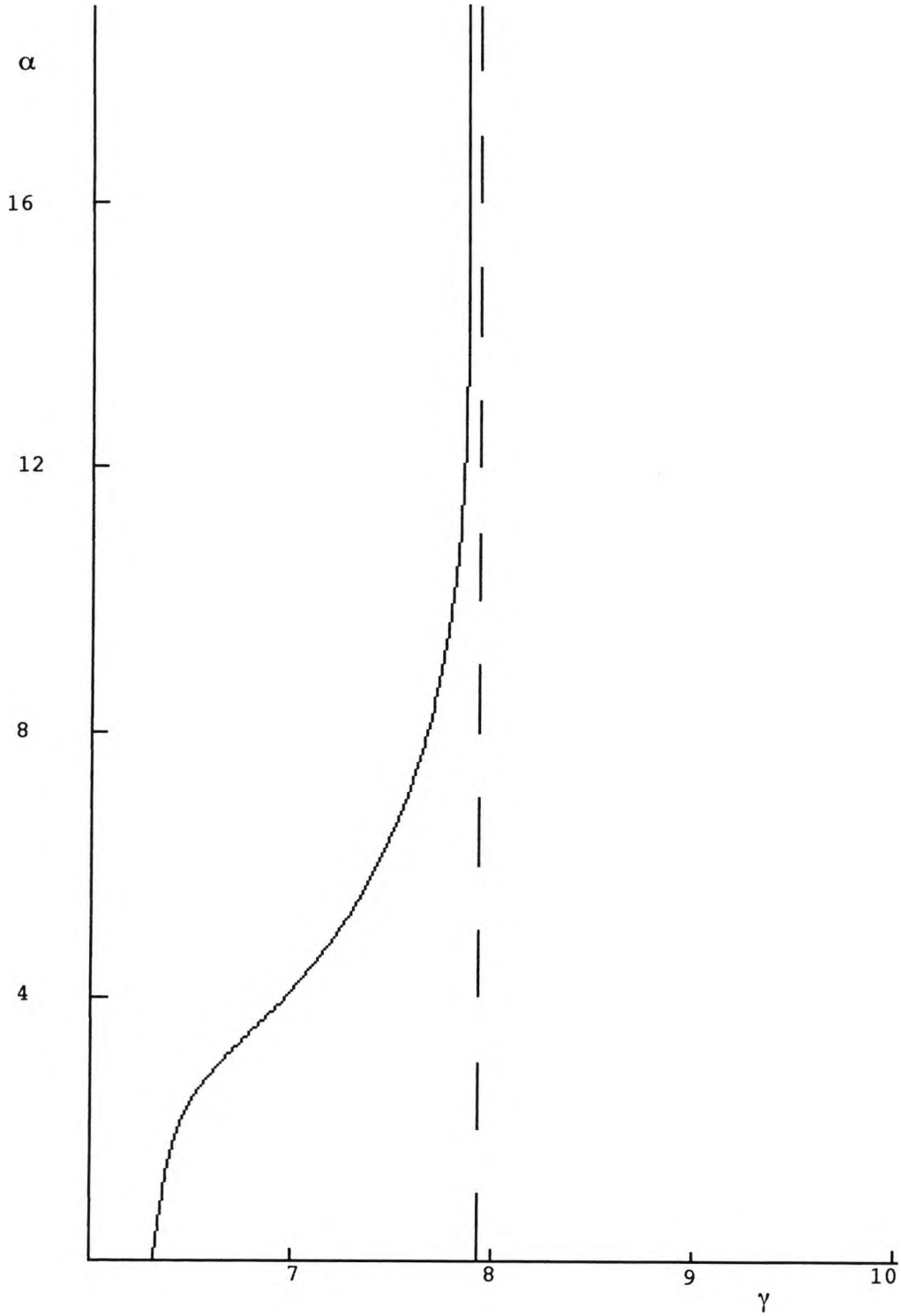

FIGURE 1.6. The upper branch of the neutral curve stemming from $\gamma_0 = 6.30$ with the asymptote at $\gamma_b = 7.85$.

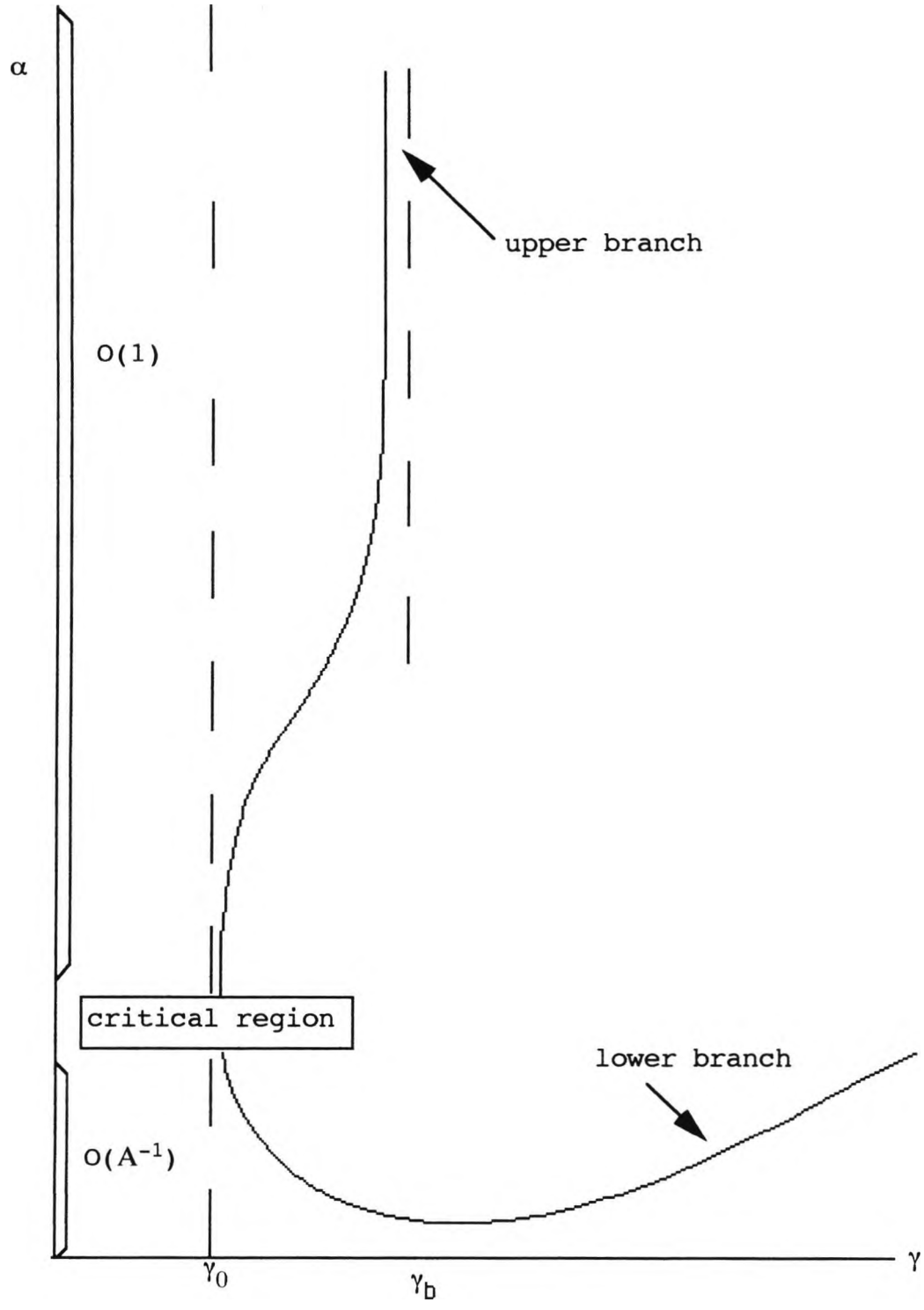

FIGURE 1.7. Schematic diagram of the neutral stability curve in the (γ, α)- plane as $A \to \infty$.

CHAPTER TWO : LARGE RAYLEIGH NUMBER SOLUTION NEAR THE CRITICAL POINT AT INFINITE PRANDTL NUMBER

2.1 Introduction

The form of the solution of the linear stability equations for stationary disturbances with infinite Prandtl number in the limiting case $A \to \infty$ and in the neighbourhood of the critical value, γ_0, of the convective parameter γ, is considered in this chapter.

In Section 2.2 the linear stability equations are stated and appropriate scales for the vertical wavenumber α and the vertical stratification γ are identified. This leads to fourth order equations for the leading terms ϕ_0 and ϕ_1 in the outer expansion of ϕ which must be solved subject to appropriate boundary conditions at the walls, $x = \pm 1/2$. Near the centre, the solution enters a critical layer and asymptotic forms as $|x| \to 0$ of the leading order solution ϕ_0, and the corresponding temperature θ_0, are derived in Section 2.3. Similarly the asymptotic forms as $|x| \to 0$ of the second order terms, ϕ_1 and θ_1, are derived in Section 2.4. The form of the overall outer solution as $x \to 0\pm$ is summarized in Section 2.5 and this allows the relevant critical layer solution to be formulated in Chapter 3. The various constants which arise in the outer solution can only be determined following the derivation of the bridging conditions for ϕ_0 and ϕ_1 across the critical layer.

2.2 Formulation of the Solution for $A \to \infty$

Consider the solution of the stability equations (1.2.30)-(1.2.31) for stationary convection (c=0) in the form

$$\psi = A(\Psi(x) + \phi(x)e^{i\alpha z}), \quad T = \beta z + \Theta(x) + \theta(x)e^{i\alpha z}. \qquad (2.2.1)$$

In the case of infinite Prandtl number the perturbation functions ϕ and θ satisfy the following linear stability equations

$$\phi'''' - 2\alpha^2\phi'' + \alpha^4\phi = \theta', \qquad (2.2.2)$$

$$\theta'' - \alpha^2\theta = i\alpha A(\Theta'\phi - \Psi'\theta) - 4\gamma^4\phi', \qquad (2.2.3)$$

to be solved subject to the boundary conditions

$$\phi = \phi' = \theta = 0. \qquad (x = \pm 1/2) \qquad (2.2.4)$$

at the vertical planes. As indicated in Chapter 1, solutions of this system in the limit as $A \to \infty$ appear to exist only above a critical value of the convective parameter γ equal to $\gamma_0 \approx 6.30$, where the corresponding wavenumber α is small. Here the form of the solution in the neighbourhood of γ_0 is investigated in detail.

It emerges that the appropriate scales for α and γ which capture the form of the neutral curve near γ_0 are given by

$$\alpha = \alpha_0 A^{-1/3}, \quad A \to \infty, \qquad (2.2.5)$$

$$\gamma = \gamma_0 + \gamma_1 A^{-2/3} + \ldots, \quad A \to \infty. \qquad (2.2.6)$$

At this stage the simplest explanation of this lies in the fact

that the correction terms to the leading order theory described briefly in Chapter 1 then contribute in the most general way to the outer expansion, as evidenced by the appearance of terms proportional to α_0^2, $1/i\alpha_0$ and γ_1 in the equation for the first correction term ϕ_1 in the solution for ϕ (see (2.4.1) below). The theory could be developed with more general forms in (2.2.5) and (2.2.6) but other powers of A simply lead to an appropriate limiting form of the neutral curve to be identified eventually in Chapter 3.

From (2.2.5) and (2.2.6) appropriate expansions for the base flow functions Θ and Ψ are

$$\Theta(x,\gamma) = \Theta_0(x) + \gamma_1 \; A^{-2/3}\Theta_1(x) + \ldots, \quad A\to\infty \; , \tag{2.2.7}$$

$$\Psi(x,\gamma) = \Psi_0(x) + \gamma_1 \; A^{-2/3}\Psi_1(x) + \ldots, \quad A\to\infty \; , \tag{2.2.8}$$

where $\Theta_0(x) = \Theta(x,\gamma_0)$, $\Theta_1(x) = \Theta_\gamma(x,\gamma_0)$, $\Psi_0 = \Psi(x,\gamma_0)$, $\Psi_1 = \Psi_\gamma(x,\gamma_0)$ and the subscript γ denotes partial differentiation with respect to γ. The formulae for Θ_0, Θ_1, Ψ_0 and Ψ_1 may be deduced from (1.2.19) and (1.2.20).

Solutions for the perturbation functions ϕ and θ, of the form

$$\phi = \phi_0 + A^{-2/3}\phi_1 + \cdots, \quad A\to\infty \tag{2.2.9}$$

$$\theta = \theta_0 + A^{-2/3}\theta_1 + \ldots, \quad A\to\infty \tag{2.2.10}$$

are assumed and substitution of (2.2.7)-(2.2.10) into equations (2.2.2) and (2.2.3), and equating terms of like powers of A, leads to the following equations and boundary conditions for ϕ_0

, ϕ_1, θ_0 and θ_1:

$$\theta_0 = \frac{\Theta_0'}{\Psi_0'}\phi_0 \ , \tag{2.2.11}$$

$$\phi_0'''' = \theta_0' \ , \tag{2.2.12}$$

$$\theta_1 = \frac{\Theta_0'}{\Psi_0'}\phi_1 + \gamma_1\frac{\Theta_1'\phi_0 - \Psi_1'\theta_0}{\Psi_0'} - \frac{\theta_0'' + 4\gamma_0^4\phi_0'}{i\alpha_0\Psi_0'} \ , \tag{2.2.13}$$

$$\phi_1'''' = \theta_1' + 2\alpha_0^2\phi_0'' \ , \tag{2.2.14}$$

$$\phi_0 = \phi_0' = \phi_1 = \phi_1' = 0, \qquad (x = \pm 1/2). \tag{2.2.15}$$

Here it is assumed that the stream function satisfies the boundary conditions $\phi = \phi' = 0$ at $x = \pm 1/2$ while conditions for θ cannot be specified in view of the loss of the second derivative term θ'' in (2.2.3). The validity of this procedure will be confirmed in Chapter 3 by considering the solution in inner regions of thickness order $A^{-2/9}$ near each vertical wall, $x=\pm 1/2$, where the necessary adjustment to the full boundary conditions (2.2.4) is made. In fact from (2.2.11), the leading order term in the outer solution for the temperature, θ_0, is consistent with the thermal condition $\theta = 0$ in (2.2.4) so that the role of these inner wall regions is a relatively minor one.

At the centre-line, $x = 0$, the base flow velocity Ψ_0' vanishes and so the systems (2.2.11)-(2.2.14) are, in general, singular

there. Thus the outer solution developed here also breaks down in the neighbourhood of $x=0$ where a thermal critical layer occurs. The outer solution is thus valid in separate regions $-1/2<x<0$ and $0<x<1/2$ either side of the critical layer (see Figure 2.1). The method by which the solution can be found in each of these regions is discussed in the following section.

2.3 Leading Order Outer Solution

The equation for ϕ_0 is

$$\phi_0'''' - \frac{d}{dx}\left(\frac{\Theta_0'}{\Psi_0'}\phi_0\right) = 0 \qquad (2.3.1)$$

and this can be integrated once to give the third order equation

$$\phi_0''' - \frac{\Theta_0'}{\Psi_0'}\phi_0 = k_0 \ , \qquad (2.3.2)$$

where k_0 is an arbitrary constant. Equation (2.3.2) is to be solved subject to the boundary conditions $\phi_0 = \phi_0' = 0$ at $x = \pm 1/2$. Thus the solution in $x<0$ can be written in the form

$$\phi_0 = \sigma_1^- f_1(x) + \sigma_2^- f_2(x) \ , \qquad (2.3.3)$$

where σ_1^- and σ_2^- are complex constants and f_1 and f_2 are real

functions of x uniquely defined in the interval $-1/2 < x < 0$ by

$$f_1''' - \frac{\Theta_0'}{\Psi_0'} f_1 = 0; \quad (f_1,\ f_1',\ f_1'') = (0,0,1) \text{ at } x=-1/2 \ , \tag{2.3.4}$$

$$f_2''' - \frac{\Theta_0'}{\Psi_0'} f_2 = 1; \quad (f_2,\ f_2',\ f_2'') = (0,0,0) \text{ at } x=-1/2 \ . \tag{2.3.5}$$

Since the base profiles Θ_0' and Ψ_0' are even and odd functions of x respectively, it follows that the appropriate solution in $x>0$ is

$$\phi_0 = \sigma_1^+ f_1(-x) + \sigma_2^+ f_2(-x) \ , \tag{2.3.6}$$

where σ_1^+ and σ_2^+ are further complex constants.

The form of the solution as $x \to 0$ is now considered. The expansions of Θ_0' and Ψ_0' about the centre line $x=0$ are

$$\Theta_0' = \mu_0 + \mu_2 x^2 + \mu_4 x^4 + \mu_6 x^6 + \ldots, \quad x \to 0\pm \ , \tag{2.3.7}$$

$$\Psi_0' = \omega_1 x + \omega_3 x^3 + \omega_5 x^5 + \omega_7 x^7 + \ldots, \quad x \to 0\pm \ , \tag{2.3.8}$$

where μ_i and ω_i are real constants whose values are given in Table 2.1. It follows that the functions f_i (i=1,2) have the general asymptotic forms

$$f_i = a_i + b_i x + c_{i0} x^2 \ln|x| + c_i x^2 + d_i x^3 + e_{i0} x^4 \ln|x| + e_i x^4 + g_i x^5 + h_{i0} x^6 \ln|x| + h_i x^6 + \ldots, \quad x \to 0-, \tag{2.3.9}$$

where the logarithmic terms are generated by the singularity

associated with the vanishing of the base flow velocity Ψ_0'. The constants a_i, b_i and c_i must be determined from a numerical solution of (2.3.4) and (2.3.5) which is undertaken in Chapter 4, and the remaining constants c_{i0}, d_i, e_{i0},... can be expressed in terms of these as follows

$$c_{i0} = a_i s_0/2, \qquad d_i = (b_i s_0 + i-1)/6$$

$$e_{i0} = c_{i0} s_0/24, \qquad e_i = (a_i s_1 + c_i s_0 - 26e_{i0})/24$$

$$g_i = (b_i s_1 + d_i s_0)/60, \qquad h_{i0} = (c_{i0} s_1 + e_{i0} s_0)/120,$$

$$h_i = (a_i s_2 + c_i s_1 + e_i s_0 - 74h_{i0})/120 \ . \qquad (2.3.10)$$

Here the real constants s_0, s_1 and s_2, are defined by

$$s_0 = \mu_0/\omega_1, \qquad s_1 = (\mu_2\omega_1 - \mu_0\omega_3)/\omega_1^2,$$

$$s_2 = [\mu_4\omega_1^2 - \mu_2\omega_1\omega_3 + \mu_0(\omega_3^2 - \omega_1\omega_5)]/\omega_1^3. \qquad (2.3.11)$$

The numerical values of s_0, s_1 and s_2 are given in Table 2.3.

From (2.3.3) and (2.3.6) the asymptotic expansion of ϕ_0 as $x \to 0\pm$ can now be written in the form

$$\phi_0 = a_0^{\pm} + b_0^{\pm}x + c_{00}^{\pm}\, x^2 \ln|x| + c_0^{\pm}x^2 + d_0^{\pm}x^3 + e_{00}^{\pm}\, x^4 \ln|x| + e_0^{\pm}x^4 + g_0^{\pm}x^5 + h_{00}^{\pm}\, x^6 \ln|x| + h_0^{\pm}x^6 + \ldots, \qquad (2.3.12)$$

where, introducing the vector notation $\underline{v}_0^{\pm} = (a_0^{\pm}, \mp b_0^{\pm}, c_{00}^{\pm}, c_0^{\pm}, \mp d_0^{\pm}\ldots)$, $\underline{v}_1 = (a_1, b_1, c_{10},\ldots)$, $\underline{v}_2 = (a_2, b_2, c_{20},\ldots)$, the relations between $a_0^{\pm}$, $b_0^{\pm}$,... and the real constants $a_1, b_1, \ldots$, $a_2, b_2, \ldots$ are given, in vector form, by the following formulae

$$\underline{v}_0^{\pm} = \sigma_1^{\pm}\, \underline{v}_1 + \sigma_2^{\pm}\, \underline{v}_2 \ . \qquad (2.3.13)$$

Thus the asymptotic expansions of ϕ_0 as $|x|\to 0$ are determined in terms of the complex constants $\sigma_1^{\pm}$, $\sigma_2^{\pm}$, and the vectors $\underline{v}_1$ and $\underline{v}_2$ which, in principle at least, are known from the solution of the two systems for f_1 and f_2.

Asymptotic forms of θ_0 as $|x|\to 0$ can be deduced from those for ϕ_0 using equation (2.2.11). Thus

$$\theta_0 = A_0^{\pm}/x + B_0^{\pm} + C_{00}^{\pm} x\ln|x| + C_0^{\pm}x + D_0^{\pm}x^2 + E_{00}^{\pm}x^3\ln|x| + E_0^{\pm}x^3 + \ldots, x\to 0\pm , \qquad (2.3.14)$$

where the constants $A_0^{\pm}$, ..., $E_0^{\pm}$ are defined by

$$A_0^{\pm} = s_0a_0^{\pm}, \qquad B_0^{\pm} = s_0b_0^{\pm}, \qquad C_{00}^{\pm} = s_0c_{00}^{\pm},$$

$$C_0^{\pm} = s_0c_0^{\pm} + s_1a_0^{\pm}, \qquad D_0^{\pm} = s_0d_0^{\pm} + s_1b_0^{\pm}, \qquad E_{00}^{\pm} = s_0e_{00}^{\pm} + s_1c_{00}^{\pm},$$

$$E_0^{\pm} = s_0e_0^{\pm} + s_1c_0^{\pm} + s_2a_0^{\pm} . \qquad (2.3.15)$$

The above asymptotic forms of ϕ_0 and θ_0, given by (2.3.12) and (2.3.14), provide the behaviour of the leading order outer solution of the stability equations as $|x|\to 0$. The next step is to carry out a similar analysis of the second order outer solutions, for ϕ_1 and θ_1.

2.4 Second Order Outer Solution

Here we are concerned with finding the outer solutions for ϕ_1 and θ_1. The equation for ϕ_1 is

$$\phi_1'''' - \frac{d}{dx}\left(\frac{\Theta_0'}{\Psi_0'}\phi_1\right) = \frac{d}{dx}\left(2\alpha_0^2\phi_0' + \gamma_1\frac{\Theta_1'\phi_0 - \Psi_1'\theta_0}{\Psi_0'} - \frac{\theta_0'' + 4\gamma_0^4\phi_0'}{i\alpha_0\Psi_0'}\right) \quad (2.4.1)$$

and this can be integrated once to give the third order equation

$$\phi_1''' - \frac{\Theta_0'}{\Psi_0'}\phi_1 = 2\alpha_0^2\phi_0' + \gamma_1\frac{\Theta_1'\phi_0 - \Psi_1'\theta_0}{\Psi_0'} - \frac{\theta_0'' + 4\gamma_0^4\phi_0'}{i\alpha_0\Psi_0'} + k_1 , \quad (2.4.2)$$

where k_1 is an arbitrary constant. This is to be solved subject to the boundary conditions $\phi_1 = \phi_1' = 0$ at $x = \pm 1/2$. The general solution for ϕ_1 can be written in the form

$$\phi_1 = \bar{\phi}_1 + 2\alpha_0^2\phi_{11} + \gamma_1\phi_{12} - \phi_{13}/i\alpha_0 , \quad (2.4.3)$$

where the functions $\bar{\phi}_1$, ϕ_{11}, ϕ_{12} and ϕ_{13} satisfy the following equations and boundary conditions:

$$\bar{\phi}_1''' - \frac{\Theta_0'}{\Psi_0'}\bar{\phi}_1 = \bar{k}_1 ; \quad \bar{\phi}_1 = \bar{\phi}_1' = 0 \quad (x = \pm 1/2), \quad (2.4.4)$$

$$\phi_{11}''' - \frac{\Theta_0'}{\Psi_0'}\phi_{11} = \phi_0' ; \quad \phi_{11} = \phi_{11}' = 0 \quad (x = \pm 1/2), \quad (2.4.5)$$

$$\phi_{12}''' - \frac{\Theta_0'}{\Psi_0'}\phi_{12} = \frac{\Theta_1'\Psi_0' - \Theta_0'\Psi_1'}{(\Psi_0')^2}\phi_0 ; \quad \phi_{12} = \phi_{12}' = 0 \quad (x = \pm 1/2), \quad (2.4.6)$$

$$\phi'''_{13} - \frac{\Theta_0'}{\Psi_0'}\,\phi_{13} = \frac{\theta_0'' + 4\gamma_0^4\phi_0'}{\Psi_0'}\ ;\ \phi_{13} = \phi'_{13} = 0 \quad (x = \pm 1/2). \qquad (2.4.7)$$

Starting with equation (2.4.4), the solution for $\bar{\phi}_1$ in $x < 0$ can be written in the form

$$\bar{\phi}_1 = \bar{\sigma}_1^- f_1(x) + \bar{\sigma}_2^- f_2(x), \qquad (2.4.8)$$

where $\bar{\sigma}_1^-$ and $\bar{\sigma}_2^-$ are complex constants. Symmetry properties of the base flow functions Θ_0' and Ψ_0' then allow the solution in $x > 0$ to be written as

$$\bar{\phi}_1 = \bar{\sigma}_1^+ f_1(-x) + \bar{\sigma}_2^+ f_2(-x), \qquad (2.4.9)$$

where $\bar{\sigma}_1^+$ and $\bar{\sigma}_2^+$ are further complex constants. Here the real functions f_1 and f_2 are those defined by (2.3.4) and (2.3.5). The asymptotic forms of $\bar{\phi}_1$ as $|x| \to 0$ are given by

$$\bar{\phi}_1 = \bar{a}_1^{\pm} + \bar{b}_1^{\pm} x + \bar{c}_{10}^{\pm} x^2 \ln|x| + \bar{c}_1^{\pm} x^2 + \bar{d}_1^{\pm} x^3 + \bar{e}_{10}^{\pm} x^4 \ln|x| + \bar{e}_1^{\pm} x^4 + \bar{g}_1^{\pm} x^5 + \bar{h}_{10}^{\pm} x^6 \ln|x| + \bar{h}_1 x^6 + \ldots, \qquad (2.4.10)$$

where the constants $\bar{a}_1^{\pm}$, $\bar{b}_1^{\pm}$,... are defined in terms of the real constants $a_1, b_1, \ldots, a_2, b_2, \ldots$ by the relation

$$\underline{\bar{v}}_1^{\pm} = \bar{\sigma}_1^{\pm}\,\underline{v}_1 + \bar{\sigma}_2^{\pm}\,\underline{v}_2. \qquad (2.4.11)$$

where $\underline{v}_1$, $\underline{v}_2$ are the vectors defined in Section 2.3 above and $\underline{\bar{v}}_1^{\pm} = (\bar{a}_1^{\pm}, \mp\bar{b}_1^{\pm}, \bar{c}_{10}^{\pm}, \bar{c}_1^{\pm}, \mp\bar{d}_1^{\pm}, \ldots)$.

Next we consider equation (2.4.5), where the solution for ϕ_{11} in $x < 0$ can be written as

$$\phi_{11} = \sigma_1^- f_{11}(x) + \sigma_2^- f_{21}(x). \qquad (2.4.12)$$

Here f_{11}, f_{21} are real functions of x uniquely defined by

$$f_{i1}''' - \frac{\Theta_0'}{\Psi_0'} f_{i1} = f_i' \; ; \; (f_{i1}, f_{i1}', f_{i1}'') = (0,0,0) \quad \text{at } x = -1/2 \qquad (2.4.13)$$

and by using symmetry the solution for ϕ_{11} in $x>0$ can be written in the form

$$\phi_{11} = \sigma_1^+ f_{11}(-x) + \sigma_2^+ f_{21}(-x). \qquad (2.4.14)$$

The asymptotic behaviour of the real functions f_{i1} (i=1,2) as $x \to 0-$ is given by

$$f_{i1} = a_{i1} + b_{i1}x + c_{i10}x^2\ln|x| + c_{i1}x^2 + d_{i1}x^3 + e_{i10}x^4\ln|x| + e_{i1}x^4 + g_{i1}x^5 + h_{i10}x^6\ln|x| + h_{i1}x^6 + \ldots \qquad (2.4.15)$$

Here the real constants a_{i1}, b_{i1} and c_{i1} must be determined by a numerical solution to be undertaken in Chapter 4, and the remaining constants are obtained in terms of these by substituting (2.4.15), together with (2.3.7)-(2.3.9), into equation (2.4.13) and equating terms of like powers in x. Thus

$$c_{i10} = a_{i1}s_0/2, \quad d_{i1} = (b_{i1}s_0 + b_i)/6, \quad e_{i10} = (2c_{i0} + c_{i10}s_0)/24,$$

$$e_{i1} = (2c_i + c_{i0} - 26e_{i10} + c_{i1}s_0 + a_{i1}s_1)/24 \; . \qquad (2.4.16)$$

From (2.4.12) and (2.4.14) the asymptotic forms of ϕ_{11} as $|x| \to 0$ are given by

$$\phi_{11} = a_{11}^{\pm} + b_{11}^{\pm}x + c_{110}^{\pm}x^2\ln|x| + c_{11}^{\pm}x^2 + d_{11}^{\pm}x^3 + e_{110}^{\pm}x^4\ln|x| + e_{11}^{\pm}x^4 + \ldots, \qquad (2.4.17)$$

where the constants $a_{11}^{\pm}, b_{11}^{\pm}, \ldots$ are defined in terms of the real constants $a_{11}, b_{11}, \ldots, a_{21}, b_{21}, \ldots$, by the vector relations

$$\underline{v}_{11}^{\pm} = \sigma_1^{\pm} \underline{v}_{11} + \sigma_2^{\pm} \underline{v}_{21} \ , \qquad (2.4.18)$$

where $\underline{v}_{11}^{\pm} = (a_{11}^{\pm}, \mp b_{11}^{\pm}, c_{110}^{\pm}, c_{11}^{\pm}, \mp d_{11}^{\pm}, \ldots)$, $\underline{v}_{11} = (a_{11}, b_{11}, c_{110}, \ldots)$ and $\underline{v}_{21} = (a_{21}, b_{21}, c_{210}, \ldots)$.

The solution for ϕ_{12} in $x < 0$ can be written in the form

$$\phi_{12} = \sigma_1^{-} f_{12}(x) + \sigma_2^{-} f_{22}(x) \ , \qquad (2.4.19)$$

where the functions f_{i2} $(i=1,2)$ are real and uniquely defined by

$$f'''_{i2} - \frac{\Theta_0'}{\Psi_0'} f_{i2} = \frac{\Theta_1' \Psi_0' - \Theta_0' \Psi_1'}{(\Psi_0')^2} f_i ;$$

$$(f_{i2}, f'_{i2}, f''_{i2}) = (0,0,0) \text{ at } x = -1/2. \qquad (2.4.20)$$

Symmetries of the base flow functions Θ_0' Ψ_0', Θ_1' and Ψ_1' then allow the solution in $x > 0$ to be written as

$$\phi_{12} = \sigma_1^{+} f_{12}(-x) + \sigma_2^{+} f_{22}(-x). \qquad (2.4.21)$$

The next step is to consider the form of ϕ_{12} as $|x| \to 0$ but before doing so, we need the appropriate expansions of the base flow functions Θ_1' and Ψ_1' about $x=0$. These are given by

$$\Theta_1' = \tilde{\mu}_0 + \tilde{\mu}_2 \, x^2 + \tilde{\mu}_4 \, x^4 + \ldots \quad (x \to 0), \qquad (2.4.22)$$

$$\Psi_1' = \tilde{\omega}_1 \, x + \tilde{\omega}_3 \, x^3 + \tilde{\omega}_5 \, x^5 + \ldots \quad (x \to 0), \qquad (2.4.23)$$

where $\tilde{\mu}_0$, ..., $\tilde{\omega}_1$, ... are real constants whose numerical values are given in Table 2.2. The asymptotic forms of f_{i2} as $x \to 0-$ are given by

$$f_{i2} = a_{i2} + b_{i2}x + c_{i20}x^2\ln|x| + c_{i2}x^2 + d_{i2}x^3 + e_{i20}x^4\ln|x| + e_{i2}x^4 + \ldots \qquad (2.4.24)$$

Here, again, the real constants a_{i2}, b_{i2} and c_{i2} are determined by a numerical solution undertaken in Chapter 4, and substitution of (2.3.9),(2.4.24) and the appropriate base flow expansions into (2.4.20) leads to the determination of the remaining constants c_{i20}, d_{i2},... as

$$c_{i20} = [s_0a_{i2} + (r_0 - s_0q_0)a_i]/2, \quad d_{i2} = [s_0b_{i2} + (r_0 - q_0s_0)b_i]/6,$$

$$e_{i20} = [s_0c_{i20} + (r_0 - q_0s_0)c_{i0}]/24,$$

$$e_{i2} = [s_0c_{i2} + s_1a_{i2} + r_0c_i + r_1a_i - q_0(s_0c_i + s_1a_i) - s_0q_1a_i - 26e_{i20}]/24, \qquad (2.4.25)$$

where the constants

$$r_0 = \tilde{\mu}_0/\omega_1, \qquad q_0 = \tilde{\omega}_1/\omega_1 ,$$

$$r_1 = (\tilde{\mu}_2 - \tilde{\mu}_0\omega_3/\omega_1)/\omega_1, \qquad q_1 = (\tilde{\omega}_3 - \tilde{\omega}_1\omega_3/\omega_1)/\omega_1 . \qquad (2.4.26)$$

The values of r_0, r_1, q_0 and q_1 are given in Table 2.3. We can now write the asymptotic forms of ϕ_{12} as $|x| \to 0$ as

$$\phi_{12} = a_{12}^{\pm} + b_{12}^{\pm}x + c_{120}^{\pm}x^2\ln|x| + c_{12}^{\pm}x^2 + d_{12}^{\pm}x^3 + e_{120}^{\pm}x^4\ln|x| + e_{12}^{\pm}x^4 + \ldots, \qquad (2.4.27)$$

where the constants $a_{12}^{\pm}$, $b_{12}^{\pm}$,... are defined in terms of the

real constants a_{12}, b_{12},..., and a_{22}, b_{22},..., by the vector relation

$$\underline{v}_{12}^{\pm} = \sigma_1^{\pm}\,\underline{v}_{12} + \sigma_2^{\pm}\,\underline{v}_{22}, \tag{2.4.28}$$

where $\underline{v}_{12}^{\pm} = (a_{12}^{\pm},\ \mp b_{12}^{\pm},\ c_{120}^{\pm},\ c_{12}^{\pm},\ \mp d_{12}^{\pm},\ldots)$, $\underline{v}_{12} = (a_{12}, b_{12}, c_{120},\ldots)$ and $\underline{v}_{22} = (a_{22}, b_{22}, c_{220},\ldots)$.

Finally we consider equation (2.4.7) where the solution for ϕ_{13} in $x<0$ can be written as

$$\phi_{13} = \sigma_1^{-} f_{13}(x) + \sigma_2^{-} f_{23}(x). \tag{2.4.29}$$

Here the functions f_{i3} (i=1,2) are real and satisfy the equations and boundary conditions

$$f'''_{i3} - \frac{\Theta_0'}{\Psi_0'} f_{i3} = \frac{1}{\Psi_0'}\left(\frac{d^2}{dx^2}\left\{\frac{\Theta_0' f_i}{\Psi_0'}\right\}\right) + \frac{4\gamma_0^4 f_i'}{\Psi_0'}, \tag{2.4.30}$$

$$f_{i3} = f'_{i3} = 0 \quad \text{at } x = -1/2\ . \tag{2.4.31}$$

The second derivative of f_{i3} does not vanish as $x\to -1/2$ in this case but the third boundary condition at $x=-1/2$ can be taken as the requirement that the finite part of f''_{i3} vanishes as $x\to -1/2$, equivalent to the local behaviour

$$f_{i3} \sim 0 + 0.X + D_{i20}\,X^2 \ln|X| + 0.X^2 + \ldots, \tag{2.4.32}$$

where $X=x+1/2$ and D_{i20} is a known constant (see Chapter 4). By symmetry, the solution for ϕ_{13} in $x>0$ can be written in the

form

$$\phi_{13} = -\sigma_1^+ f_{13}(-x) - \sigma_2^+ f_{23}(-x). \qquad (2.4.33)$$

The asymptotic behaviours of f_{i3} as $x\to 0-$ are given by

$$f_{i3} = \delta_{i3}/x + a_{i3} + b_{i30}\, x\ln|x| + b_{i3}\, x + c_{i30}\, x^2\ln|x| + c_{i3}\, x^2 + d_{i30}\, x^3\ln|x| + d_{i3}\, x^3 + \ldots, \qquad (2.4.34)$$

where the constants a_{i3}, b_{i3} and c_{i3} are determined numerically in Chapter 4. The remaining constants are obtained in terms of a_{i3}, b_{i3} and c_{i3} by substituting (2.3.9),(2.4.34) and the appropriate base flow expansions into equation (2.4.30) and equating terms of like powers of x. This leads to the formulae

$$\delta_{i3} = -s_0 a_{i3}/3\omega_1, \qquad b_{i30} = (-s_0\omega_1\delta_{i3} - s_0 c_{i0} + 2a_i\omega_3 s_0/\omega_1)/\omega_1,$$

$$c_{i30} = s_0 a_{i3}/2 + (s_0 d_i + s_1 b_i + 2\gamma_0^4 b_i)/\omega_1,$$

$$d_{i30} = [\omega_1 s_0 b_{i30} + (6e_{i0}s_0 + 6c_{i0}s_1) + 8\gamma_0^4 c_{i0}]/6\omega_1,$$

$$d_{i3} = [s_0 b_{i3} - 11 d_{i30} + s_1\delta_{i3} + 2s_0 a_i(\omega_3^2 - \omega_1\omega_5)/\omega_1^3 + 4\gamma_0^4(2c_i + c_{i0})/\omega_1 + (6e_i s_0 + 5s_0 e_{i0} + 6s_1 c_i + 5s_1 c_{i0} + 6s_2 a_i)/\omega_1 - (s_0\omega_3 c_{i0})/\omega_1^2]/6\ . \qquad (2.4.35)$$

We can now construct the asymptotic forms of ϕ_{13} as $|x|\to 0$ which are given by

$$\phi_{13} = \delta^{\pm}_{13}/x + a^{\pm}_{13} + b^{\pm}_{130}\, x\ln|x| + b^{\pm}_{13}\, x + c^{\pm}_{130}\, x^2\ln|x| + c^{\pm}_{13}\, x^2 + d^{\pm}_{130}\, x^3\ln|x| + d^{\pm}_{13}\, x^3 + \ldots, \qquad (2.4.36)$$

where $\delta^{\pm}_{13}$, $a^{\pm}_{13}$,... are defined in terms of the real constants $\delta_{13}, a_{13}, \ldots, \delta_{23}, a_{23}, \ldots$ by the vector relation

$$\underline{v}_{13}^{\pm} = \sigma_1^{\pm} \underline{v}_{13} + \sigma_2^{\pm} \underline{v}_{23} \ , \tag{2.4.37}$$

where $\underline{v}_{13}^{\pm} = (\delta_{13}^{\pm}, \mp a_{13}^{\pm}, b_{130}^{\pm}, b_{13}^{\pm}, \mp c_{130}^{\pm}, \mp c_{13}^{\pm}, \ldots)$, $\underline{v}_{13} = (\delta_{13}, a_{13}, b_{130}, b_{13}, \ldots)$ and $\underline{v}_{23} = (\delta_{23}, a_{23}, b_{230}, b_{23}, \ldots)$.

The next step is to combine equations (2.4.10), (2.4.17), (2.4.27) and (2.4.36) in the overall solution (2.4.3), to obtain the general form of ϕ_1 as $|x| \to 0$. Thus

$$\phi_1 = \delta_1^{\pm}/x + a_1^{\pm} + b_{10}^{\pm} x\ln|x| + b_1^{\pm} x + c_{10}^{\pm} x^2\ln|x| + c_1^{\pm} x^2 + d_{10}^{\pm} x^3\ln|x| + d_1^{\pm} x^3 + \ldots, \quad x \to 0\pm, \tag{2.4.38}$$

where $\delta_1^{\pm}$, $a_1^{\pm}$, ...are defined by the vector relations

$$\underline{v}_1^{\pm} = \overline{\underline{v}}_1^{\pm} + 2\alpha_0^2 \underline{v}_{11}^{\pm} + \gamma_1 \underline{v}_{12}^{\pm} - \underline{v}_{13}^{\pm}/i\alpha_0 \ , \tag{2.4.39}$$

where

$$\underline{v}_1^{\pm} = (\delta_1^{\pm}, a_1^{\pm}, b_{10}^{\pm}, b_1^{\pm}, c_{10}^{\pm}, c_1^{\pm}, d_{10}^{\pm}, d_1^{\pm}, \ldots), \tag{2.4.40}$$

$$\overline{\underline{v}}_1^{\pm} = (0, \overline{a}_1^{\pm}, 0, \mp\overline{b}_1^{\pm}, \overline{c}_{10}^{\pm}, \overline{c}_1^{\pm}, 0, \mp\overline{d}_1^{\pm}, \ldots), \tag{2.4.41}$$

$$\underline{v}_{11}^{\pm} = (0, a_{11}^{\pm}, 0, \mp b_{11}^{\pm}, c_{110}^{\pm}, c_{11}^{\pm}, 0, \mp d_{11}^{\pm}, \ldots), \tag{2.4.42}$$

$$\underline{v}_{12}^{\pm} = (0, a_{12}^{\pm}, 0, \mp b_{12}^{\pm}, c_{120}^{\pm}, c_{12}^{\pm}, 0, \mp d_{12}^{\pm}, \ldots), \tag{2.4.43}$$

$$\underline{v}_{13}^{\pm} = (\delta_{13}^{\pm}, \mp a_{13}^{\pm}, b_{13}^{\pm}, b_{130}^{\pm}, \mp c_{130}^{\pm}, \mp c_{13}^{\pm}, d_{130}^{\pm}, d_{13}^{\pm}, \ldots) \tag{2.4.44}$$

and where $\overline{\underline{v}}_1^{\pm}$, $\underline{v}_{11}^{\pm}$ and $\underline{v}_{12}^{\pm}$ are extensions of the vectors defined in (2.4.11), (2.4.18) and (2.4.28). We now have a complete asymptotic form for the solution ϕ_1 as $|x| \to 0$.

The corresponding form of θ_1 is now obtained from equation (2.2.13), leading to the result

$$\theta_1 = \Delta_1^{\pm}/x^4 + A_1^{\pm}/x^2 + B_1^{\pm}/x + C_{10}^{\pm} \ln|x| + C_1^{\pm} + \ldots, x \to 0\pm, \quad (2.4.45)$$

where the constants $\Delta_1^{\pm}$,....., $C_1^{\pm}$ are given by

$$\Delta_1^{\pm} = -2A_0^{\pm}\nu_1/i\alpha_0 \ , \quad (2.4.46)$$

$$A_1^{\pm} = \delta_1^{\pm}s_0 - (\nu_1 C_{00}^{\pm} + 2\nu_2 A_0^{\pm})/i\alpha_0 \quad (2.4.47)$$

$$B_1^{\pm} = s_0 a_1^{\pm} + \gamma_1(r_0 a_0^{\pm} - q_0 A_0^{\pm}) - (2\nu_1 D_0^{\pm} + 4\gamma_0\nu_1 b_0^{\pm})/i\alpha_0, \quad (2.4.48)$$

$$C_{10}^{\pm} = s_0 b_{10}^{\pm} - (8\gamma_0^4 \nu_1 c_{00}^{\pm} + 6\nu_1 E_{00}^{\pm})/i\alpha_0 \quad (2.4.49)$$

$$C_1^{\pm} = (s_0 b_1^{\pm} + s_1\delta_1^{\pm}) + \gamma_1(r_0 b_0^{\pm} - q_0 B_0^{\pm}) - [\nu_2 C_{00}^{\pm} + 2\nu_3 A_0^{\pm} + \nu_1(5E_{00}^{\pm} + 6E_0^{\pm}) + 4\gamma_0^4 \nu_1(2c_0^{\pm} + c_{00}^{\pm})]/i\alpha_0. \quad (2.4.50)$$

and

$$\nu_1 = 1/\omega_1, \qquad \nu_2 = -\omega_3/\omega_1, \qquad \nu_3 = \omega_3^2 - \omega_1\omega_5/\omega_1^3 \ . \quad (2.4.51)$$

The values of ν_1, ν_2, and ν_3 are given in Table 2.3.

The above asymptotic solutions for ϕ_1 and θ_1, defined by equations (2.4.38) and (2.4.45) respectively, represent the forms of the second order terms in the outer solution of the stability equations as $|x| \to 0$. The next step is to combine the results for ϕ_0, ϕ_1 and θ_0, θ_1, as given by (2.3.12), (2.4.38) and (2.3.14), (2.4.45) respectively, and to write down the overall asymptotic forms of the perturbation functions ϕ and θ as $|x| \to 0$. This is described in the next section.

2.5 Summary

Using equation (2.2.9), we can write the overall asymptotic forms of ϕ as $x \to 0\pm$:

$$\phi = a_0^{\pm} + b_0^{\pm}x + c_{00}^{\pm}\, x^2 \ln|x| + c_0^{\pm}x^2 + d_0^{\pm}x^3 + e_{00}^{\pm}\, x^4 \ln|x| + e_0^{\pm}x^4 + g_0^{\pm}x^5 + h_{00}^{\pm}\, x^6 \ln|x| + h_0^{\pm}x^6 + \cdots + A^{-2/3}(\delta_1^{\pm}/x + a_1^{\pm} + b_{10}^{\pm}x\ln|x| + b_1^{\pm}x + c_{10}^{\pm}x^2\ln|x| + c_1^{\pm}x^2 + d_{10}^{\pm}x^3\ln|x| + d_1^{\pm}x^3 + \ldots) + \ldots \quad (2.5.1)$$

Likewise the asymptotic forms of θ as $x \to 0\pm$ are

$$\theta = A_0^{\pm}/x + B_0^{\pm} + C_{00}^{\pm}\, x\ln|x| + C_0^{\pm}x + D_0^{\pm}\, x^2 + E_{00}^{\pm}\, x^3\ln|x| + E_0^{\pm}\, x^3 + \ldots + A^{-2/3}(\Delta_1^{\pm}/x^4 + A_1^{\pm}/x^2 + B_1^{\pm}/x^2 + C_{10}^{\pm}\ln|x| + C_1^{\pm} + \ldots) \quad (2.5.2)$$

The above forms of ϕ and θ, represent the complete asymptotic behaviour of the outer solution as $x \to 0\pm$. Since these forms are singular, the need for a critical layer in the neighbourhood of $x = 0$ is evident, wherein it is expected that the thermal gradient term $\theta''(x)$ will become significant. Thus we need to write the above asymptotic forms of ϕ and θ in terms of an appropriate inner variable, which will allow the outer solution to be matched with corresponding inner solutions for ϕ and θ in the critical layer. Consideration of the critical layer solution will lead to the derivation of bridging conditions needed to complete the determination of the remaining unknown parameters in the outer solution and to determine the form of the neutral stability curve near γ_0. The inner forms of ϕ and θ are discussed in the next chapter.

i	μ_i	ω_i
0	-0.27267	0.00000
1	0.00000	-0.00339
2	10.65360	0.00000
3	0.00000	-0.04544
4	71.51070	0.00000
5	0.00000	0.17756
6	-186.27000	0.00000
7	0.00000	0.34053
8	-267.92400	0.00000
9	0.00000	-0.36958
10	232.62700	0.00000
11	0.00000	0.27063
12	141.95300	0.00000
13	0.00000	0.13556
14	-60.94880	0.00000
15	0.00000	0.05120
16	-20.45560	0.00000
17	0.00000	-0.01494
18	5.22375	0.00000
19	0.00000	-0.00352
20	1.10728	0.00000

TABLE 2.1. Values of the real constants μ_i and ω_i (i=0,..,20).

i	$\tilde{\mu}_i$	$\tilde{\omega}_i$
0	-0.04129	0.00000
1	0.00000	0.00396
2	-5.69997	0.00000
3	0.00000	-0.00687
4	56.22620	0.00000
5	0.00000	-0.09500
6	-18.63890	0.00000
7	0.00000	0.26774
8	-380.81500	0.00000
9	0.00000	-0.03698
10	171.01800	0.00000
11	0.00000	-0.38466
12	291.91900	0.00000
13	0.00000	0.09966
14	-83.51520	0.00000
15	0.00000	0.10693
16	-55.05700	0.00000
17	0.00000	-0.02047
18	10.47540	0.00000
19	0.00000	-0.00947
20	3.6835	0.00000

TABLE 2.2. Values of the real constants $\tilde{\mu}_i$ and $\tilde{\omega}_i$ (i=0,..,20).

s_0	80.54847	s_1	-4228.50775
s_2	39866.68584		
ν_1	-295.40954	ν_2	3965.79800
ν_3	37744.78737		
q_0	-1.17012	q_1	29.13334
r_0	12.17643	r_1	1520.35936

TABLE 2.3. Values of the real constants s_i, ν_i, (i = 0,1,2), q_i and r_i .

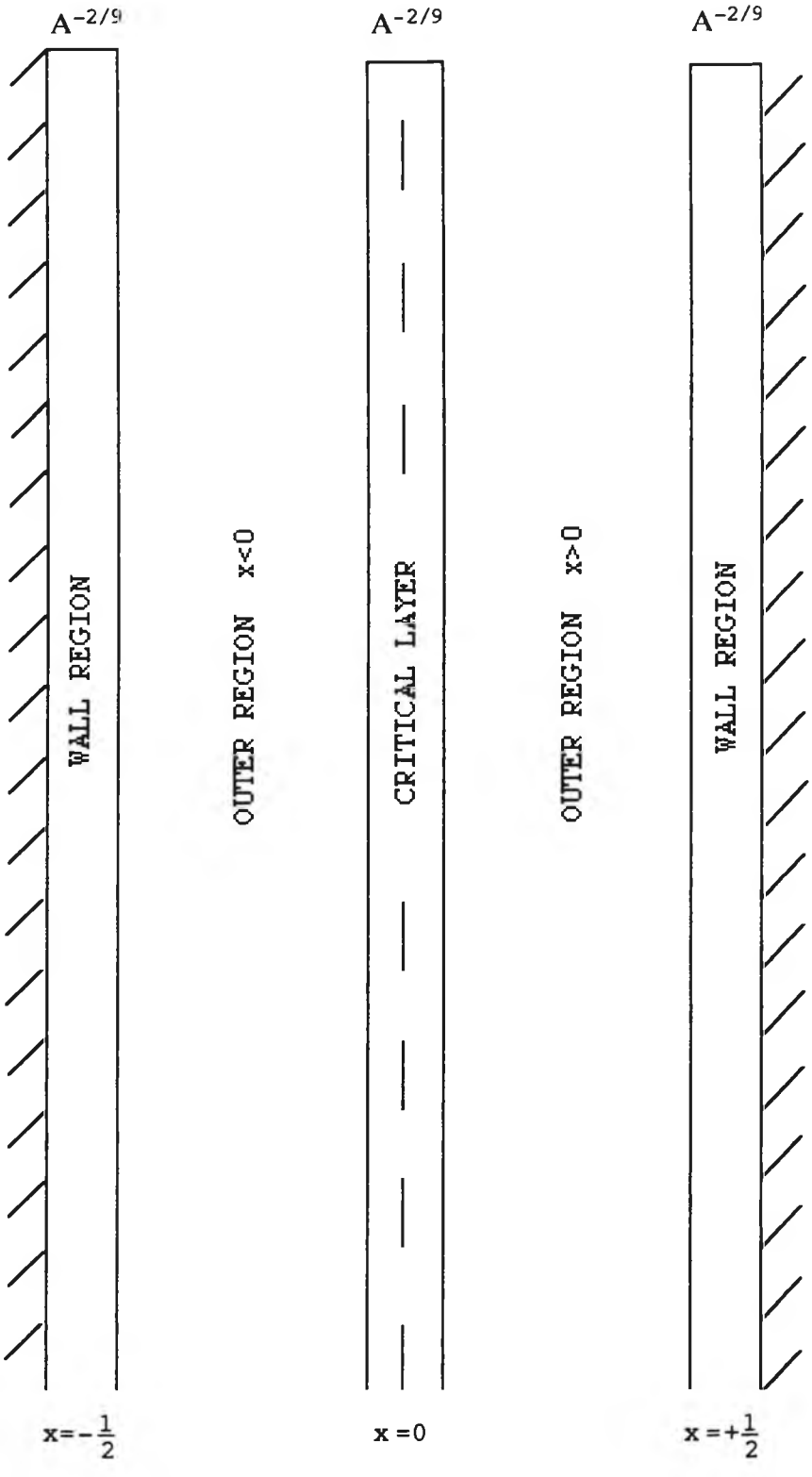

FIGURE 2.1. Schematic diagram of the asymptotic structure of the flow in the limit $A \to \infty$.

CHAPTER THREE : CRITICAL LAYER SOLUTION

3.1 Introduction

The inner forms of the outer solutions for ϕ and θ as $|x| \to 0$, obtained in Chapter 2, are now written in terms of an appropriate inner variable ξ, where $x = A^{-2/9}\xi$. This inner region is a thermal critical layer and the forms of ϕ and θ obtained in Section 3.2 determine the asymptotic expansion of the critical layer solution. Consideration of the critical layer solution leads to the determination of two sets of bridging conditions associated with the outer solutions for ϕ_0 and ϕ_1 respectively. These bridging conditions are derived in Section 3.3 for the leading order solution, and in Section 3.4 for the second order solution. In Section 3.5 the validity of the outer solution in the neighbourhood of each vertical plane $x = \pm 1/2$, is considered. It is found that inner regions of lateral extent order $A^{-2/9}$ are also relevant there, although these have no significant influence on the instability. It is shown in Section 3.6 that these inner regions allow the necessary adjustment of the solution to the full boundary conditions at the vertical planes. The bridging conditions obtained in Sections 3.3 and 3.4 lead firstly to the determination of γ_0 and secondly to the determination of γ_1 as a function of α_0. The latter result constitutes the neutral stability curve and allows the critical wavelength of the disturbance to be found following appropriate numerical calculations to be undertaken in Chapter 4. The form of the neutral stability curve is derived in Section 3.7.

3.2 Critical Layer

This section is concerned with setting up the appropriate expansions for the perturbation functions ϕ and θ within a critical layer along the centre-line, x=0, of the vertical planes. Initially this involves writing the limiting form of the outer solution for small x, given in Chapter 2, in terms of a new variable, ξ, which it is appropriate to use for the inner solution within the critical layer. This variable is chosen so that, within the critical layer, the thermal gradient term θ'' becomes significant, from which it follows that ξ should be defined by

$$x = A^{-2/9}\xi \ . \qquad (3.2.1)$$

The inner limit of the outer solution (2.5.1)and (2.5.2) may now be expressed in terms of ξ as follows. For the stream function

$$\begin{aligned}\phi \ = & \ a_0^{\pm} + A^{-2/9} b_0^{\pm}\xi - \frac{2}{9}A^{-4/9}\ln A\, c_{00}^{\pm}\xi^2 + A^{-4/9}[(c_{00}^{\pm}\ln|\xi| + c_0^{\pm})\xi^2 + \\ & \delta_1^{\pm}\xi^{-1}] + A^{-6/9}(d_0^{\pm}\xi^3 + a_1^{\pm}) - \frac{2}{9}A^{-8/9}\ln A\,(e_{00}^{\pm}\xi^4 + b_{10}^{\pm}\xi) + \\ & A^{-8/9}[(e_{00}^{\pm}\ln|\xi| + e_0^{\pm})\xi^4 + (b_{10}^{\pm}\ln|\xi| + b_1^{\pm})\xi] - \frac{2}{9}A^{-10/9}\ln A\, c_{10}^{\pm}\xi^2 + \\ & A^{-10/9}[g_0^{\pm}\xi^5 + (c_{10}^{\pm}\ln|\xi| + c_1^{\pm})\xi^2] - \frac{2}{9}A^{-12/9}\ln A(h_{00}^{\pm}\xi^6 + d_{10}\xi^3) + \\ & A^{-12/9}[(h_0^{\pm} + h_{00}^{\pm}\ln|\xi|)\xi^6 + (d_{10}^{\pm}\ln|\xi| + d_1^{\pm})\xi^3] + \ldots \ , \qquad (3.2.2)\end{aligned}$$

and for the temperature

$$\begin{aligned}\theta \ = & \ A^{2/9}(A_0^{\pm}\xi^{-1} + \Delta_1^{\pm}\xi^{-4}) + B_0^{\pm} - \frac{2}{9}A^{-2/9}\ln A\, C_{00}^{\pm}\xi + A^{-2/9}[(C_{00}^{\pm}\ln|\xi| + \\ & B_0^{\pm})\xi + c_1^{\pm}\xi^{-2}] + A^{-4/9}(D_0^{\pm}\xi^2 + B_1^{\pm}\xi^{-1}) - \frac{2}{9}A^{-6/9}\ln A\,(E_{00}^{\pm}\xi^3 + C_{10}^{\pm}) + \\ & A^{-6/9}[(E_{00}^{\pm}\ln|\xi| + E_0^{\pm})\xi^3 + C_{10}^{\pm}\ln|\xi| + C_1^{\pm}] + \ldots \ . \qquad (3.2.3)\end{aligned}$$

These forms now suggest that within the critical layer the

solutions for ϕ and θ should be expanded in the forms

$$\phi = \tilde{\phi}_0 + A^{-2/9}\tilde{\phi}_1 + A^{-4/9}\ln A\,\tilde{\phi}_{20} + A^{-4/9}\tilde{\phi}_2 + A^{-6/9}\tilde{\phi}_3 + A^{-8/9}\ln A\,\tilde{\phi}_{40} + A^{-8/9}\tilde{\phi}_4 + A^{-10/9}\ln A\,\tilde{\phi}_{50} + A^{-10/9}\tilde{\phi}_5 + A^{-12/9}\ln A\,\tilde{\phi}_{60} + A^{-12/9}\tilde{\phi}_6 + \ldots, \quad A\to\infty, \tag{3.2.4}$$

$$\theta = A^{2/9}\,\tilde{\theta}_0 + \tilde{\theta}_1 + A^{-2/9}\ln A\,\tilde{\theta}_{20} + A^{-2/9}\tilde{\theta}_2 + A^{-4/9}\tilde{\theta}_3 + A^{-6/9}\ln A\,\tilde{\theta}_{40} + A^{-6/9}\tilde{\theta}_4 + A^{-8/9}\ln A\,\tilde{\theta}_{50} + A^{-8/9}\tilde{\theta}_5 + A^{-10/9}\ln A\,\tilde{\theta}_{60} + A^{-10/9}\tilde{\theta}_6 + \ldots, \quad A\to\infty, \tag{3.2.5}$$

where $\tilde{\phi}_i, \tilde{\theta}_i$ (i=0,1,2,...) and $\tilde{\phi}_{i0}, \tilde{\theta}_{i0}$ (i=2,4,5,...)are functions of the inner variable ξ.

We shall also require the forms of the base functions $\partial\Psi/\partial x$ and $\partial\Theta/\partial x$ within the critical layer. From (1.2.19) and (1.2.20) the relevant expansions are

$$\partial\Theta/\partial x = \mu_0 + A^{-4/9}\mu_2\xi^2 + A^{-6/9}\bar{\mu}_0\gamma_1 + A^{-8/9}\mu_4\xi^4 + \ldots, A\to\infty, \tag{3.2.6}$$

$$\partial\Psi/\partial x = A^{-2/9}\omega_1\xi + A^{-6/9}\omega_3\xi^3 + A^{-8/9}\bar{\omega}_1\gamma_1\xi + \ldots, A\to\infty, \tag{3.2.7}$$

where the coefficients are those given in Tables 2.1 and 2.2. We are now in a position to proceed to find the inner solution in the critical layer and hence obtain the appropriate bridging conditions for the outer solution across the line x=0.

3.3 Leading Order Bridging Conditions

In this section, we begin the process of finding the critical layer solution by substituting the forms of $\partial\Theta/\partial x$ and $\partial\Psi/\partial x$, defined by (3.2.6)and (3.2.7), and the forms of ϕ and θ,

defined by (3.2.4) and (3.2.5), into equations (2.2.2) and (2.2.3) and balancing terms of like powers of A.

Thus from terms of order $A^{8/9}$ we find the equation for $\tilde{\phi}_0$ is given by

$$\tilde{\phi}_0^{iv} = 0, \tag{3.3.1}$$

from which it follows that

$$\tilde{\phi}_0 = \tilde{a}_0 + \tilde{b}_0 \xi + \tilde{c}_0 \xi^2 + \tilde{d}_0 \xi^3. \tag{3.3.2}$$

From (3.2.2) the boundary conditions for $\tilde{\phi}_0$ are

$$\tilde{\phi}_0 \to a^{\pm}_0 \quad \text{as } \xi \to \pm\infty, \tag{3.3.3}$$

and it follows that $\tilde{a}_0 = a^{\pm}_0$ and $\tilde{b}_0 = \tilde{c}_0 = \tilde{d}_0 = 0$. Thus the first bridging condition across the critical layer is

$$a^{+}_0 = a^{-}_0 \tag{3.3.4}$$

and the solution for $\tilde{\phi}_0$ is simply

$$\tilde{\phi}_0 = a^{+}_0 . \tag{3.3.5}$$

Similarly, from terms of order $A^{6/9}$ the equation for $\tilde{\phi}_1$ is found to be

$$\tilde{\phi}_1^{iv} = 0, \tag{3.3.6}$$

with solution

$$\tilde{\phi}_1 = \tilde{a}_1 + \tilde{b}_1 \xi + \tilde{c}_1 \xi^2 + \tilde{d}_1 \xi^3 . \tag{3.3.7}$$

From (3.2.2) the boundary conditions are

$$\tilde{\phi}_1 \sim b_0^{\pm}\,\xi + 0 \quad \text{as } \xi \to \pm\infty \tag{3.3.8}$$

and it follows that $\tilde{b}_1 = b_0^{\pm}$ and $\tilde{a}_1 = \tilde{c}_1 = \tilde{d}_1 = 0$. Thus the second bridging condition across the critical layer is

$$b_0^{+} = b_0^{-} \tag{3.3.9}$$

and the solution for $\tilde{\phi}_1$ is

$$\tilde{\phi}_1 = b_0^{+}\,\xi\,. \tag{3.3.10}$$

From terms of order $A^{4/9}\ln A$, the equation for $\tilde{\phi}_{20}$ is found to be

$$\tilde{\phi}_{20}^{\,iv} = 0, \tag{3.3.11}$$

with solution

$$\tilde{\phi}_{20} = \tilde{a}_{20} + \tilde{b}_{20}\,\xi + \tilde{c}_{20}\,\xi^2 + \tilde{d}_{20}\,\xi^3 \tag{3.3.12}$$

and since the boundary conditions are, from (3.2.2),

$$\tilde{\phi}_{20} \sim -\frac{2}{9}c_{00}^{\pm}\,\xi^2 + 0.\xi + 0 \text{ as } \xi \to \pm\infty, \tag{3.3.13}$$

we have $\tilde{a}_{20} = \tilde{b}_{20} = \tilde{d}_{20} = 0$ and

$$\tilde{\phi}_{20} = \tilde{c}_{20}\,\xi^2 \text{ with } \tilde{c}_{20} = -\frac{2}{9}c_{00}^{\pm}, \tag{3.3.14}$$

This result requires $c_{00}^{+} = c_{00}^{-}$ but this is the case since, from (2.3.10) and (2.3.13), $c_{00}^{\pm} = a_0^{\pm}s_0/2$ and $a_0^{+} = a_0^{-}$ by (3.3.4).

From terms of order $A^{4/9}$, $\tilde{\phi}_2$ is found to satisfy the equation

$$\tilde{\phi}_2^{\,iv} = \tilde{\theta}_0', \tag{3.3.15}$$

where $\tilde{\theta}_0$ is the leading term in the temperature field, to be considered below (see(3.3.24)). From (3.2.2) the boundary conditions for $\tilde{\phi}_2$ are,

$$\tilde{\phi}_2 \sim c_{00}^{\pm}\, \xi^2 \ln|\xi| + c_0^{\pm}\, \xi^2 + \delta_1^{\pm}\, \xi^{-1} \quad \text{as } \xi \to \pm\infty. \tag{3.3.16}$$

Further equations and boundary conditions for $\tilde{\phi}_3, \ldots, \tilde{\phi}_6$ are obtained in succession as follows:

$$\left.\begin{aligned} &\tilde{\phi}_3^{\,iv} = \tilde{\theta}_1', \\ &\tilde{\phi}_3 \sim d_0^{\pm}\, \xi^3 + a_1^{\pm}, \quad \xi \to \pm\infty \end{aligned}\right\} \tag{3.3.17}$$

$$\left.\begin{aligned} &\tilde{\phi}_{40}^{\,iv} = \tilde{\theta}_{20}' \\ &\tilde{\phi}_{40} \sim -\tfrac{2}{9} e_{00}^{\pm}\, \xi^4 - \tfrac{2}{9} b_{10}^{\pm}\, \xi, \quad \xi \to \pm\infty \end{aligned}\right\} \tag{3.3.18}$$

$$\left.\begin{aligned} &\tilde{\phi}_4^{\,iv} = \tilde{\theta}_2', \\ &\tilde{\phi}_4 \sim e_{00}^{\pm}\, \xi^4 \ln|\xi| + e_0^{\pm}\, \xi^4 + b_{10}^{\pm}\, \xi \ln|\xi| + b_1^{\pm}\, \xi, \quad \xi \to \pm\infty \end{aligned}\right\} \tag{3.3.19}$$

$$\left.\begin{aligned} &\tilde{\phi}_{50}^{\,iv} = 0, \\ &\tilde{\phi}_{50} \sim -\tfrac{2}{9} c_{10}^{\pm}\, \xi^2, \quad \xi \to \pm\infty \end{aligned}\right\} \tag{3.3.20}$$

$$\left.\begin{aligned} &\tilde{\phi}_5^{\,iv} = \tilde{\theta}_3', \\ &\tilde{\phi}_5 \sim g_0^{\pm}\, \xi^5 + c_{10}^{\pm}\, \xi^2 \ln|\xi| + c_1^{\pm}\, \xi^2, \quad \xi \to \pm\infty \end{aligned}\right\} \tag{3.3.21}$$

$$\left.\begin{aligned} &\tilde{\phi}_{60}^{iv} = \tilde{\theta}_{40}' , \\ &\tilde{\phi}_{60} \sim -\frac{2}{9} h_{00}^{\pm} \xi^6 - \frac{2}{9} d_{10}^{\pm} \xi^3 , \ \xi \to \pm\infty \end{aligned}\right\} \qquad (3.3.22)$$

$$\left.\begin{aligned} &\tilde{\phi}_6^{iv} = \tilde{\theta}_4' , \\ &\tilde{\phi}_6 \sim h_{00}^{\pm} \xi^6 \ln|\xi| + h_0^{\pm} \xi^6 + d_{10}^{\pm} \xi^3 \ln|\xi| + d_1^{\pm} \xi^3 , \ \xi \to \pm\infty . \end{aligned}\right\} \qquad (3.3.23)$$

In (3.3.21) and (3.3.23) we have used the fact that $\tilde{\phi}_0'' = \tilde{\phi}_1'' = 0$ in order to simplify the equations.

Equations for the unknown temperature functions $\tilde{\theta}_0, \ldots \tilde{\theta}_4$ are obtained by substituting the form of θ, as defined by (3.2.5), along with (3.2.6) and (3.2.7) into equation (2.2.3). At order $A^{6/9}$ this leads to the following equation for $\tilde{\theta}_0$:

$$\tilde{\theta}_0'' + i\alpha_0\omega_1 \xi \tilde{\theta}_0 = i\alpha_0 \mu_0 \tilde{\phi}_0 , \qquad (3.3.24)$$

and from (3.2.3) the relevant boundary conditions are

$$\tilde{\theta}_0 \sim A_0^{\pm} \xi^{-1} + \Delta_1^{\pm} \xi^{-4} , \quad \xi \to \pm\infty , \qquad (3.3.25)$$

where $A_0^+ = A_0^- = s_0 a_0^+$. This system can be expressed in the form

$$\hat{\theta}_0'' - i\hat{\xi}\,\hat{\theta}_0 = -i , \qquad \hat{\theta}_0 \sim \hat{\xi}^{-1} , \ (\hat{\xi} \to \pm\infty), \qquad (3.3.26)$$

by making the transformations

$$\xi = (-\alpha_0\omega_1)^{1/3} \hat{\xi}, \qquad \tilde{\theta} = -\alpha_0\mu_0 a_0^+ (-\alpha_0\omega_1)^{-2/3} \hat{\theta}_0(\hat{\xi}) \qquad (3.3.27)$$

and using the fact that $\tilde{\phi}_0 = a_0^+$ in the right-hand side of (3.3.24). Consider now the modified system

$$\hat{\theta}_0'' - i\hat{\xi}\,\hat{\theta}_0 = -ie^{-\varepsilon|\hat{\xi}|}, \quad \hat{\theta}_0 \to 0 \text{ as } |\hat{\xi}| \to \infty \tag{3.3.28}$$

and let $\bar{\theta}_0(p)$ denote the Fourier transform of $\hat{\theta}_0$, so that

$$\hat{\theta}_0 = (1/2\pi) \int_{-\infty}^{\infty} \bar{\theta}_0 e^{-ip\hat{\xi}}\, dp, \quad \bar{\theta}_0(0) = \int_{-\infty}^{\infty} \hat{\theta}_0\, d\hat{\xi}. \tag{3.3.29}$$

Taking the Fourier transform of (3.3.28) gives

$$d\bar{\theta}_0/dp + p^2\bar{\theta}_0 = 2i\varepsilon/(p^2+\varepsilon^2) \tag{3.3.30}$$

and the solution for $\bar{\theta}_0$ obtained by multiplying (3.3.30) by a suitable integrating factor, is

$$\bar{\theta}_0 = 2i\varepsilon\, e^{-p^3/3} \int_{-\infty}^{p} (e^{p^3/3}/(p^2+\varepsilon^2))dp. \tag{3.3.31}$$

Consideration of the solution for $\bar{\theta}_0$ in (3.3.31),in the limit as $\varepsilon \to 0$, leads to the result

$$\bar{\theta}_0(0) = i\pi \tag{3.3.32}$$

and hence

$$\int_{-\infty}^{\infty} \tilde{\theta}_0\, d\xi = i\pi\mu_0 a_0^+/\omega_1 . \tag{3.3.33}$$

Returning to the solution for $\tilde{\phi}_2$, equation (3.3.15) may be integrated once to give $\tilde{\phi}_2''' = \tilde{\theta}_0$ and it follows from (3.3.24) that

$$\tilde{\phi}_2^{v} + i\alpha_0\omega_1\xi\tilde{\phi}_2''' = i\alpha_0\mu_0 a_0^+ . \tag{3.3.34}$$

Two integrations give the third order equation

$$\tilde{\phi}_2''' + i\alpha_0\omega_1\xi\tilde{\phi}_2' - 2i\alpha_0\omega_1\tilde{\phi}_2 = i\alpha_0\mu_0 a_0^+\xi^2/2 + M_1\xi + M_2, \tag{3.3.35}$$

where M_1 and M_2 are arbitrary constants whose values are

determined from the boundary conditions (3.3.16) as $M_1 = M_2 = 0$. It is expected that a solution of this equation for $\tilde{\phi}_2$ can now be found consistent with the boundary conditions (3.3.16) provided the constants $c_0^{\pm}$ satisfy a certain relation. This can be found by noting that

$$\tilde{\phi}_2'' = \int_0^{\xi} \tilde{\theta}_0 \, d\xi + \tilde{k}_2 \ , \tag{3.3.36}$$

where $\tilde{k}_2$ is a constant corresponding to one of the complementary solutions, $\tilde{k}_2\xi^2/2$, of (3.3.35). Letting $\xi \to \pm\infty$, it follows that

$$\lim_{\Delta\to\infty} \left[\tilde{\phi}_2''(\Delta) - \tilde{\phi}_2''(-\Delta) \right] = \int_{-\infty}^{\infty} \tilde{\theta}_0 \, d\xi \ , \tag{3.3.37}$$

giving

$$c_0^+ - c_0^- = (1/2) \int_{-\infty}^{\infty} \tilde{\theta}_0 \, d\xi . \tag{3.3.38}$$

The integral on the right-hand side was evaluated in (3.3.33) and gives the result

$$c_0^+ = c_0^- + i\mu_0 \pi a_0^+ / 2\omega_1 , \tag{3.3.39}$$

which represents the third bridging condition across the critical layer.

At order $A^{4/9}$ the equation for $\tilde{\theta}_1$ is determined as

$$\tilde{\theta}_1'' + i\alpha_0 \omega_1 \xi \tilde{\theta}_1 = i\alpha_0 \mu_0 b_0^+ \xi \tag{3.3.40}$$

and, from (3.2.3), the boundary conditions are

$$\tilde{\theta}_1 \sim \mu_0 b_0^{\pm} / \omega_1 , \quad \xi \to \pm\infty \ . \tag{3.3.41}$$

Here the solution $\tilde{\phi}_1 = b_0^+ \xi$ has been used on the right-hand side

of (3.3.40) and it should be recalled that $b_0^+ = b_0^-$. Thus by inspection

$$\tilde{\theta}_1 = \mu_0 b_0^+/\omega_1 \tag{3.3.42}$$

is the required solution. Returning to the equation for $\tilde{\phi}_3$, since $\tilde{\phi}_3^{iv} = \tilde{\theta}_1' = 0$, it follows that

$$\tilde{\phi}_3 = \tilde{a}_3 + \tilde{b}_3 \xi + \tilde{c}_3 \xi^2 + \tilde{d}_3 \xi^3 \tag{3.3.43}$$

and from the boundary conditions (3.3.17) it follows that $\tilde{b}_3 = \tilde{c}_3 = 0$ and $\tilde{a}_3 = a_1^{\pm}$, $\tilde{d}_3 = d_0^{\pm}$. Thus

$$d_0^+ = d_0^- , \tag{3.3.44}$$

$$a_1^+ = a_1^- \tag{3.3.45}$$

and the solution for $\tilde{\phi}_3$ is

$$\tilde{\phi}_3 = d_0^+ \xi^3 + a_1^+ . \tag{3.3.46}$$

Equation (3.3.44) represents the fourth bridging condition across the critical layer for the outer solution ϕ_0.

At this stage of the analysis we have four bridging conditions across the critical layer for the outer solution ϕ_0. These are summarized as follows:

$$a_0^+ = a_0^-, \tag{3.3.47}$$

$$b_0^+ = b_0^-, \tag{3.3.48}$$

$$c_0^+ = c_0^- + i\pi\mu_0 a_0^+/2\omega_1, \tag{3.3.49}$$

$$d_0^+ = d_0^- \ . \qquad (3.3.50)$$

Bridging conditions across the critical layer for the second order solution ϕ_1 are obtained in the next section.

3.4 Second Order Bridging Conditions

As explained in Section 3.3, in order to obtain the bridging conditions for ϕ_1 , we need to proceed with the determination of higher order terms in the critical layer solution. The equation and boundary conditions for $\tilde{\theta}_{20}$ are

$$\left.\begin{aligned} &\tilde{\theta}_{20}'' + i\alpha_0\omega_1\xi\tilde{\theta}_{20} = i\alpha_0\mu_0\tilde{\phi}_{20} \ , \\ &\tilde{\theta}_{20} \sim -\tfrac{2}{9}c_{00}^{\pm}\xi \ , \quad \xi\to\pm\infty \ , \end{aligned}\right\} \qquad (3.4.1)$$

where $\tilde{\phi}_{20} = -\frac{2}{9}c_{00}^{\pm}\xi^2$, and $C_{00}^+ = C_{00}^- = s_0c_{00}^+$. It is easily verified that the required solution is $\tilde{\theta}_{20} = -\frac{2}{9}s_0c_{00}^+\xi$. Since $\tilde{\phi}_{40}^{iv} = \tilde{\theta}_{20}'$, it follows from (3.3.18) that

$$\tilde{\phi}_{40}' = \tilde{b}_{40} + 4\tilde{e}_{40}\xi^3 \ , \qquad (3.4.2)$$

where $\tilde{b}_{40} = -\frac{2}{9}b_{10}^+ = -\frac{2}{9}b_{10}^-$ and $\tilde{e}_{40} = -\frac{2}{9}e_{00}^+ = -\frac{2}{9}e_{00}^-$, consistent with the fact that $e_{00}^+ = s_0c_{00}^+/24$.

The equation for $\tilde{\theta}_2$ is

$$\tilde{\theta}_2'' + i\alpha_0\omega_1\xi\tilde{\theta}_2 = R \qquad (3.4.3)$$

where

$$R = i\alpha_0(a_0^+ \mu_2 \xi^2 + \mu_0 \tilde{\phi}_2 - \omega_3 \xi^3 \tilde{\theta}_0) \qquad (3.4.4)$$

and from (3.2.3) the boundary conditions are

$$\tilde{\theta}_2 \sim C_{00}^{\pm} \xi \ln|\xi| + B_0^{\pm} \xi + c_1^{\pm}/\xi \quad \text{as} \quad \xi \to \pm\infty \ . \qquad (3.4.5)$$

Using the relation $\tilde{\phi}_4''' = \tilde{\theta}_2$ obtained from (3.3.19) one integration of equation (3.4.3) gives

$$\tilde{\phi}_4^{iv} + i\alpha_0 \omega_1 \xi \tilde{\phi}_4'' - i\alpha_0 \omega_1 \tilde{\phi}_4' = \int_0^{\xi} R\, d\xi + \tilde{k}_4 \ , \qquad (3.4.6)$$

where $\tilde{k}_4$ is an arbitrary constant. Now using the outer behaviours

$$\tilde{\phi}_4 \sim e_{00}^{\pm} \xi^4 \ln|\xi| + e_0^{\pm} \xi^4 + b_{10}^{\pm} \xi \ln|\xi| + b_1^{\pm} \xi \ , \ \xi \to \pm\infty , \qquad (3.4.7)$$

given by (3.3.19) and the fact that $e_0^+ - e_0^- = s_0(c_0^+ - c_0^-)/24$, substitution into (3.4.6) gives the following relation:

$$i\alpha_0\omega_1(b_1^+ - b_1^-) = \boldsymbol{F} \int_{-\Delta}^{\Delta} R\, d\xi + s_0(c_0^+ - c_0^-) \qquad (3.4.8)$$

where $\boldsymbol{F}$ denotes the finite part of the integral in the limit as $\Delta \to \infty$. The right-hand side of (3.4.8) involves non-zero contributions from integrals of the form

$$I_1 = \boldsymbol{F} \int_{-\Delta}^{\Delta} \tilde{\phi}_2 \, d\xi \qquad (3.4.9)$$

and

$$I_2 = \boldsymbol{F} \int_{-\Delta}^{\Delta} \xi^3 \tilde{\theta}_0 \, d\xi . \qquad (3.4.10)$$

These may be evaluated using integration by parts and making use of (3.3.16) to give

$$I_1 = 2(c_0^+ - c_0^-)/3i\alpha_0\omega_1 \qquad (3.4.11)$$

$$I_2 = -4(c_0^+ - c_0^-)/i\alpha_0\omega_1 \ . \qquad (3.4.12)$$

Substitution of these results into (3.4.8) with R given by (3.4.4) and making use of (3.3.49) then yields

$$b_1^+ - b_1^- = \mu_0\pi(\mu_0 - 12\omega_3)a_0^+/6\alpha_0\omega_1^3. \qquad (3.4.13)$$

The relation $a_1^+ = a_1^-$ obtained in (3.3.45) represents the first bridging condition across the critical layer for the outer solution ϕ_1, while equation (3.4.13) represents the second.

The second bridging condition for the outer solution ϕ_1 is now confirmed by an analytical solution for $\tilde{\theta}_2$ which can be obtained in the form

$$\tilde{\theta}_2 = \lambda_1\tilde{\phi}_2' + \lambda_2\xi\,\tilde{\phi}_2'' + \lambda_3\xi^2\,\tilde{\phi}_2''' + \lambda_4\xi^3\,\tilde{\phi}_2^{iv} + \lambda_5\xi \ . \qquad (3.4.14)$$

Substitution into (3.4.3) and a balancing of like terms requires that the constants λ_i are given by

$$\lambda_1 = -3\omega_3/7\omega_1 + \mu_0/2\omega_1 \ ; \quad \lambda_2 = 3\omega_3/7\omega_1 ; \quad \lambda_3 = -3\omega_3/14\omega_1$$

$$\lambda_4 = \omega_3/7\omega_1 ; \quad \lambda_5 = a_0^+\{-\mu_0^2/2 + 2\omega_1\mu_2 - 15\mu_0\omega_3/7\}/2\omega_1^2 \ . \qquad (3.4.15)$$

An exact solution for $\tilde{\phi}_4$ can now also be obtained by three integrations of the equation $\tilde{\phi}_4''' = \tilde{\theta}_2$ to yield

$$\tilde{\phi}_4 = \tilde{\lambda}_1\xi\tilde{\phi}_2'' + [\tilde{\lambda}_2 + \lambda_4\xi^3]\tilde{\phi}_2' + \tilde{\lambda}_3\xi^2\tilde{\phi}_2 + (\tilde{\lambda}_4 + \lambda_5)\xi^4 + \tilde{\beta}_1\xi^2/2 + \tilde{\beta}_2\xi + \tilde{\beta}_3 \qquad (3.4.16)$$

where in (3.4.16) we have used (3.3.35) to obtain expressions

for $\int \tilde{\phi}_2 \, d\xi$ and $\int\left(\int \tilde{\phi}_2 \, d\xi\right) d\xi$ and the constants $\tilde{\lambda}_i$ (i=1,...5) are given by

$$\tilde{\lambda}_1 = (7\mu_0 + 204\omega_3)/168i\alpha_0\omega_1^2; \qquad \tilde{\lambda}_2 = (7\mu_0 - 180\omega_3)/56i\alpha_0\omega_1^2;$$

$$\tilde{\lambda}_3 = (7\mu_0 - 48\omega_3)/168\omega_1; \qquad \tilde{\lambda}_4 = \mu_0 a^+_0(-49\mu_0 - 276\omega_3)/4032\omega_1^2 \tag{3.4.17}$$

where $\tilde{\beta}_1$, $\tilde{\beta}_2$ and $\tilde{\beta}_3$ are arbitrary constants of integration. Substitution of the appropriate forms of $\tilde{\phi}_2''$, $\tilde{\phi}_2'$ and $\tilde{\phi}_2$ as $\xi \to \pm\infty$ into (3.4.16) shows that the coefficients $b^{\pm}_1$ of the linear terms in ξ as $\xi \to \pm\infty$ are given by

$$b^{\pm}_1 = c^{\pm}_{00}(3\tilde{\lambda}_1 + \tilde{\lambda}_2) + 2c^{\pm}_0(\tilde{\lambda}_1 + \tilde{\lambda}_2) + \delta^{\pm}_1(\tilde{\lambda}_3 - \tilde{\lambda}_2) + \tilde{\beta}_2 \tag{3.4.18}$$

and this leads to the relation

$$b^+_1 - b^-_1 = 2(\tilde{\lambda}_1 + \tilde{\lambda}_2)(c^+_0 - c^-_0).$$

Substitution of $\tilde{\lambda}_1$ and $\tilde{\lambda}_2$ from (3.4.17) confirms the bridging condition

$$b^+_1 - b^-_1 = \mu_0\pi(\mu_0 - 12\omega_3)a^+_0/6\alpha_0\omega_1^3 \tag{3.4.19}$$

obtained in (3.4.13). Also the choice $\tilde{\beta}_1=0$ ensures that $\tilde{\phi}_4$ contains no quadratic term in ξ as $\xi \to \pm\infty$, as required by (3.4.7).

Given that $c^+_{10}=c^-_{10}$, the solution of (3.3.20) for $\tilde{\phi}_{50}$ is simply

$$\tilde{\phi}_{50} = -\frac{2}{9}c^+_{10}\xi^2 + \tilde{b}_{50}\xi + \tilde{a}_{50}, \tag{3.4.20}$$

where the values of $\tilde{a}_{50}$ and $\tilde{b}_{50}$ will not be required.

Next we consider the equation for $\tilde{\theta}_3$ which is determined at order one from substitution of (3.2.4), (3.2.5) and the relevant base flow expansions into (2.2.3):

$$\tilde{\theta}_3'' + i\alpha_0\omega_1\xi\tilde{\theta}_3 = i\alpha_0[\mu_0\gamma_1\tilde{\phi}_0 + \mu_2\xi^2\tilde{\phi}_1 + \mu_0\tilde{\phi}_3 - \omega_3\xi^3\tilde{\theta}_1 - \gamma_1\omega_1\xi\tilde{\theta}_0] - 4\gamma_0^4\tilde{\phi}_1'. \tag{3.4.21}$$

The boundary conditions obtained from (3.2.3) are

$$\tilde{\theta}_3 \sim D_0^{\pm}\xi^2 + B_1^{\pm}/\xi, \quad \xi \to \pm\infty, \tag{3.4.22}$$

where $D_0^+ = D_0^-$. The equation $\tilde{\phi}_5^{iv} = \tilde{\theta}_3'$ may be integrated twice to yield

$$\tilde{\phi}_5'' = \int_0^{\xi} \tilde{\theta}_3\, d\xi + \tilde{k}_5, \tag{3.4.23}$$

where $\tilde{k}_5$ is a constant of integration, and by considering the expression $(\phi_5'' - D_0^+\xi^3/3)(\pm\Delta)$, where Δ is a large value of ξ, we obtain

$$\lim_{\Delta\to\infty}[(\tilde{\phi}_5'' - D_0^+\xi^3/3)(\Delta) - (\tilde{\phi}_5'' - D_0^+\xi^3/3)(-\Delta)] = \int_{-\infty}^{\infty}(\tilde{\theta}_3 - D_0^+\xi^2)\, d\xi. \tag{3.4.24}$$

The boundary conditions for $\tilde{\phi}_5$ require that

$$\tilde{\phi}_5'' - D_0^+\xi^2/3 \sim 2c_{10}^{\pm}\ln|\xi| + (3c_{10}^{\pm} + 2c_1^{\pm}), \quad \xi \to \pm\infty \tag{3.4.25}$$

and since $c_{10}^+ = c_{10}^-$, we obtain

$$c_1^+ - c_1^- = \frac{1}{2}\int_{-\infty}^{\infty}(\tilde{\theta}_3 - D_0^+\xi^2)\, d\xi. \tag{3.4.26}$$

This relation represents the third bridging condition for ϕ_1 across the critical layer. Fortunately the precise form of the

integral on the right-hand side is not needed in the final analysis that leads to the equation of the neutral curve and so the value of the integral has not been calculated.

The equation for $\tilde{\theta}_{40}$, obtained by equating terms of order $A^{-6/9}\ln A$, is given by

$$\tilde{\theta}_{40}'' + i\alpha_0\omega_1\xi\tilde{\theta}_{40} = i\alpha_0[\mu_0\tilde{\phi}_{40} + \mu_2\xi^2\tilde{\phi}_{20} - \omega_3\xi^3\tilde{\theta}_{20}] - 4\gamma_0^4\tilde{\phi}_{20}. \qquad (3.4.27)$$

Substitution of $\tilde{\phi}_{40}$, $\tilde{\phi}_{20}$ and $\tilde{\theta}_{20}$ into the above equation gives

$$\tilde{\theta}_{40}'' + i\alpha_0\omega_1\xi\tilde{\theta}_{40} = \rho_1\xi^4 + \rho_2\xi, \qquad (3.4.28)$$

where

$$\rho_1 = i\alpha_0(\mu_0\tilde{e}_{40} + \mu_2\tilde{c}_{20} - \omega_3 s_0\tilde{c}_{20}), \quad \rho_2 = i\alpha_0(\mu_0\tilde{b}_{40} - 8\tilde{c}_{20}\gamma_0^4/i\alpha_0) \qquad (3.4.29)$$

and $\tilde{b}_{40}$ and $\tilde{e}_{40}$ are defined below (3.4.2). The required solution satisfying the outer behaviour

$$\tilde{\theta}_{40} \sim -\frac{2}{9}E_{00}^{\pm}\xi^3 - \frac{2}{9}C_{10}^{\pm}, \quad \xi\to\pm\infty \qquad (3.4.30)$$

is found by inspection as

$$\tilde{\theta}_{40} = (\rho_1\xi^3 + \rho_2 - 6\rho_1/i\alpha_0\omega_1)/i\alpha_0\omega_1 \qquad (3.4.31)$$

given that $E_{00}^{+} = E_{00}^{-}$ and since $\tilde{\phi}_{60}''' = \tilde{\theta}_{40}$ it follows that

$$\tilde{\phi}_{60} = \rho_1\xi^6/120i\alpha_0\omega_1 + (\rho_2 - 6\rho_1/i\alpha_0\omega_1)\xi^3/6i\alpha_0\omega_1 + \tilde{c}_{60}\xi^2 + \tilde{b}_{60}\xi + \tilde{a}_{60}, \qquad (3.4.32)$$

where $\tilde{a}_{60}$, $\tilde{b}_{60}$ and $\tilde{c}_{60}$ are constants of integration. This solution is consistent with the outer behaviour for $\tilde{\phi}_{60}$ defined by (3.3.22),

$$\tilde{\phi}_{60} \sim -\frac{2}{9}h^{\pm}_{00}\xi^6 - \frac{2}{9}d^{\pm}_{10}\xi^3, \quad \xi\to\pm\infty \ , \tag{3.4.33}$$

given that $h^{\pm}_{00} = (s_0^3 + 24s_0s_1)a^{\pm}_0/5760$ and that $d^{+}_{10} = d^{-}_{10}$.

The final bridging condition across the critical layer for the outer solution ϕ_1 is obtained by considering the equation $\tilde{\phi}_6''' = \tilde{\theta}_4 + \tilde{k}_6$, together with the outer forms

$$\tilde{\phi}_6''' \sim 120h^{\pm}_{00}\xi^3\ln|\xi| + (74h^{\pm}_{00} + 120h^{\pm}_0)\xi^3 + 6d^{\pm}_{10} + 6d^{\pm}_1, \ \xi\to\pm\infty, \tag{3.4.34}$$

$$\tilde{\theta}_4 \sim E^{\pm}_{00}\xi^3\ln|\xi| + E^{\pm}_0\xi^3 + C^{\pm}_{10}\ln|\xi| + C^{\pm}_1, \quad \xi\to\pm\infty \ , \tag{3.4.35}$$

defined by (3.2.2) and (3.2.3) respectively. This gives the relation $d^{+}_1 - d^{-}_1 = (C^{+}_1 - C^{-}_1)/6$, and substitution for $C^{+}_1 - C^{-}_1$ from (2.4.50) yields

$$d^{+}_1 - d^{-}_1 = \mu_0\pi a^{+}_0[s_0(\mu_0 - 12\omega_3)/6 - (4\gamma_0^4 + 3s_1 + s_0^2/8)\omega_1]/6\omega_1^3\alpha_0 \tag{3.4.36}$$

where s_0 is the constant defined in (2.3.11).

The four bridging conditions for the outer solution ϕ_1 are now summarized as follows:

$$a^{+}_1 = a^{-}_1 \ , \tag{3.4.37}$$

$$b^{+}_1 = b^{-}_1 + \mu_0\pi(\mu_0 - 12\omega_3)a^{+}_0/6\alpha_0\omega_1^3 \ , \tag{3.4.38}$$

$$c^{+}_1 = c^{-}_1 + \frac{1}{2}\int_{-\infty}^{\infty}(\tilde{\theta}_3 - D^{+}_0\xi^2)d\xi \ , \tag{3.4.39}$$

$$d^{+}_1 = d^{-}_1 + \mu_0\pi a^{+}_0[s_0(\mu_0 - 12\omega_3)/6 - (4\gamma_0^4 + 3s_1 + s_0^2/8)\omega_1]/6\omega_1^3\alpha_0 . \tag{3.4.40}$$

The critical layer enables the outer solutions in $-1/2<x<0$ and $0<x<1/2$ to be joined smoothly across the centre-line $x=0$

and the two sets of bridging conditions (3.3.47)-(3.3.50) and (3.4.37)-(3.4.40) will be used in Section 3.7 below to complete the outer solution, to determine γ_0 and to determine a relationship between α_0 and γ_1 equivalent to the local form of the neutral stability curve near γ_0. However, it is also important to confirm that the outer solution can adjust to the full boundary conditions at each vertical plane, and this entails consideration of further inner solutions in the neighbourhood of x=±1/2. These wall regions are considered in the next two sections.

3.5 Wall Region

This section is concerned with the validity of our solution of the stability equations near the walls x=±1/2. We first set out the form of the outer solution as x→-1/2, based on the assumptions made about the boundary conditions for the outer functions f_i, f_{ij} (i=1,2; j=1,2,3) and then consider the local solution of the linear stability equations

$$\phi'''' - 2\alpha^2\phi'' + \alpha^4\phi = \theta', \qquad (3.5.1)$$

$$\theta'' - \alpha^2\theta = i\alpha A(\Theta'\phi - \Psi'\theta) - 4\gamma^4\phi', \qquad (3.5.2)$$

$$\phi = \phi' = \theta = 0 \quad \text{at } x = \pm 1/2 \qquad (3.5.3)$$

in which

$$\alpha = A^{-1/3}\alpha_0, \quad A\to\infty, \qquad (3.5.4)$$

$$\gamma = \gamma_0 + A^{-2/3}\gamma_1 + \ldots, \quad A\to\infty. \qquad (3.5.5)$$

Near the wall the base flow functions

$$\Theta = \Theta_0 + \gamma_1 A^{-2/3} \Theta_1 + \ldots; \qquad \Psi = \Psi_0 + \gamma_1 A^{-2/3} \Psi_1 + \ldots, \tag{3.5.6}$$

may be expanded as follows. Let $X = x + 1/2$, so that $X = 0$ when $x = -1/2$. Using Taylor expansions about $X = 0$, we obtain

$$\Theta_0' = \sum_{i=0} \bar{\mu}_i X^i \quad , \; X \to 0 \; , \tag{3.5.7}$$

$$\Theta_1' = \sum_{i=0} \hat{\mu}_i X^i \quad , \; X \to 0 \; , \tag{3.5.8}$$

where $\bar{\mu}_i$, $\hat{\mu}_i$ $(i=0,1,2\ldots)$ are real constants; their numerical values, obtained from evaluating Θ_0' and Θ_1' using (1.2.19) are given in Table 3.1. Similarly, expansions for Ψ_0' and Ψ_1' are given by

$$\Psi_0' = \sum_{i=0} \bar{\omega}_i X^i, \qquad X \to 0, \tag{3.5.9}$$

$$\Psi_1' = \sum_{i=0} \hat{\omega}_i X^i, \qquad X \to 0, \tag{3.5.10}$$

where $\bar{\omega}_i$, $\hat{\omega}_i$ $(i=1,2\ldots)$, are real constants whose numerical values are given in Table 3.2.

The boundary conditions assumed for the outer functions f_i $(i=1,2)$ at $x = \pm 1/2$ are given by equations (2.3.4) and (2.3.5). Thus

$$f_1 = X^2/2 + \sum_{i=3} A_{1i} X^i, \qquad X \to 0, \tag{3.5.11}$$

$$f_2 = \sum_{i=3} A_{2i} X^i, \qquad X \to 0, \tag{3.5.12}$$

where A_{ji} $(j=1,2)$ are real constants whose formulae are given in Appendix I and whose values are given in Table 3.3. The solution for the leading order outer solution ϕ_0, in $x<0$, is

given by

$$\phi_0 = \bar{\sigma_1} f_1(x) + \bar{\sigma_2} f_2(x), \tag{3.5.13}$$

so that ϕ_0 has the form

$$\phi_0 = J_2 X^2 + J_3 X^3 + J_4 X^4 + J_5 X^5 + \ldots, \quad X \to 0, \tag{3.5.14}$$

where the constants $J_2, J_3, \ldots$ are given by

$$J_2 = \bar{\sigma_1}/2, \; J_i = \bar{\sigma_1} A_{1i} + \bar{\sigma_2} A_{2i}, \; (i=3,4\ldots). \tag{3.5.15}$$

Next we consider the behaviour of the functions f_{ij} $(i=1,2;$ $j=1,2,3)$, as $X \to 0$. The boundary conditions for the functions f_{ij} at $x=-1/2$ are given in (2.4.13), (2.4.15), (2.4.31) and (2.4.32) and it follows that as $X \to 0$

$$f_{11} = \sum_{i=3}^{\infty} B_{1i} X^i, \tag{3.5.16}$$

$$f_{21} = \sum_{i=3}^{\infty} B_{2i} X^i, \tag{3.5.17}$$

$$f_{12} = \sum_{i=3}^{\infty} C_{1i} X^i, \tag{3.5.18}$$

$$f_{22} = \sum_{i=3}^{\infty} C_{2i} X^i, \tag{3.5.19}$$

$$f_{13} = D_{120} X^2 \ln|X| + D_{13} X^3 + D_{140} X^4 \ln|X| + D_{14} X^4 + \ldots, \tag{3.5.20}$$

$$f_{23} = D_{220} X^2 \ln|X| + D_{23} X^3 + D_{240} X^4 \ln|X| + D_{24} X^4 + \ldots, \tag{3.5.21}$$

where B_{ji}, C_{ji} and D_{ji}, D_{ji0}, $(j=1,2)$ are real constants whose formulae are given in Appendix I and whose numerical values are given in Tables 3.4-3.5. The solution for ϕ_1 in $x<0$ is given by

$$\phi_1(x) = \bar{\sigma_1} f_1(x) + \bar{\sigma_2} f_2(x) + 2\alpha_0^2 [\bar{\sigma_1} f_{11}(x) + \bar{\sigma_2} f_{21}(x)] + \gamma_1 [\bar{\sigma_1} f_{12}(x) + \bar{\sigma_2} f_{22}(x)] - [\bar{\sigma_1} f_{13}(x) + \bar{\sigma_2} f_{23}(x)]/i\alpha_0 \tag{3.5.22}$$

and it therefore follows that

$$\phi_1 = K_{20} X^2 \ln|X| + K_2 X^2 + K_3 X^3 + K_{40} X^4 \ln|X| + \ldots, X \to 0, \quad (3.5.23)$$

where

$$K_{20} = -[\bar{\sigma_1} D_{120} + \bar{\sigma_2} D_{220}]/i\alpha_0, \qquad K_2 = \bar{\sigma_1}/2,$$

$$K_3 = \bar{\sigma_1} A_{13} + \bar{\sigma_2} A_{23} + 2\alpha_0^2 (\bar{\sigma_1} C_{13} + \bar{\sigma_2} C_{23}) + \gamma_1 (\bar{\sigma_1} B_{13} + \bar{\sigma_2} B_{23}) -$$
$$(\bar{\sigma_1} D_{13} + \bar{\sigma_2} D_{23})/i\alpha_0$$

$$K_{40} = -[\sigma_1 D_{140} + \sigma_2 D_{240}]/i\alpha_0 . \quad (3.5.24)$$

We may also deduce the forms of θ_0 and θ_1 as $X \to 0$ using relations (2.2.11) and (2.2.13). The leading order temperature field has the form

$$\theta_0 = R_1 X + R_2 X^2 + R_3 X^3 + \ldots, \qquad X \to 0, \quad (3.5.25)$$

where the real constants $R_1, R_2, \ldots$ are defined as

$$R_1 = J_2 \bar{\mu}_0 / \bar{\omega}_1 , \quad R_2 = J_3 \bar{\mu}_0 / \bar{\omega}_1 - J_2 \bar{\mu}_0 \bar{\omega}_2 / \bar{\omega}_1^2 ,$$

$$R_3 = (J_4 \bar{\mu}_0 + J_2 \bar{\mu}_2)/\bar{\omega}_1 - (J_3 \bar{\mu}_0 \bar{\omega}_2 + J_2 \bar{\mu}_0 \bar{\omega}_3)/\bar{\omega}_1^2 + J_2 \bar{\mu}_0 \bar{\omega}_2^2 / \bar{\omega}_1^3 . \quad (3.5.26)$$

Similarly, the second order temperature field θ_1 is given by

$$\theta_1 = T_0 X^{-1} + T_1 + T_{20} X \ln|X| + T_2 X + \ldots, \quad (3.5.27)$$

where

$$T_0 = 2(J_2 \bar{\mu}_0 \bar{\omega}_2 - J_3 \bar{\mu}_0 \bar{\omega}_1)/i\alpha_0 \bar{\omega}_1^3 ,$$

$$T_1 = [8\bar{\mu}_0(J_3\bar{\omega}_2 - J_2\bar{\omega}_2^2/\bar{\omega}_1) + 6J_2\bar{\mu}_0\bar{\omega}_3 - 6\bar{\omega}_1(J_4\bar{\mu}_0 + J_2\bar{\mu}_2) - 8J_2\gamma_0^4\bar{\omega}_1^2]/i\alpha_0\bar{\omega}_1^3,$$

$$T_{20} = \bar{\mu}_0 K_{20}/\bar{\omega}_1 . \qquad (3.5.28)$$

Combining the results (3.5.14), (3.5.23), (3.5.25) and (3.5.27) and recalling that in the outer region

$$\phi = \phi_0 + A^{-2/3}\phi_1 + \ldots, \qquad \theta = \theta_0 + A^{-2/3}\theta_1 + \ldots, \qquad (3.5.29)$$

it follows that as $X \to 0$ the overall solutions for the stream function and temperature perturbations have the form

$$\phi = J_2X^2 + J_3X^3 + \ldots + A^{-2/3}(K_{20}X^2\ln|X| + K_2X^2 + K_3X^3 + \ldots) + \ldots, \qquad (3.5.30)$$

$$\theta = R_1X + R_2X^2 + \ldots + A^{-2/3}(T_0X^{-1} + T_1 + T_{20}X\ln|X| + \ldots) + \ldots . \qquad (3.5.31)$$

These results represent the form of the outer solution as $X \to 0$ and it is clear that the wall conditions (3.5.3) are not satisfied in full by the outer solutions. An adjustment must occur in a region close to the wall and the solution there is considered in the next section.

3.6 Wall Region Solution

The singular behaviour evident in (3.5.31) and (3.5.30) is caused by the absence of the highest derivative θ'' in the outer approximation to the heat equation. Within the wall region this conduction term must come into play, requiring a local variation on the scale η defined by

$$X = A^{-2/9}\eta . \qquad (3.6.1)$$

Writing the inner limit (3.5.30) and (3.5.31) of the outer solution in terms of the variable η, it follows that as $\eta\to\infty$ the wall region solution must match with the form

$$\phi = A^{-4/9} J_2 \eta^2 + A^{-6/9} J_3 \eta^3 + A^{-8/9} J_4 \eta^4 - \frac{2}{9} A^{-10/9} \ln A \, K_{20} \eta^2 + A^{-10/9} (J_5 \eta^5 + K_{20} \eta^2 \ln\eta + K_2 \eta^2) + \ldots, \quad \eta\to\infty, \tag{3.6.2}$$

$$\theta = A^{-2/9} R_1 \eta + A^{-4/9} (R_2 \eta^2 + T_0/\eta) + A^{-6/9} (R_3 \eta^4 + T_1) - \frac{2}{9} A^{-8/9} \ln A \, T_{20} \eta^2 + A^{-8/9} (R_4 \eta^4 + T_{22} \eta \ln\eta + T_2 \eta) + \ldots, \quad \eta\to\infty. \tag{3.6.3}$$

This suggests that the inner expansions for ϕ and θ in the wall region have the form

$$\phi = A^{-4/9} \bar{\phi}_0 + A^{-6/9} \bar{\phi}_1 + A^{-8/9} \bar{\phi}_2 + A^{-10/9} \ln A \, \bar{\phi}_{30} + A^{-10/9} \bar{\phi}_3 + \ldots, \tag{3.6.4}$$

$$\theta = A^{-2/9} \bar{\theta}_0 + A^{-4/9} \bar{\theta}_1 + A^{-6/9} \bar{\theta}_2 + A^{-8/9} \ln A \, \bar{\theta}_{30} + A^{-8/9} \bar{\theta}_3 + \ldots, \tag{3.6.5}$$

where $\bar{\phi}_i$, $\bar{\theta}_i$ and $\bar{\phi}_{i0}$, $\bar{\theta}_{i0}$ are functions of η. Substitution of (3.6.4) and (3.6.5) into equations (3.5.1) and use of the appropriate inner versions of the base flow functions (3.5.7)-(3.5.10) leads successively to the following results.

At order $A^{4/9}$ in (3.5.1) we obtain

$$\bar{\phi}_0^{iv} = 0, \tag{3.6.6}$$

to be solved subject to

$$\bar{\phi}_0 = \bar{\phi}_0' = 0 \quad (\eta=0), \qquad \bar{\phi}_0 \sim J_2 \eta^2 \quad (\eta\to\infty). \tag{3.6.7}$$

The required solution is clearly

$$\bar{\phi}_0 = J_2\eta^2. \tag{3.6.8}$$

At order $A^{2/9}$ we obtain

$$\bar{\phi}_1^{iv} = 0, \tag{3.6.9}$$

with boundary conditions

$$\bar{\phi}_1 = \bar{\phi}_1' = 0 \quad (\eta=0), \quad \bar{\phi}_1 \sim J_3\eta^3 + 0.\eta^2 \quad (\eta\to\infty). \tag{3.6.10}$$

The required solution is

$$\bar{\phi}_1 = J_3\eta^3. \tag{3.6.11}$$

At order one we obtain

$$\bar{\phi}_2^{iv} = \bar{\theta}_0', \tag{3.6.12}$$

where the solution for $\bar{\theta}_0$ is to be considered below.

At order $A^{-2/9}\ln A$ it is found that

$$\bar{\phi}_{30}^{iv} = 0 \tag{3.6.13}$$

and the boundary conditions are

$$\bar{\phi}_{30} = \bar{\phi}_{30}' = 0 \quad (\eta=0), \quad \bar{\phi}_{30} \sim -2K_{20}\eta^2/9 \quad (\eta\to\infty). \tag{3.6.14}$$

The required solution is

$$\bar{\phi}_{30} = -2K_{20}\eta^2/9. \tag{3.6.15}$$

At order $A^{-2/9}$ we obtain

$$\bar{\phi}_3^{iv} = \bar{\theta}_1' , \tag{3.6.16}$$

with boundary conditions

$$\bar{\phi}_3 = \bar{\phi}_3' = 0 \quad (\eta=0), \quad \bar{\phi}_3 \sim J_5\eta^5 + K_{20}\eta^2 \ln\eta + K_2\eta^2 \quad (\eta\to\infty). \tag{3.6.17}$$

One integration gives

$$\bar{\phi}_3''' = \bar{\theta}_1 + \bar{k}_3 , \tag{3.6.18}$$

where $\bar{k}_3$ is a real constant; the solution for $\bar{\theta}_1$ will be discussed below.

In the heat equation (3.5.2), substitution of (3.6.4) and (3.6.5) into equation (3.5.2), and equating terms of like powers of A, leads successively to the following results. At order $A^{2/9}$

$$\bar{\theta}_0' + i\alpha_0\bar{\omega}_1\eta\bar{\theta}_0 = i\alpha_0\bar{\mu}_0\bar{\phi}_0 \tag{3.6.19}$$

and since $\bar{\phi}_0 = J_2\eta^2$, it follows that

$$\bar{\theta}_0'' + i\alpha_0\bar{\omega}_1\eta\bar{\theta}_0 = i\alpha_0\bar{\mu}_0 J_2\eta^2 . \tag{3.6.20}$$

The boundary conditions for $\bar{\theta}_0$ are

$$\bar{\theta}_0 = 0 \ (\eta=0), \quad \bar{\theta}_0 \sim R_1\eta \quad (\eta\to\infty), \tag{3.6.21}$$

where R_1 is given by (3.5.26). By inspection the required solution is

$$\bar{\theta}_0 = R_1\eta, \tag{3.6.22}$$

indicating that the leading order temperature field in the

outer solution is effectively unchanged across the wall region.

Returning to equation (3.6.12) the solution for $\bar{\phi}_2$ is obtained by integrating $\bar{\theta}_0$ in (3.6.12) three times and applying the boundary conditions

$$\bar{\phi}_2' = \bar{\phi}_2 = 0 \quad (\eta=0), \qquad \bar{\phi}_2 \sim J_4\eta^4 \quad (\eta\to\infty). \tag{3.6.23}$$

This leads to the solution

$$\bar{\phi}_2 = J_4\eta^4. \tag{3.6.24}$$

At order one the equation for $\bar{\theta}_1$ is found to be

$$\bar{\theta}_1'' + i\alpha_0\bar{\omega}_1\eta\bar{\theta}_1 = i\alpha_0\bar{\mu}_0\bar{\phi}_1 - i\alpha_0\bar{\omega}_2\eta^2\bar{\theta}_0, \tag{3.6.25}$$

and since $\bar{\phi}_1 = J_3\eta^3$ and $\bar{\theta}_0 = R_1\eta$, this reduces to the form

$$\bar{\theta}_1'' + r_1\eta\bar{\theta}_1 = r_2\eta^3, \tag{3.6.26}$$

where

$$r_1 = i\alpha_0\bar{\omega}_1, \qquad r_2 = i\alpha_0\bar{\mu}_0(J_3 - R_1\bar{\omega}_2/\bar{\mu}_0). \tag{3.6.27}$$

The boundary conditions for $\bar{\theta}_1$ are

$$\bar{\theta}_1 = 0 \quad (\eta=0), \quad \bar{\theta}_1 \sim R_2\eta^2 + T_0\eta^{-1} \quad (\eta\to\infty), \tag{3.6.28}$$

where $T_0 = 2(J_2\bar{\mu}_0\bar{\omega}_2 - J_3\bar{\mu}_0\bar{\omega}_1)/i\alpha_0\bar{\omega}_1^3$. By using the transformation

$$\bar{\theta}_1 = \bar{\theta} + r_2\eta^2/r_1, \tag{3.6.29}$$

the system (3.6.26), (3.6.27) can be written in the simplified form

$$\bar{\theta}'' + r_1\eta\bar{\theta} = -2r_2/r_1 \;; \bar{\theta} = 0 \;\; (\eta=0), \;\; \bar{\theta} \sim T_0\eta^{-1} \;\; (\eta\to\infty), \qquad (3.6.30)$$

for which the general solution can be expressed in terms of Airy functions (Abramowitz & Stegun, p.446):

$$\bar{\theta} = m_1 Ai(c\eta) + m_2 Bi(c\eta) + 2\pi r_2 Gi(c\eta)/r_1c^2 \qquad (3.6.31)$$

where $c = (-r_1)^{-1/3} = (-i\alpha_0\bar{\omega}_1)^{1/3}$ and m_1 and m_2 are arbitrary constants. It is convenient to choose the argument of the Airy function in the sector $|\arg z|<\pi/3$ of the complex plane so that c is defined by $c = e^{-\pi i/6}(\alpha_0\bar{\omega}_1)^{1/3}$ and the choice $m_2 = 0$ then ensures that the solution does not grow exponentially as $\eta\to\infty$. Indeed since $Gi(c\eta) \sim 1/\pi c\eta$ as $\eta\to\infty$, it then follows that $\bar{\theta} \sim T_0\eta^{-1}$ as $\eta\to\infty$, as required. Finally, application of the boundary condition $\bar{\theta}_1 = 0$ at $\eta = 0$ gives $m_1 = -2r_2\pi/3^{1/2}r_1c^2$. The final solution for $\bar{\theta}_1$ is thus

$$\bar{\theta}_1 = r_2\eta^2/r_1 - 2r_2\pi A_i(c\eta)/3^{1/2}r_1c^2 + 2\pi r_2 Gi(c\eta)/r_1c^2 \qquad (3.6.32)$$

In the solution for $\bar{\phi}_3$ it is seen from (3.6.18) that the term $\bar{\theta}_1$ will generate a logarithmic contribution of order $\eta^2\ln\eta$ as $\eta\to\infty$, consistent with the outer boundary condition (3.6.17). At this stage , we have seen that the wall region admits solutions for both the temperature and the stream function which allow the outer solution to adjust smoothly to the full boundary conditions at the vertical plane. This involves significant adjustment in the temperature field at order $A^{-4/9}$ and a corresponding adjustment in the stream function field at order $A^{-10/9}$. This gives confidence in the boundary conditions assumed for the outer functions ϕ_0 and ϕ_1, suggesting that the overall solution structure will be consistent in the limit as

$A \to \infty$.

In the next section we return to the question of the completion of the outer solution and the derivation of the neutral stability curve, making use of the bridging conditions across the critical layer derived in Sections 3.3 and 3.4.

3.7 Neutral Stability Curve

Derivation of the neutral stability curve requires application of the bridging conditions to the outer solutions for ϕ_0 and ϕ_1 across the centre-line, x=0. We recall that in x<0, the solution for ϕ_0 is given by

$$\phi_0 = \sigma_1^- f_1(x) + \sigma_2^- f_2(x), \qquad (3.7.1)$$

where σ_1^- and σ_2^- are complex constants and that in x>0

$$\phi_0 = \sigma_1^+ f_1(-x) + \sigma_2^+ f_2(-x), \qquad (3.7.2)$$

where σ_1^+, σ_2^+ are further complex constants. The real functions f_1, f_2 are uniquely defined by the solution of (2.3.5) and (2.3.4). The forms of the functions f_i (i=1,2) as $x \to 0-$ are given by

$$f_i(x) = a_i + b_i x + c_{i0} x^2 \ln|x| + c_i x^2 + d_i x^3 + \ldots, \qquad (3.7.3)$$

where the constants a_i, b_i, c_{i0}, c_i and d_i are related to those in the general forms of ϕ_0 as $x \to 0\pm$,

$$\phi_0 = a_0^{\pm} + b_0^{\pm} x + c_{00}^{\pm} x^2 \ln|x| + c_0^{\pm} x^2 + d_0^{\pm} x^3 + \ldots, \qquad (3.7.4)$$

by the formulae

$$\underline{v}_0^{\pm} = \sigma_1^{\pm}\,\underline{v}_1 + \sigma_2^{\pm}\,\underline{v}_2 \ , \tag{3.7.5}$$

where the vectors $\underline{v}_0^{\pm}$, $\underline{v}_1$ and $\underline{v}_2$ are those defined in Chapter 2. These are now substituted into the bridging conditions (3.3.47)-(3.3.50) for $a_0^{\pm}$, $b_0^{\pm}$, $c_0^{\pm}$ and $d_0^{\pm}$ to give

$$(\sigma_1^- - \sigma_1^+)a_1 + (\sigma_2^- - \sigma_2^+)a_2 = 0, \tag{3.7.6}$$

$$(\sigma_1^- + \sigma_1^+)b_1 + (\sigma_2^- + \sigma_2^+)b_2 = 0, \tag{3.7.7}$$

$$(\sigma_1^- - \sigma_1^+)c_1 + (\sigma_2^- - \sigma_2^+)c_2 = -i\pi s_0(\sigma_1^- a_1 + \sigma_2^- a_2)/2, \tag{3.7.8}$$

$$(\sigma_1^- + \sigma_1^+)d_1 + (\sigma_2^- + \sigma_2^+)d_2 = 0 \ . \tag{3.7.9}$$

The system of equations (3.7.6)-(3.7.9) has more than one set of solutions (Daniels 1987), but the solution of interest here is that for which ϕ_0 does not vanish on the centre-line x=0. From (3.7.7) and (3.7.9) this leads to the requirement that the determinant

$$\begin{vmatrix} b_1 & b_2 \\ d_1 & d_2 \end{vmatrix} = 0. \tag{3.7.10}$$

Since, from (2.3.10), $d_1 = b_1 s_0/6$ and $d_2 = (1 + b_2 s_0)/6$ this reduces to the requirement that $b_1 = 0$. This condition, equivalent to $f_1'(0) = 0$, effectively fixes the value of γ_0, as explained originally by Daniels (1987). The lowest value of γ for which (2.3.4) has a solution with $f_1'(0) = 0$ is $\gamma = \gamma_0 = 6.30$ and the manner in which γ_0 can be calculated numerically from (2.3.4) is discussed in Chapter 4.

Solving the above system of equations (3.7.6)-(3.7.9) now leads to the following relations between the constants σ_1^+, σ_2^-, σ_2^+ and σ_1^- :

$$\sigma_1^+ = \frac{4a_2c_1 - 4a_1c_2 + i\pi s_0 a_1 a_2}{4a_2c_1 - 4a_1c_2 - i\pi s_0 a_1 a_2}\ \sigma_1^-, \tag{3.7.11}$$

$$\sigma_2^- = \frac{i\pi s_0 a_1^{\,2}}{4a_2c_1 - 4a_1c_2 - i\pi s_0 a_1 a_2}\ \sigma_1^-, \tag{3.7.12}$$

and

$$\sigma_2^+ = -\sigma_2^-\,. \tag{3.7.13}$$

The value of σ_1^- remains arbitrary, equivalent to the fact that the original stability problem is a linear, homogeneous one. However, it is convenient to note that provided α is real the eigensolutions ϕ and θ can always be expressed in the form

$$\phi = \phi^{(o)} + i\,\phi^{(e)}\,,\quad \theta = \theta^{(e)} + i\,\theta^{(o)}, \tag{3.7.14}$$

where $\phi^{(o)}$, $\theta^{(o)}$ and $\phi^{(e)}$, $\theta^{(e)}$ are real odd and even functions of x respectively. This may be achieved in the present context by choosing $\sigma_1^- = -i(4a_2c_1 - 4a_1c_2 - i\pi s_0 a_1 a_2)$, so that for the leading order outer solution

$$\phi_0 = \phi_0^{(o)} + i\,\phi_0^{(e)}, \tag{3.7.15}$$

where

$$\phi_0^{(o)} = a_1\pi s_0[a_1 f_2(x) - a_2 f_1(x)], \tag{3.7.16}$$

and

$$\phi_0^{(e)} = (4a_1c_2 - 4a_2c_1)f_1(x). \qquad (3.7.17)$$

Just as the leading order bridging conditions involving $b_0^{\pm}$ and $d_0^{\pm}$ yield γ_0, so the second order bridging conditions involving $b_1^{\pm}$ and $d_1^{\pm}$ yield γ_1 as a function of α_0. This relation constitutes the neutral stability curve. We recall that the solution for ϕ_1 in $x<0$ is given by

$$\phi_1 = \bar{\sigma}_1^- f_1(x) + \bar{\sigma}_2^- f_2(x) + 2\alpha_0^2 [\sigma_1^- f_{11}(x) + \sigma_2^- f_{21}(x)] + \gamma_1 [\sigma_1^- f_{12}(x) + \sigma_2^- f_{22}(x)] - [\sigma_1^- f_{13}(x) + \sigma_2^- f_{23}(x)]/i\alpha_0 , \qquad (3.7.18)$$

where the real functions f_{ij} ($i=1,2$; $j=1,2,3$) are defined in Chapter 2, and $\bar{\sigma}_1^-$ and $\bar{\sigma}_2^-$ are complex constants. In $x>0$ the corresponding solution is

$$\phi_1 = \bar{\sigma}_1^+ f_1(-x) + \bar{\sigma}_2^+ f_2(-x) + 2\alpha_0^2 [\sigma_1^+ f_{11}(-x) + \sigma_2^+ f_{21}(-x)] + \gamma_1 [\sigma_1^+ f_{12}(-x) + \sigma_2^+ f_{22}(-x)] + [\sigma_1^+ f_{13}(-x) + \sigma_2^+ f_{23}(-x)]/i\alpha_0 . \qquad (3.7.19)$$

The forms of the functions f_{ij} ($i=1,2$; $j=1,2,3$) as $x \to 0$ are given in Chapter 2 and involve, in particular, the constants b_{ij} and d_{ij} which are related to those $b_1^{\pm}$ and $d_1^{\pm}$ in the general forms of ϕ_1 as $x \to 0\pm$,

$$\phi_1 = \delta_1^{\pm}/x + a_1^{\pm} + b_{10}^{\pm} x\ln|x| + b_1^{\pm} x + c_{10}^{\pm} x^2\ln|x| + c_1^{\pm} x^2 + d_{10}^{\pm} x^3\ln|x| + d_1^{\pm} x^3 + \ldots \qquad (3.7.20)$$

by the formulae

$$\underline{v}_1^{\pm} = \bar{\underline{v}}_1^{\pm} + 2\alpha_0^2 \underline{v}_{11}^{\pm} + \gamma_1 \underline{v}_{12}^{\pm} - \underline{v}_{13}^{\pm}/i\alpha_0 , \qquad (3.7.21)$$

where the vectors $\underline{v}_1^{\pm}$, $\bar{\underline{v}}_1^{\pm}$, $\underline{v}_{11}^{\pm}$, $\underline{v}_{12}^{\pm}$ and $\underline{v}_{13}^{\pm}$ are those defined in Chapter 2. These are now substituted into the bridging conditions (3.4.38) and (3.4.40) for $b_1^{\pm}$ and $d_1^{\pm}$ to yield

$$\bar{\sigma}_1^- b_1 + \bar{\sigma}_2^- b_2 + \bar{\sigma}_1^+ b_1 + \bar{\sigma}_2^+ b_2 + 2\alpha_0^2 [\sigma_1^- b_{11} + \sigma_2^- b_{21} + \sigma_1^+ b_{11} + \sigma_2^+ b_{21}] + \gamma_1[\sigma_1^- b_{12} + \sigma_2^- b_{22} + \sigma_1^+ b_{12} + \sigma_2^+ b_{22}] - [\sigma_1^- b_{13} + \sigma_2^- b_{23} - \sigma_1^+ b_{13} - \sigma_2^+ b_{23})]/i\alpha_0 = -\mu_0 \pi (\mu_0 - 12\omega_3) a_0^+ / 6\alpha_0 \omega_1^3 \qquad (3.7.22)$$

and

$$\bar{\sigma}_1^- d_1 + \bar{\sigma}_2^- d_2 + \bar{\sigma}_1^+ d_1 + \bar{\sigma}_2^+ d_2 + 2\alpha_0^2 [\sigma_1^- d_{11} + \sigma_2^- d_{21} + \sigma_1^+ d_{11} + \sigma_2^+ d_{21}] + \gamma_1[\sigma_1^- d_{12} + \sigma_2^- d_{22} + \sigma_1^+ d_{12} + \sigma_2^+ d_{22}] - [\sigma_1^- d_{13} + \sigma_2^- d_{23} - \sigma_1^+ d_{13} - \sigma_2^+ d_{23})]/i\alpha_0 = -\mu_0 \pi a_0^+ [s_0(\mu_0 - 12\omega_3)/6 - (4\gamma_0^4 + 3s_1 + s_0^2/8)\omega_1]/ 6\alpha_0 \omega_1^3 . \qquad (3.7.23)$$

Since $b_1 = 0$, $\sigma_2^+ = -\sigma_2^-$ and $a_0^+ = \sigma_1^- a_1 + \sigma_2^- a_2$, the first of these equations can be written in the simplified form

$$(\bar{\sigma}_2^- + \bar{\sigma}_2^+) b_2 + (\sigma_1^- + \sigma_1^+)(2\alpha_0^2 b_{11} + \gamma_1 b_{12}) - [(\sigma_1^- - \sigma_1^+) b_{13} + 2\sigma_2^- b_{23}]/i\alpha_0 = -\mu_0 \pi (\mu_0 - 12\omega_3)(\sigma_1^- a_1 + \sigma_2^- a_2)/6\alpha_0 \omega_1^3 \qquad (3.7.24)$$

and the second in the simplified form

$$(\bar{\sigma}_2^- + \bar{\sigma}_2^+) d_2 + (\sigma_1^- + \sigma_1^+)(2\alpha_0^2 d_{11} + \gamma_1 d_{12}) - [(\sigma_1^- - \sigma_1^+) d_{13} + 2\sigma_2^- b_{23}]/i\alpha_0 = -\mu_0 \pi a_0^+ [s_0(\mu_0 - 12\omega_3)/6 - (4\gamma_0^4 + 3s_1 + s_0^2/8)\omega_1](\sigma_1^- a_1 + \sigma_2^- a_2)/6\alpha_0 \omega_1^3 . \qquad (3.7.25)$$

Elimination of $(\bar{\sigma}_2^- + \bar{\sigma}_2^+)$ and substitution for σ_1^+, σ_2^- and σ_1^+ from (3.7.11)-(3.7.13) leads, after simplification, to a cubic equation for α_0 given by

$$\alpha_0^3 + \bar{c}_1 \alpha_0 \gamma_1 + \bar{c}_2 = 0, \qquad (3.7.26)$$

where

$$\bar{c}_1 = \frac{(b_2 d_{12} - d_2 b_{12})}{2(b_2 d_{11} - d_2 b_{11})} , \qquad (3.7.27)$$

$$\bar{c}_2 = \mu_0 \pi a_1 \frac{(\mu_0 - 12\omega_3)(s_0 b_2/6 - d_2) - \omega_1 b_2 (4\gamma_0^4 + 3s_1 + s_0^2/8)}{24\,\omega_1^3 (b_2 d_{11} - d_2 b_{11})}$$

$$+ \pi a_1 s_0 \frac{a_2 (b_2 d_{13} - d_2 b_{13}) + a_1 (d_2 b_{23} - b_2 d_{23})}{8(a_2 c_1 - a_1 c_2)(b_2 d_{11} - d_2 b_{11})} . \qquad (3.7.28)$$

This equation is the neutral stability curve from which the critical wavelength of the instability can be obtained. In order to determine the coefficients $\bar{c}_1$ and $\bar{c}_2$ it is necessary to calculate numerically the various constants a_i, b_i, c_i; a_{ij}, b_{ij}, c_{ij}, arising in the solutions for f_i and f_{ij} (i=1,2; j=1,2,3) as $x \to 0$. This task is undertaken in Chapter 4.

i	$\bar{\mu}_i$	$\hat{\mu}_i$
0	3.16092	0.50152
1	0.00000	0.00000
2	-125.37500	-58.79610
3	524.52701	333.12400
4	-828.99600	-658.02000
5	0.00000	0.00000
6	21292.09001	2420.19001
7	-3930.42010	-4992.36002
8	3105.94002	4437.91000
9	0.00000	0.00000
10	-2737.64010	-4761.17030
11	3123.65003	5951.43001
12	-1645.61010	-3396.43000
13	0.00000	0.00000
14	717.26700	1702.97000
15	-600.16200	-1524.64000
16	237.13300	640.03100
17	0.00000	0.00000
18	-61.47490	-184.99900
19	40.60910	128.95300
20	-12.83620	42.79760

TABLE 3.1. Values of the real constants $\bar{\mu}_i$ and $\hat{\mu}_i$ (i=0,..,20).

i	$\bar{\omega}_i$	$\hat{\omega}_i$
0	0.00000	0.00000
1	0.03984	-0.00662
2	-0.25000	0.00000
3	0.526821	0.08359
4	0.00000	0.00000
5	-2.08958	-0.97994
6	4.37106	2.77603
7	-3.94760	-3.13343
8	0.00000	0.00000
9	4.34938	4.80196
10	-5.45891	-6.93384
11	3.13731	4.48274
12	0.00000	0.00000
13	-1.59536	-2.77457
14	1.43024	2.72502
15	-0.60279	-1.24411
16	0.00000	0.00000
17	0.17580	0.41739
18	-0.12258	-0.311404
19	0.04079	0.110084
20	0.00000	0.000000

TABLE3.2. Values of the real constants $\bar{\omega}_i$ and $\hat{\omega}_i$ (i=0,..,20).

i	A_{1i}	A_{2i}
0	0.00000	0.00000
1	0.00000	0.00000
2	0.50000	0.00000
3	0.00000	0.16667
4	1.65303	0.00000
5	4.14945	0.22040
6	-3.37225	0.69157

TABLE 3.3. Values of the real constants A_{ji} (j=1,2; i=0,...,6).

i	B_{1i}	B_{2i}
0	0.00000	0.00000
1	0.00000	0.00000
2	0.00000	0.00000
3	0.00000	0.00000
4	0.04167	0.00000
5	0.00000	0.00833
6	0.69157	0.00000

i	C_{1i}	C_{2i}
0	0.00000	0.00000
1	0.00000	0.00000
2	0.00000	0.00000
3	0.00000	0.00000
4	0.53689	0.00000
5	2.03706	0.07158
6	-1.90329	0.33951

TABLE 3.4. Values of the real constants B_{ji} and C_{ji} ($j=1,2$; $i=0,\ldots,6$).

i	D_{1i}	D_{1i0}
0	0.00000	
1	0.00000	
2	0.00000	6249.58111
3	30180.31065	
4	20661.53915	20661.53915
5	94836.28995	51864.66976
6	273001.03277	

i	D_{2i}	D_{2i0}
0	0.00000	
1	0.00000	
2	0.00000	331.95613
3	2777.59161	
4	4072.38010	1097.46950
5	12226.50923	2754.87189
6	413.40865	

TABLE 3.5. Values of the real constants D_{ji} and D_{ji0} ($j=1,2$; $i=0,\ldots,6$).

CHAPTER FOUR : NUMERICAL METHODS AND RESULTS

4.1 Introduction

This chapter is concerned with the numerical calculations required to obtain γ_0 and the real constants a_i, b_i, c_i, a_{ij}, b_{ij} and c_{ij} (i=1,2; j=1,2,3) and hence the precise form of the cubic neutral stability curve. This in turn determines the critical wavelength of the instability. In Section 4.2, the various systems of equations and boundary conditions for f_i and f_{ij} are listed, and in Section 4.3 an appropriate numerical method of solution based on series expansions and a fourth order Runge Kutta scheme is described. The results are reported in Section 4.4 and this leads to the precise form of the neutral stability curve in Section 4.5. The critical wavenumber is found and comparisons made with both numerical results and experimental observations of the instability in slot flows.

4.2 Statement of Equations and Boundary Conditions

In this section, we summarize the system of equations and boundary conditions for the real functions f_i and f_{ij} (i=1,2; j=1,2,3), which must be solved to determine the various constants arising in the equation of the neutral stability curve.

The equations and boundary conditions for f_i (i=1,2), as

given in Chapter 2, are

$$f_1''' - \frac{\Theta_0'}{\Psi_0'} f_1 = 0; \ (f_1, f_1', f_1'') = (0,0,1) \quad \text{at } x=-1/2, \qquad (4.2.1)$$

$$f_2''' - \frac{\Theta_0'}{\Psi_0'} f_2 = 1; \ (f_2, f_2', f_2'') = (0,0,0) \quad \text{at } x=-1/2. \qquad (4.2.2)$$

The equations and boundary conditions for the functions f_{ij} (i=1,2; j=1,2,3) are

$$f_{i1} - \frac{\Theta_0'}{\Psi_0'} f_{i1} = f'_i \ ; (f_{i0}, f_{i0}', f_{i0}'') = (0,0,0) \quad \text{at } x=-1/2, \qquad (4.2.3)$$

$$f'''_{i2} - \frac{\Theta_0'}{\Psi_0'} f_{i2} = \frac{\Theta_1' \Psi_0' - \Theta_0 \Psi_1'}{(\Psi_0')^2} f_i ; (f_{i2}, f'_{i2}, f''_{i2}) = (0,0,0) \text{at } x=-1/2, \qquad (4.2.4)$$

$$f'''_{i3} - \frac{\Theta_0'}{\Psi_0'} f_{i3} = \frac{1}{\Psi_0'} \left(\frac{d^2}{dx^2} \left\{ \frac{\Theta_0' f_i}{\Psi_0'} \right\} \right) + \frac{4 \gamma_0^4 f_i'}{\Psi_0'} . \qquad (4.2.5)$$

For f_{i3} the second derivative does not vanish at x=-1/2 where the local behaviour is given by

$$f_{i3} = 0 + 0.(x+1/2) + D_{i20}(x+1/2)^2 \ln(x+1/2) + 0.(x+1/2)^2 + \ldots, \quad (x \to -1/2), \qquad (4.2.6)$$

where D_{i20} (i=1,2) are real constants whose values are given in

Table 3.5. The three zero coefficients are the three conditions needed to uniquely define the solution in this case.

The method of solution of the above systems of equations and boundary conditions is described in the next section.

4.3 Numerical Method

The numerical method employed to solve all of the systems defined in Section 4.2, in the interval [-1/2,0], was a fourth order Runge-Kutta scheme, together with a series expansion of the solution in the neighbourhood of the point x=-1/2. The expansions for the base flow functions and the real functions f_i, f_{ij} were determined in Section 3.5 and are given below. Starting with the base flow functions, and writing X = x+1/2, we have

$$\Theta_0' = \sum_{i=0}^{\infty} \bar{\mu}_i X^i \ , \qquad X \to 0 \ , \tag{4.3.1}$$

$$\Psi_0' = \sum_{i=0}^{\infty} \bar{\omega}_i X^i \ , \qquad X \to 0 \ , \tag{4.3.2}$$

where values of the real constants $\bar{\mu}_i$ and $\bar{\omega}_i$ (i=0,1,2,...,20) are given in Tables 3.1 and 3.2.

The Taylor expansion for f_1 has the form

$$f_1 = X^2/2 + \sum_{i=3}^{\infty} A_{1i} X^i, \qquad X \to 0, \tag{4.3.3}$$

where the real constants A_{1i} are obtained by substituting (4.3.1)-(4.3.3) into (4.2.1) and equating terms of like powers of X. Formulae for the real constants A_{1i} are listed in

Similarly

$$f_2 = \sum_{i=3}^{\infty} A_{2i} X^i , \quad X \to 0, \tag{4.3.4}$$

where the real constants A_{2i}, obtained in the same manner as the constants A_{1i}, are listed in Appendix I.

Next, we consider equation (4.2.3); the Taylor expansion for f_{j1} (j=1,2) is given by

$$f_{j1} = \sum_{i=3}^{\infty} B_{ji} X^i , \quad X \to 0, \tag{4.3.5}$$

where the real constants B_{ji} are also listed in Appendix I.

Before considering equation (4.2.4), we need expansions of the base flow functions Θ_1' and Ψ_1'. These are given in Section 3.5 as

$$\Theta_1' = \sum_{i=0}^{\infty} \hat{\mu}_i X^i , \quad X \to 0 , \tag{4.3.6}$$

$$\Psi_1' = \sum_{i=0}^{\infty} \hat{\omega}_i X^i , \quad X \to 0 , \tag{4.3.7}$$

where numerical values of the real constants $\hat{\mu}_i$, $\hat{\omega}_i$ are given in Tables 3.1 and 3.2. The Taylor expansions for f_{j2} (j=1,2) are then given by

$$f_{j2} = \sum_{i=3}^{\infty} C_{ji} X^i , \quad X \to 0, \tag{4.3.8}$$

and formulae for the real constants C_{ji} are given in Appendix I.

Finally, we consider equation (4.2.5), where the expansions

for f_{i3} about the point $X=0$ contain logarithmic contributions. In particular

$$f_{i3} = D_{i20}X^2\ln|X| + D_{i3}X^3 + D_{i40}X^4\ln|X| + D_{i4}X^4 + \ldots, \quad X\to 0, \tag{4.3.9}$$

where substitution of (4.3.9) and (4.3.1)-(4.3.3) into (4.2.5) yields the appropriate formulae for D_{ij} and D_{ij0} (i=1,2) which are given in Appendix I.

These expansions are used to start off the numerical integration near $x=-1/2$ and at $x=-1/2+kh$ $(k=1,2,\ldots)$ they provide initial values of f_i, f'_i, f''_i and f_{ij}, f'_{ij} and f''_{ij} needed to initiate the solution of (4.2.1)-(4.2.5) by a fourth order Runge-Kutta scheme. The Runge-Kutta integration proceeds to the neighbourhood of the origin, $x=0$, where the solutions f_i, f_{ij} are singular. In general the integration is stopped just ahead of the origin, at $x=x_s$, where x_s is small and negative and the expansions derived in Sections 2.3-2.4,

$$f_i = a_i + b_ix + c_{i0}x^2\ln|x| + c_ix^2 + d_ix^3 + e_{i0}x^4\ln|x| + e_ix^4 + g_ix^5 + h_{i0}x^6\ln|x| + h_ix^6 + \ldots, \quad x\to 0-, \tag{4.3.10}$$

$$f_{i1} = a_{i1} + b_{i1}x + c_{i10}x^2\ln|x| + c_{i1}x^2 + d_{i1}x^3 + e_{i10}x^4\ln|x| + e_ix^4 + g_{i1}x^5 + h_{i10}x^6\ln|x| + h_{i1}x^6 + \ldots, \quad x\to 0-, \tag{4.3.11}$$

$$f_{i2} = a_{i2} + b_{i2}x + c_{i20}x^2\ln|x| + c_{i2}x^2 + d_{i2}x^3 + e_{i20}x^4\ln|x| + e_{i2}x^4 + \ldots, \quad x\to 0-, \tag{4.3.12}$$

$$f_{i3} = \delta_{i3}/x + a_{i3} + b_{i30}x\ln|x| + b_{i3}x + c_{i30}x^2\ln|x| + c_{i3}x^2 + d_{i3}x^3\ln|x| + d_{i3}x^3 + \ldots., \quad x\to 0-, \tag{4.3.13}$$

are used to obtain estimates of the various constants a_i, b_i, c_i, a_{ij}, b_{ij} and c_{ij}. This is done by equating the Runge-Kutta values of f_i, f'_i, f''_i and f_{ij}, f'_{ij} and f''_{ij} at $x=x_s$ to the corresponding formulae given by the series expansions (4.3.10)-(4.3.13). In the case of each function f_i this leads to a non-homogeneous system of three equations for a_i, b_i and c_i since the remaining constants d_i,... are known in terms of a_i, b_i and c_i, from (2.3.10). Similarly, in the case of each f_{ij}, it leads to a non-homogeneous system of three equations for a_{ij}, b_{ij} and c_{ij}, since the remaining constants d_{ij},... are known in terms of these from (2.4.16), (2.4.25) and (2.4.35). For the leading order terms $f_i(i=1,2)$ there are two systems which take the form

$$a_i\Gamma_i + b_i\Lambda_i + c_i\chi_i = f_i(x_s) + K_i, \qquad (4.3.14)$$

$$a_i\Gamma'_i + b_i\Lambda'_i + c_i\chi'_i = f'_i(x_s) + K'_i, \qquad (4.3.15)$$

$$a_i\Gamma''_i + b_i\Lambda''_i + c_i\chi''_i = f''_i(x_s) + K''_i\ , \qquad (4.3.16)$$

where the real functions $\Gamma_i, \Lambda_i, \chi_i, K_i$, their first derivatives, denoted by Γ'_i, Λ'_i, χ'_i, K'_i and their second derivatives, denoted by Γ''_i, Λ''_i, χ''_i, K''_i are defined explicitly in Appendix II. Here $f_i(x_s)$, $f'_i(x_s)$ and $f''_i(x_s)$ denote the values of $f_i(x)$ and its first and second derivatives at the point x_s, obtained from the Runge-Kutta integration.

For the second order terms, f_{ij}, there are six systems (i=1,2; j=1,2,3) which take the form

$$a_{ij}\Gamma_{ij} + b_{ij}\Lambda_{ij} + c_{ij}\chi_{ij} = f_{ij}(x_s) + K_{ij}, \qquad (4.3.17)$$

$$a_{ij}\Gamma'_{ij} + b_{ij}\Lambda'_{ij} + c_{ij}\chi'_{ij} = f'_{ij}(x_s) + K'_{ij}, \qquad (4.3.18)$$

$$a_{ij}\Gamma''_{ij} + b_{ij}\Lambda''_{ij} + c_{ij}\chi''_{ij} = f''_{ij}(x_s) + K''_{ij}, \qquad (4.3.19)$$

where the real functions Γ_{ij}, Λ_{ij}, χ_{ij}, K_{ij}, their first derivatives, denoted by Γ'_{ij}, Λ'_{ij}, χ'_{ij}, K'_{ij} and their second derivatives denoted by Γ''_{ij}, Λ''_{ij}, χ''_{ij}, K''_{ij} are defined explicitly in Appendix II. Also, on the right-hand sides, $f_{ij}(x_s)$, $f'_{ij}(x_s)$ and $f''_{ij}(x_s)$ denote the values of $f_{ij}(x)$ and its first and second derivatives at the point x_s, as obtained from the Runge-Kutta integration.

In the case of the equation for f_1, it is necessary to adjust the convective parameter γ until $b_1 = f'_1(0) = 0$. This is achieved by an iterative procedure in which repeated computations across the interval $[-1/2,0]$ are carried out and the bisection method used to converge on the required value of γ. Once this value, γ_0, is known, the remaining systems of equations are solved for this single value of γ, using, in each case, one integration across the interval $[-1/2,0]$. Numerical results are discussed in the next section.

4.4 Results

The numerical solution was implemented with between 100 and 400 steps in the Runge-Kutta scheme, that is with step lengths h in the range 0.01 to 0.0025. It was established that, with 100 steps, the solution obtained was accurate only to three

significant figures , when compared with solutions obtained for 200 or 400 steps; however, the solutions obtained with 200 and 400 steps agreed to four significant figures and it was decided that the main results would be obtained using the Runge-Kutta scheme with 400 steps. Tables 4.1 and 4.2 show a comparison of results obtained for f_1 with 200 and 400 steps respectively.

Numerical experiments were carried out in which the Runge-Kutta scheme was initiated one, two and four steps away from the point x=-1/2, using the method outlined in the previous section. Starting the scheme one step or more away from x=-1/2 made no difference to the solutions obtained to five decimal places and therefore all of the solutions were computed by starting one step away from x=-1/2.

In solving equation (4.2.1), the bisection method led to the determination of γ_0 as

$$\gamma_0 = 6.29829 \ , \qquad (4.4.1)$$

consistent with results given by Daniels & Weinstein (1992). Properties of the leading order functions f_1 and f_2 are tabulated in Tables 4.2-4.3 and Figures 4.1-4.2 show both the functions and their first derivatives. The second order functions f_{ij} (i=1,2; j=1,2,3) and their first derivatives are shown in Figures 4.3-4.8 and quantitative information is contained in Tables 4.4-4.9.

In order to determine the constants a_i, b_i, c_i, a_{ij}, b_{ij} and c_{ij} accurately, the solutions of the systems of equations (4.3.14)-(4.3.19) described in the previous section were tested

for accuracy and consistency, by solving each system at several points $x_s=-kh$ $(k=0,1,2,...)$. In this way it was found to be possible to predict the values of the constants a_i, b_i, c_i, a_{ij}, b_{ij} and c_{ij} accurate to about four significant figures. Relevant results are shown in Tables 4.10-4.13, and the predicted values of the various constants are

$a_1 = 0.2413$

$b_1 = 0.000$

$c_1 = 14.13$

$a_2 = 0.02548$

$b_2 = 0.03245$

$c_2 = 1.703$

$a_{11} = 0.00395$

$b_{11} = 0.0193$

$c_{11} = 0.372$

$a_{21} = 3.12 \times 10^{-4}$

$b_{21} = 1.98 \times 10^{-3}$

$c_{21} = 3.38$

$a_{12} = -0.0137$

$b_{12} = -2.06$

$c_{12} = 11.0$

$a_{22} = -0.00367$

$b_{22} = -0.207$

$c_{22} = 1.26$

$a_{13} = 3.69 \times 10^{4}$

$b_{13} = -2.05 \times 10^{5}$

$c_{13} = 8.30 \times 10^{5}$

$a_{23} = 4.41 \times 10^{3}$

$$b_{23} = -1.68 \times 10^4$$

$$c_{23} = 1.58 \times 10^5 \ .$$

These results in combination with the formulae for d_i and d_{ij} given by (2.3.10), (2.4.16),(2.4.25) and (2.4.35) also give

$$d_1 = 0.000$$

$$d_2 = 0.610$$

$$d_{11} = 0.255$$

$$d_{21} = 0.0321$$

$$d_{12} = -27.7$$

$$d_{22} = -2.77$$

$$d_{13} = 4.01 \times 10^6$$

$$d_{23} = 6.04 \times 10^5$$

4.5 Neutral Stability Curve

Consider the equation of the neutral stability curve derived in Section 3.7,

$$\alpha_0^3 + \bar{c}_1 \alpha_0 \gamma_1 + \bar{c}_2 = 0 \ , \qquad (4.5.1)$$

where the real constants $\bar{c}_1$ and $\bar{c}_2$ are given in terms of the constants a_i, b_i, c_i and a_{ij}, b_{ij}, c_{ij} by the formulae (3.7.28) and (3.7.27). Inserting the numerical values gives

$$\bar{c}_1 = -53.37 \qquad (4.5.2)$$

$$\bar{c}_2 = 1.677 \times 10^7 \ . \qquad (4.5.3)$$

Using the transformation

$$\alpha_0 = \bar{\alpha}_0 \bar{c}_2^{1/3} , \quad \gamma_1 = -\bar{\gamma}_1 \bar{c}_2^{2/3} / \bar{c}_1 , \tag{4.5.4}$$

equation (4.5.1) can be written as

$$\bar{\alpha}_0^3 - \bar{\alpha}_0 \bar{\gamma}_1 + 1 = 0 , \tag{4.5.5}$$

from which we obtain

$$\bar{\gamma}_1 = (1 + \bar{\alpha}_0^3)/\bar{\alpha}_0 . \tag{4.5.6}$$

The minimum value of $\bar{\gamma}_1$, obtained by setting $d\bar{\gamma}_1/d\bar{\alpha}_0 = 0$, occurs when

$$\bar{\alpha}_0 = (1/2)^{1/3} \tag{4.5.7}$$

and the corresponding value of $\bar{\gamma}_1$ is given by

$$\bar{\gamma}_1 = 3(2)^{-2/3} . \tag{4.5.8}$$

Figure 4.9 shows the graph of $\bar{\gamma}_1$ as a function of $\bar{\alpha}_0$. Substitution of the values of $\bar{c}_1$ and $\bar{c}_2$ into the formulae (4.5.4) gives the critical value of the wavenumber as

$$\alpha_{0crit} = 203.2 \tag{4.5.9}$$

and the minimum value of γ_1 as

$$\gamma_{1\,min} = 2320 . \tag{4.5.10}$$

Thus the overall vertical wavenumber at the onset of instability is predicted to be

$$\alpha_{crit} \sim \alpha_{0crit} A^{-1/3} = 203.2\, A^{-1/3}, \qquad A \to \infty. \tag{4.5.11}$$

This result can be compared with the predictions of various

numerical results and experimental observations for high Prandtl number fluids, as summarized in Table 4.14. In the present theory the Prandtl number is assumed to be infinite, while the previous results shown in Table 4.12 are for Prandtl numbers in the range $\sigma = 900$ to 1000. The results obtained by Elder (1965) are from experimental observations in a slot with a vertical aspect ratio between 1 and 60 and with Prandtl number $\sigma \approx 1000$. Vest and Arpaci's (1969) results are from experimental observations in a vertical slot with Prandtl number $\sigma \approx 1000$. De Vahl Davis and Mallinson (1975) obtained their results by solving numerically the full, nonlinear Boussinesq equations for a vertical slot of aspect ratio 10 and for a Prandtl number, $\sigma = 1000$. Bergholz' (1978) result was obtained by a numerical solution of the full linear stability equations using the Galerkin method, for a Prandtl number $\sigma = 1000$, and for the convective paremeter $\gamma = 6.98$. The present prediction of the critical wavenumber is seen to be in reasonable agreement particularly with the results of Bergholz' stability analysis and Elder's experiments.

Figures 4.10-4.14 show the development of the instability near the critical point, as given by (1.2.26), (3.7.16), (3.7.17) and (4.5.11) for increasing values of the amplitude ε. The vertical scale is chosen to be equivalent to a Rayleigh number $A \simeq 10^5$. The results indicate flow patterns for the smaller values of ε in good agreement with experimental observations and full numerical simulations.

x	f_1	f_1'	f_1''
-0.49750	0.00000	0.00250	1.00013
-0.49000	0.00005	0.01001	1.00207
-0.47000	0.00045	0.03019	1.02002
-0.45000	0.00126	0.05095	1.05940
-0.43000	0.00250	0.07274	1.12356
-0.41000	0.00418	0.09608	1.21562
-0.39000	0.00635	0.12157	1.33844
-0.37000	0.00906	0.14984	1.49462
-0.35000	0.01237	0.18159	1.68635
-0.33000	0.01635	0.21754	1.91524
-0.31000	0.02111	0.25845	2.18196
-0.29000	0.02673	0.30507	2.48570
-0.27000	0.03335	0.35811	2.82342
-0.25000	0.04110	0.41819	3.18866
-0.23000	0.05013	0.48576	3.56982
-0.21000	0.06058	0.56096	3.94769
-0.19000	0.07262	0.64345	4.29185
-0.17000	0.08636	0.73210	4.55534
-0.15000	0.10193	0.82465	4.66679
-0.13000	0.11935	0.91705	4.51821
-0.11000	0.13856	1.00257	3.94480
-0.09000	0.15933	1.07033	2.68834
-0.07000	0.18114	1.10276	0.31965
-0.05000	0.20302	1.07054	-3.96396
-0.03000	0.22319	0.91952	-12.06993
-0.01000	0.23818	0.51580	-32.27270
0.00000	0.24125	0.00810	1.97E+13

TABLE 4.1. 200-step Runge-Kutta solution for f_1.

x	f_1	f_1'	f_1''
-0.49750	0.00000	0.00250	1.00012
-0.49000	0.00005	0.01001	1.00206
-0.47000	0.00045	0.03019	1.02002
-0.45000	0.00126	0.05095	1.05939
-0.43000	0.00250	0.07274	1.12356
-0.41000	0.00418	0.09608	1.21561
-0.39000	0.00635	0.12157	1.33843
-0.37000	0.00906	0.14984	1.49461
-0.35000	0.01237	0.18159	1.68634
-0.33000	0.01635	0.21754	1.91523
-0.31000	0.02111	0.25845	2.18195
-0.29000	0.02673	0.30507	2.48569
-0.27000	0.03335	0.35810	2.82341
-0.25000	0.04110	0.41819	3.18864
-0.23000	0.05013	0.48576	3.56980
-0.21000	0.06058	0.56096	3.94767
-0.19000	0.07262	0.64344	4.29182
-0.17000	0.08636	0.73210	4.55531
-0.15000	0.10193	0.82465	4.66677
-0.13000	0.11935	0.91705	4.51818
-0.11000	0.13856	1.00256	3.94477
-0.09000	0.15933	1.07032	2.68832
-0.07000	0.18114	1.10276	0.31965
-0.05000	0.20302	1.07054	-3.96394
-0.03000	0.22318	0.91951	-12.06986
-0.01000	0.23818	0.51580	-32.27237
0.00000	0.24125	0.00405	-4.14E+11

TABLE 4.2. 400-step Runge-Kutta solution for f_1.

x	f_2	f_2'	f_2''
-0.49750	0.00000	0.00000	0.00250
-0.49000	0.00000	0.00005	0.01000
-0.47000	0.00000	0.00045	0.03014
-0.45000	0.00002	0.00126	0.05067
-0.43000	0.00006	0.00248	0.07196
-0.41000	0.00012	0.00414	0.09439
-0.39000	0.00023	0.00627	0.11841
-0.37000	0.00038	0.00889	0.14446
-0.35000	0.00059	0.01206	0.17301
-0.33000	0.00086	0.01583	0.20450
-0.31000	0.00122	0.02027	0.23930
-0.29000	0.00168	0.02543	0.27767
-0.27000	0.00225	0.03140	0.31967
-0.25000	0.00294	0.03824	0.36506
-0.23000	0.00378	0.04602	0.41309
-0.21000	0.00479	0.05477	0.46228
-0.19000	0.00598	0.06450	0.51004
-0.17000	0.00737	0.07514	0.55212
-0.15000	0.00899	0.08650	0.58174
-0.13000	0.01084	0.09825	0.58837
-0.11000	0.01292	0.10978	0.55549
-0.09000	0.01522	0.12004	0.45674
-0.07000	0.01770	0.12732	0.24761
-0.05000	0.02027	0.12867	-0.15602
-0.03000	0.02277	0.11852	-0.95524
-0.01000	0.02485	0.08291	-3.02405
0.00000	0.02548	0.03288	-83445742364

TABLE 4.3. 400-step Runge-Kutta solution for f_2.

x	f_{11}	f_{11}'	f_{11}''
-0.49750	0.00000	0.00000	0.00000
-0.49000	0.00000	0.00000	0.00005
-0.47000	0.00000	0.00000	0.00045
-0.45000	0.00000	0.00002	0.00127
-0.43000	0.00000	0.00006	0.00252
-0.41000	0.00000	0.00013	0.00426
-0.39000	0.00001	0.00023	0.00653
-0.37000	0.00001	0.00039	0.00942
-0.35000	0.00002	0.00061	0.01304
-0.33000	0.00004	0.00092	0.01749
-0.31000	0.00006	0.00132	0.02293
-0.29000	0.00009	0.00184	0.02950
-0.27000	0.00013	0.00251	0.03737
-0.25000	0.00019	0.00335	0.04672
-0.23000	0.00027	0.00439	0.05766
-0.21000	0.00037	0.00566	0.07028
-0.19000	0.00050	0.00721	0.08454
-0.17000	0.00066	0.00906	0.10019
-0.15000	0.00086	0.01122	0.11664
-0.13000	0.00111	0.01372	0.13272
-0.11000	0.00141	0.01652	0.14630
-0.09000	0.00177	0.01953	0.15361
-0.07000	0.00219	0.02257	0.14779
-0.05000	0.00267	0.02527	0.11531
-0.03000	0.00320	0.02680	0.02357
-0.01000	0.00373	0.02503	-0.26642
0.00000	0.00395	0.01936	-6780869476

TABLE 4.4. 400-step Runge-Kutta solution for f_{11}.

x	f_{21}	f_{21}'	f_{21}''
-0.49750	0.00000	0.00000	0.00000
-0.49000	0.00000	0.00000	0.00000
-0.47000	0.00000	0.00000	0.00000
-0.45000	0.00000	0.00000	0.00002
-0.43000	0.00000	0.00000	0.00006
-0.41000	0.00000	0.00000	0.00012
-0.39000	0.00000	0.00001	0.00023
-0.37000	0.00000	0.00001	0.00038
-0.35000	0.00000	0.00002	0.00060
-0.33000	0.00000	0.00004	0.00089
-0.31000	0.00000	0.00006	0.00128
-0.29000	0.00000	0.00009	0.00177
-0.27000	0.00001	0.00013	0.00239
-0.25000	0.00001	0.00019	0.00316
-0.23000	0.00001	0.00026	0.00409
-0.21000	0.00002	0.00035	0.00521
-0.19000	0.00003	0.00047	0.00652
-0.17000	0.00004	0.00061	0.00802
-0.15000	0.00005	0.00079	0.00969
-0.13000	0.00007	0.00100	0.01145
-0.11000	0.00009	0.00125	0.01317
-0.09000	0.00012	0.00152	0.01457
-0.07000	0.00015	0.00182	0.01515
-0.05000	0.00019	0.00212	0.01385
-0.03000	0.00024	0.00235	0.00813
-0.01000	0.00029	0.00235	-0.01290
0.00000	0.00031	0.00200	25188657784

TABLE 4.5. 400-step Runge-Kutta solution for f_{21}.

x	f_{12}	f_{12}'	f_{12}''
-0.49750	0.00000	0.00000	0.00004
-0.49000	0.00000	0.00000	0.00071
-0.47000	0.00000	0.00007	0.00696
-0.45000	0.00000	0.00033	0.02109
-0.43000	0.00002	0.00097	0.04475
-0.41000	0.00005	0.00220	0.07954
-0.39000	0.00011	0.00424	0.12699
-0.37000	0.00022	0.00737	0.18855
-0.35000	0.00041	0.01189	0.26552
-0.33000	0.00071	0.01810	0.35883
-0.31000	0.00115	0.02635	0.46874
-0.29000	0.00178	0.03696	0.59429
-0.27000	0.00265	0.05021	0.73240
-0.25000	0.00381	0.06629	0.87644
-0.23000	0.00532	0.08522	1.01408
-0.21000	0.00723	0.10667	1.12381
-0.19000	0.00960	0.12975	1.16971
-0.17000	0.01242	0.15265	1.09332
-0.15000	0.01568	0.17206	0.80134
-0.13000	0.01924	0.18231	0.14646
-0.11000	0.02285	0.17398	-1.10336
-0.09000	0.02598	0.13179	-3.31798
-0.07000	0.02773	0.03084	-7.11107
-0.05000	0.02655	-0.17040	-13.60541
-0.03000	0.01976	-0.54749	-25.37105
-0.01000	0.00237	-1.28077	-53.12595
0.00000	-0.01373	-2.05861	2.53E13

TABLE 4.6. 400-step Runge-Kutta solution for f_{12}.

x	f_{22}	f_{22}'	f_{22}''
-0.49750	0.00000	0.00000	0.00000
-0.49000	0.00000	0.00000	0.00000
-0.47000	0.00000	0.00000	0.00005
-0.45000	0.00000	0.00000	0.00024
-0.43000	0.00000	0.00001	0.00072
-0.41000	0.00000	0.00003	0.00163
-0.39000	0.00000	0.00008	0.00315
-0.37000	0.00000	0.00017	0.00547
-0.35000	0.00001	0.00031	0.00877
-0.33000	0.00002	0.00052	0.01321
-0.31000	0.00003	0.00084	0.01892
-0.29000	0.00005	0.00129	0.02591
-0.27000	0.00008	0.00189	0.03405
-0.25000	0.00013	0.00266	0.04291
-0.23000	0.00019	0.00360	0.05159
-0.21000	0.00027	0.00471	0.05838
-0.19000	0.00038	0.00591	0.06034
-0.17000	0.00051	0.00706	0.05247
-0.15000	0.00066	0.00789	0.02662
-0.13000	0.00082	0.00791	-0.03047
-0.11000	0.00097	0.00632	-0.14008
-0.09000	0.00105	0.00174	-0.33685
-0.07000	0.00100	-0.00811	-0.67923
-0.05000	0.00067	-0.02710	-1.27560
-0.03000	-0.00019	-0.06240	-2.37614
-0.01000	-0.00204	-0.13140	-5.02699
0.00000	-0.00367	-0.20507	2.45E+12

TABLE 4.7. 400-step Runge-Kutta solution for f_{22}.

x	$10^{-3} f_{13}$	$10^{-6} f_{13}'$	$10^{-8} f_{13}''$
-0.49750	-0.00024	-0.00017	-0.00056
-0.49000	-0.00286	-0.00050	-0.00037
-0.47000	-0.01897	-0.00105	-0.00020
-0.45000	-0.04335	-0.00135	-0.00011
-0.43000	-0.07199	-0.00148	-0.00003
-0.41000	-0.10175	-0.00147	0.00004
-0.39000	-0.12974	-0.00131	0.00012
-0.37000	-0.15297	-0.00099	0.00020
-0.35000	-0.16817	-0.00050	0.00029
-0.33000	-0.17161	0.00019	0.00040
-0.31000	-0.15894	0.00112	0.00053
-0.29000	-0.12511	0.00231	0.00067
-0.27000	-0.06445	0.00380	0.00082
-0.25000	0.02898	0.00559	0.00096
-0.23000	0.16059	0.00760	0.00104
-0.21000	0.33330	0.00965	0.00097
-0.19000	0.54384	0.01128	0.00058
-0.17000	0.77543	0.01153	-0.00048
-0.15000	0.98365	0.00850	-0.00286
-0.13000	1.06858	-0.00169	-0.00795
-0.11000	0.81718	-0.02702	-0.01875
-0.09000	-0.22667	-0.08531	-0.04290
-0.07000	-3.10081	-0.22205	-0.10398
-0.05000	-10.53872	-0.58568	-0.30294
-0.03000	-32.43577	-1.94647	-1.42089
-0.01000	-156.49761	-18.96095	-38.26245
0.00000	-17590.21100	-44161.68500	-3.47E+49

TABLE 4.8. 400-step Runge-Kutta solution for f_{13}.

x	$10^{-2} f_{23}$	$10^{-5} f_{23}'$	$10^{-7} f_{23}''$
-0.49750	-0.00012	-0.00009	-0.00029
-0.49000	-0.00150	-0.00026	-0.00019
-0.47000	-0.00975	-0.00053	-0.00008
-0.45000	-0.02141	-0.00062	-0.00001
-0.43000	-0.03350	-0.00057	0.00006
-0.41000	-0.04332	-0.00039	0.00013
-0.39000	-0.04803	-0.00006	0.00021
-0.37000	-0.04444	0.00045	0.00030
-0.35000	-0.02883	0.00115	0.00041
-0.33000	0.00331	0.00211	0.00055
-0.31000	0.05735	0.00335	0.00071
-0.29000	0.13972	0.00495	0.00089
-0.27000	0.25789	0.00694	0.00110
-0.25000	0.42013	0.00936	0.00131
-0.23000	0.63477	0.01217	0.00149
-0.21000	0.90842	0.01522	0.00153
-0.19000	1.24239	0.01810	0.00128
-0.17000	1.62539	0.01991	0.00038
-0.15000	2.01917	0.01874	-0.00186
-0.13000	2.32976	0.01068	-0.00685
-0.11000	2.34734	-0.01252	-0.01777
-0.09000	1.60952	-0.06945	-0.04269
-0.07000	-0.95637	-0.20798	-0.10653
-0.05000	-8.21111	-0.58481	-0.31605
-0.03000	-30.58159	-2.01382	-1.49651
-0.01000	-160.69222	-19.97643	-40.40887
0.00000	-18573.07412	-46642.11203	-3.67E+49

TABLE 4.9. 400-step Runge-Kutta solution for f_{23}.

i	x_s=-ih	a_1	b_1	c_1
1	-0.00125	0.24125	0.00000	14.11680
2	-0.00250	0.24125	0.00000	14.12940
3	-0.00375	0.24125	0.00000	14.13020
4	-0.00500	0.24125	0.00000	14.13040
5	-0.00625	0.24125	0.00000	14.13050
6	-0.00750	0.24125	0.00000	14.13050
7	-0.00875	0.24125	0.00000	14.13050
8	-0.01000	0.24125	0.00000	14.13050

i	x_s=-ih	a_2	b_2	c_2
1	-0.00125	0.02548	0.03245	1.70084
2	-0.00250	0.02548	0.03245	1.70217
3	-0.00375	0.02548	0.03245	1.70226
4	-0.00500	0.02548	0.03245	1.70229
5	-0.00625	0.02548	0.03245	1.70232
6	-0.00750	0.02548	0.03245	1.70237
7	-0.00875	0.02548	0.03246	1.70244

TABLE 4.10. Values of the constants a_i, b_i and c_i.

i	x_s=-ih	a_{11}	b_{11}	c_{11}
1	-0.00125	0.00395	0.01929	0.37173
2	-0.00250	0.00395	0.01929	0.37193
3	-0.00375	0.00395	0.01929	0.37194
4	-0.00500	0.00395	0.01929	0.37195
5	-0.00625	0.00395	0.01929	0.37196
6	-0.00750	0.00395	0.01929	0.37196
7	-0.00875	0.00395	0.01929	0.37196
8	-0.00100	0.00395	0.01929	0.37196

i	x_s=-ih	a_{12}	b_{12}	c_{12}
1	-0.00125	-0.01373	-2.06367	10.89810
2	-0.00250	-0.01373	-2.06359	10.93540
3	-0.00375	-0.01373	-2.06351	10.94930
4	-0.00500	-0.01373	-2.06343	10.95900
5	-0.00625	-0.01373	-2.06334	10.96680
6	-0.00750	-0.01373	-2.06325	10.97340
7	-0.00875	-0.01373	-2.06316	10.97930

TABLE 4.11. Values of the constants a_{1j}, b_{1j} and c_{1j} (j=1,2).

i	x_s=-ih	a_{13}	b_{13}	c_{13}
1	-0.00125	-1.61×10^{11}	-2.58×10^{14}	-1.03×10^{17}
2	-0.00250	35930.5	-2.07×10^{6}	-6.93×10^{8}
3	-0.00375	36780.8	-391813	-4.69×10^{7}
4	-0.00500	36889.2	-241165	-6.00×10^{6}
5	-0.00625	36912.8	-215795	-680211
6	-0.00750	36920	-209598	377053
7	-0.00875	36922.9	-207629	656338
8	-0.00100	36924.4	-206845	748322
9	-0.01125	36925.5	-206454	785216
10	-0.01250	36926.4	-206209	803175
11	-0.01375	36927.3	-206026	813703
12	-0.01500	36928.3	-205870	820920
13	-0.01625	36929.3	-205729	826450
14	-0.01750	36930.3	-205598	830987
15	-0.01875	36931.4	-205474	834846

TABLE 4.12. Values of the constants a_{13}, b_{13} and c_{13}.

i	x_s=-ih	a_{23}	b_{23}	c_{23}
1	-0.00125	2057.64	-8.0×10^{6}	-5.38×10^{9}
2	-0.00250	4304.28	-213736	-7.32×10^{7}
3	-0.00375	4394.24	-36490.4	-4.88×10^{6}
4	-0.00500	4405.74	-20556.3	-565661
5	-0.00625	4408.26	-17866	-2488.59
6	-0.00750	4409.04	-17205.8	109606
7	-0.00875	4409.36	-16994.4	139321
8	-0.00100	4409.53	-16909.4	149157
9	-0.01125	4409.65	-16866.5	153127
10	-0.01250	4409.75	-16839.6	155072
11	-0.01375	4409.86	-16819.3	156216
12	-0.01500	4409.96	-16802.2	157003
13	-0.01625	4410.7	-16786.7	157608
14	-0.01750	4410.19	-16772.3	158105
15	-0.01875	4410.31	-16758.6	158530

TABLE 4.13. Values of the constants a_{23}, b_{23} and c_{23}.

Previous Studies	h	A	α	Presentstudy
Elder† (1965)	19	490000	2.4	2.58
Vest & Arpaci† (1969)	20	370000	3.5	2.83
deVahl Davis & Mallinson* (1975)	10	940000	2.56	2.07
Bergholz† (1978)	20	360576	2.59	2.85

TABLE 4.14. Comparison of the value of the critical wavenumber given by (4.5.11) with the results of previous studies near† and above* the onset of secondary instability.

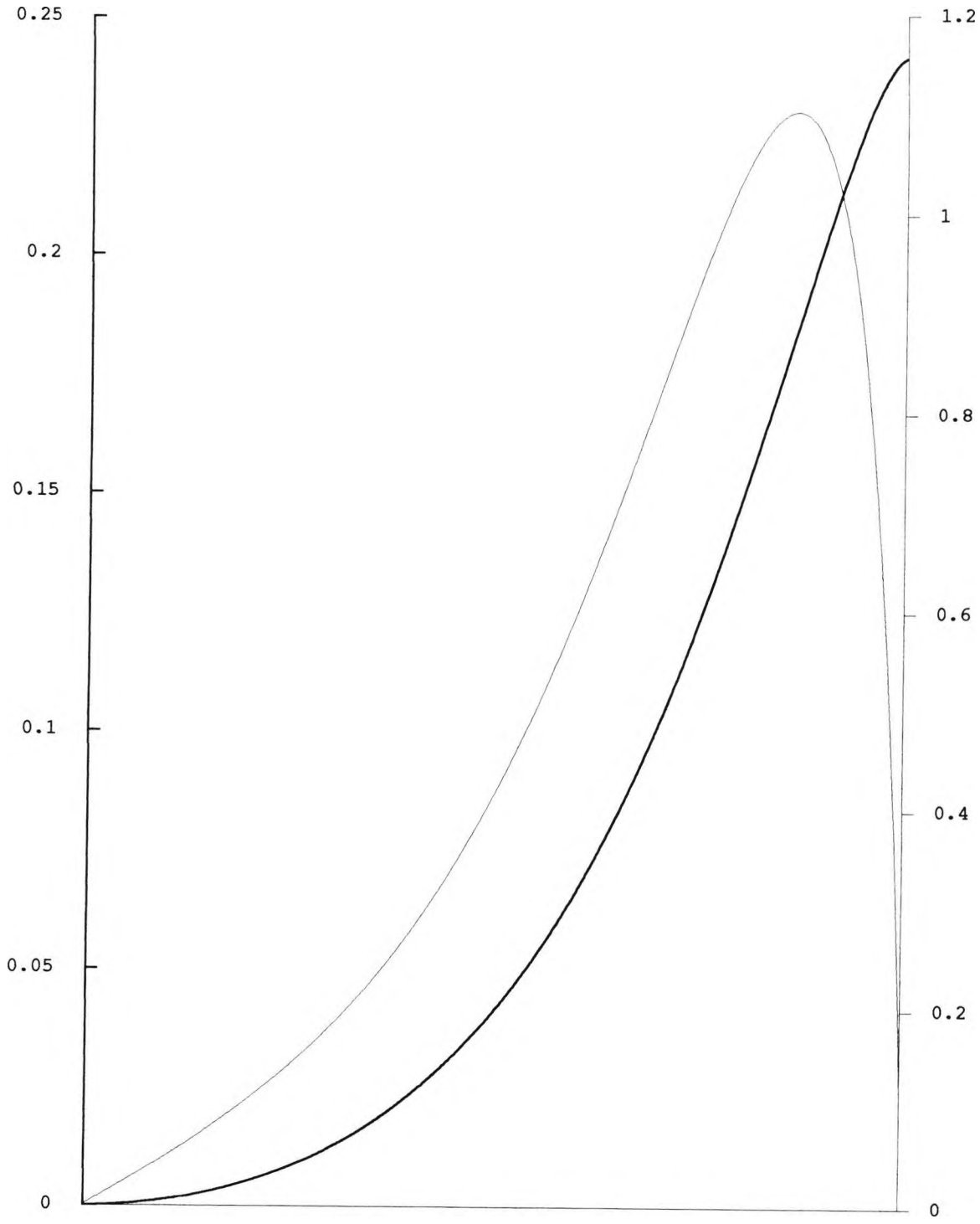

FIGURE 4.1. The outer function f_1 —— and its derivative —— at the critical point γ_0 in the interval [-0.5,0].

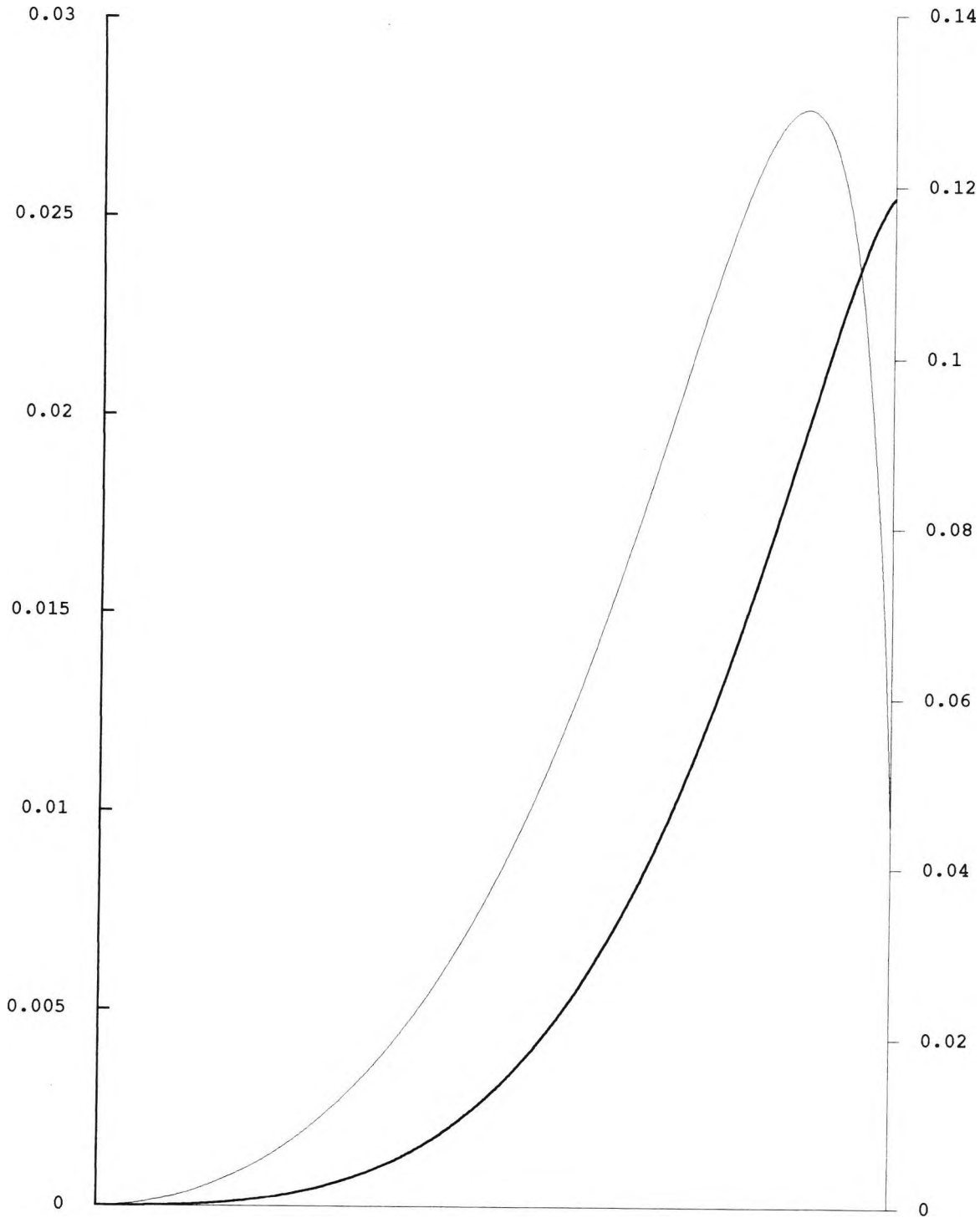

FIGURE 4.2. The outer function f_2 —— and its derivative —— in the interval [-0.5,0].

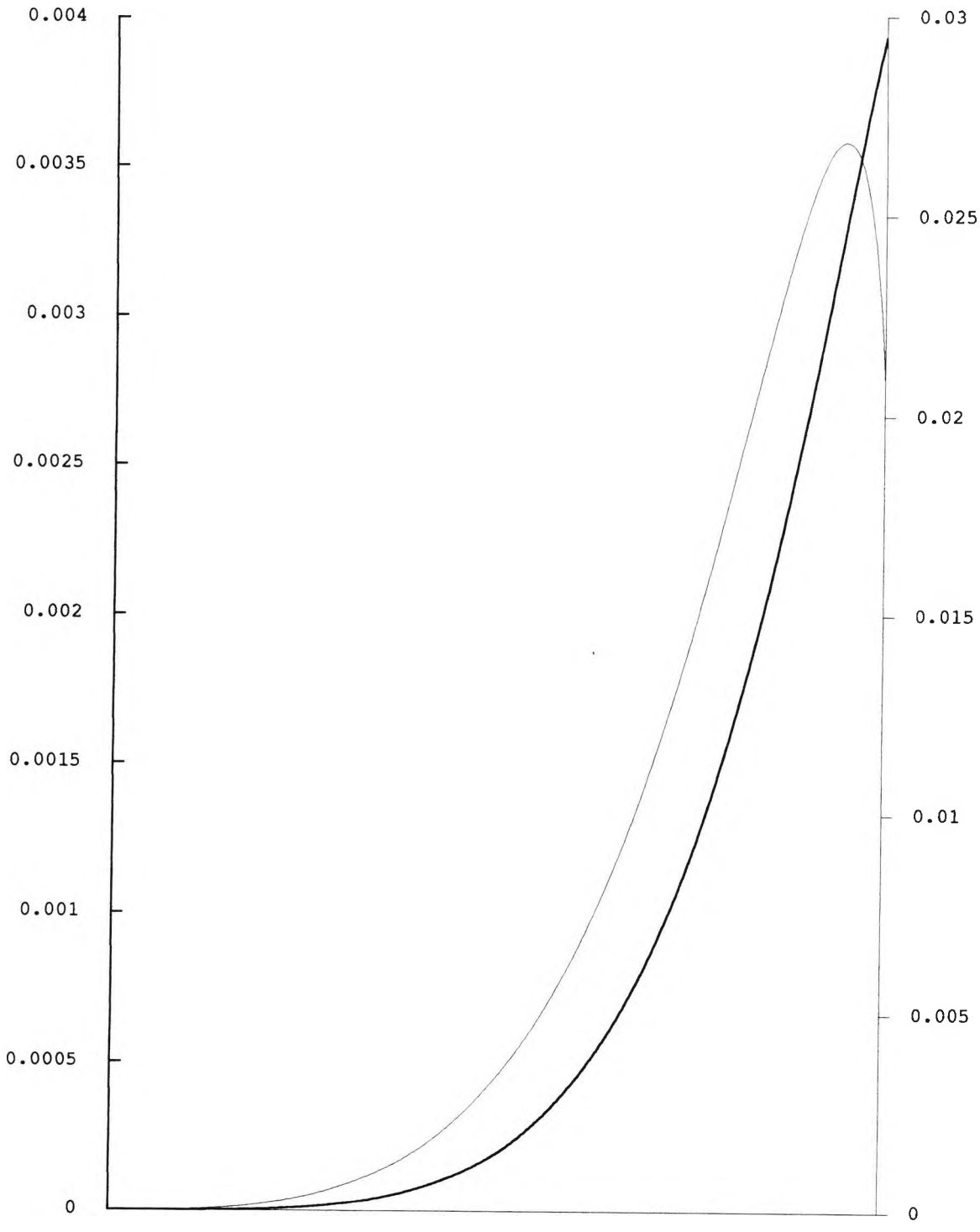

FIGURE 4.3. The outer function f_{11} —— and its derivative —— in the interval [-0.5,0].

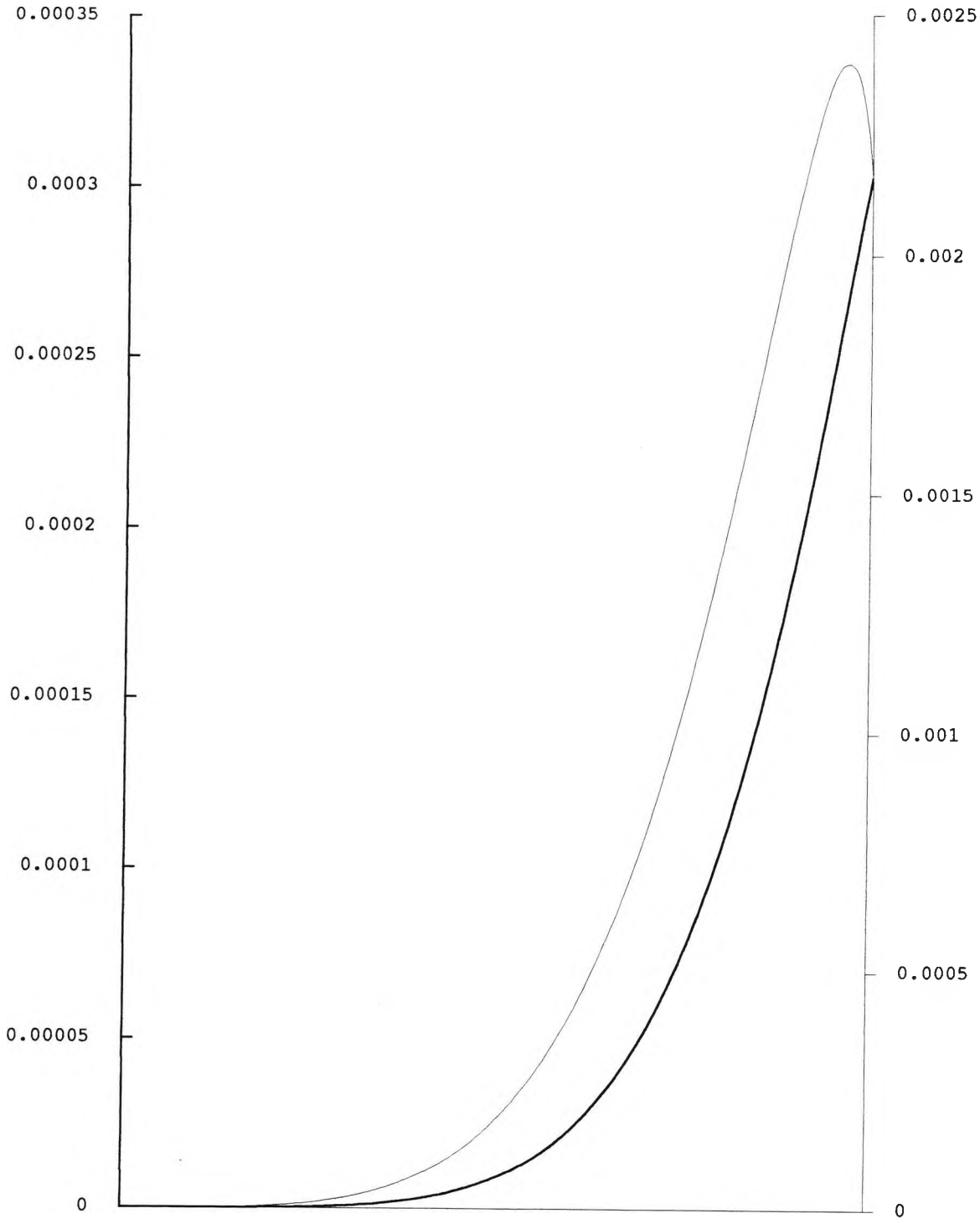

FIGURE 4.4. The outer function f_{21} —— and its derivative f'_{21} —— in the interval [-0.5,0].

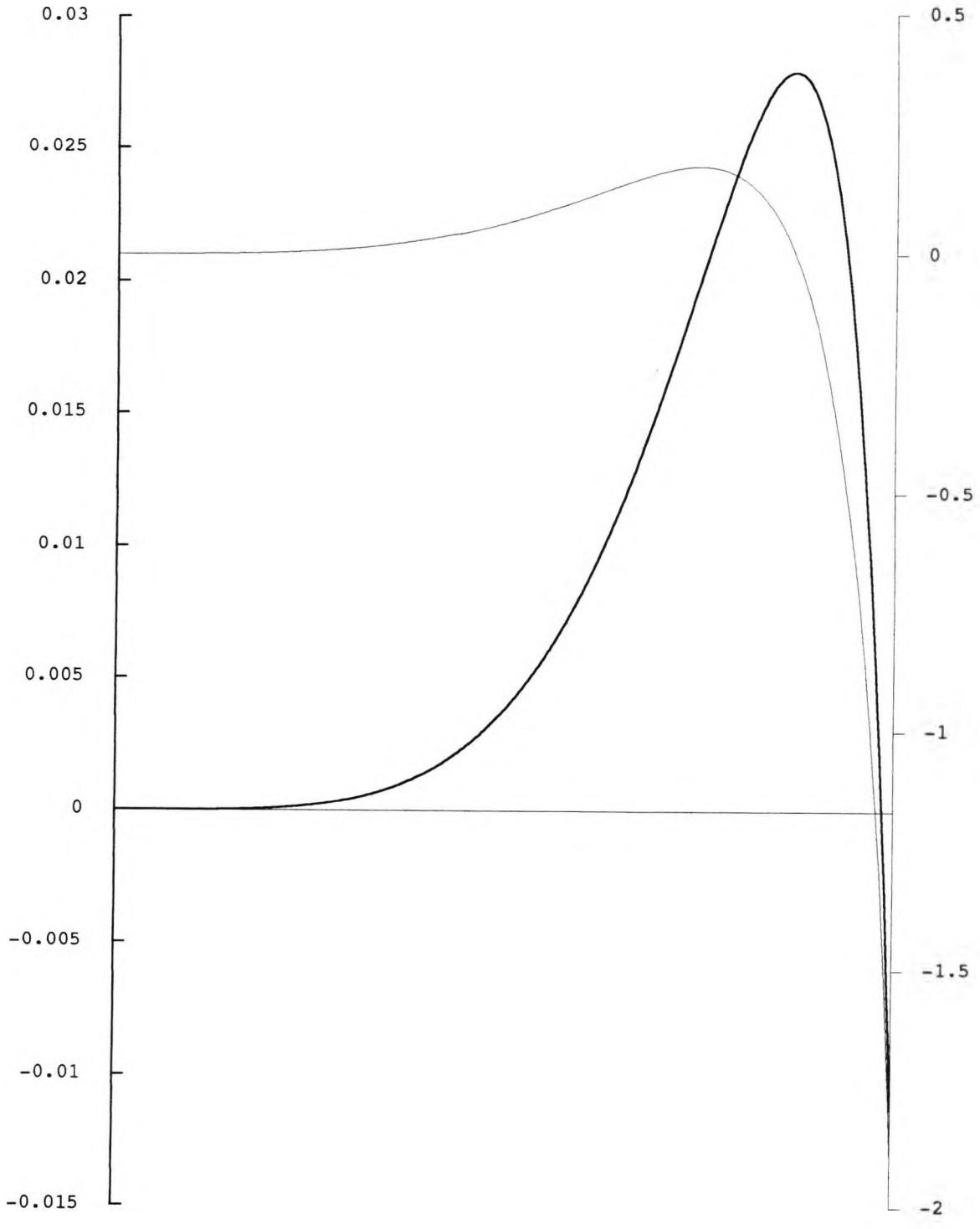

FIGURE 4.5. The outer function f_{12} —— and its derivative —— in the interval [-0.5,0].

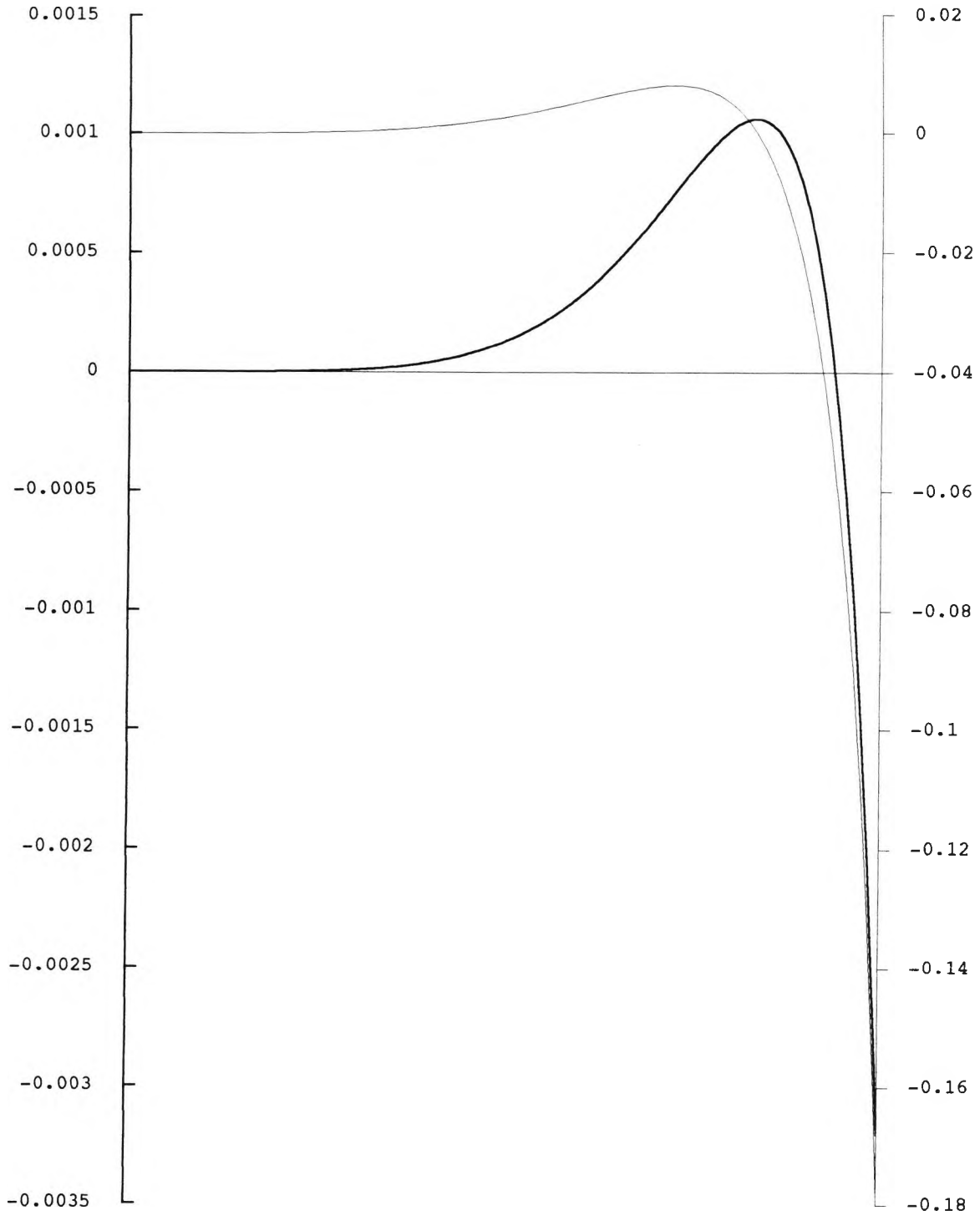

FIGURE 4.6. The outer function f_{22} —— and its derivative —— in the interval [-0.5,0].

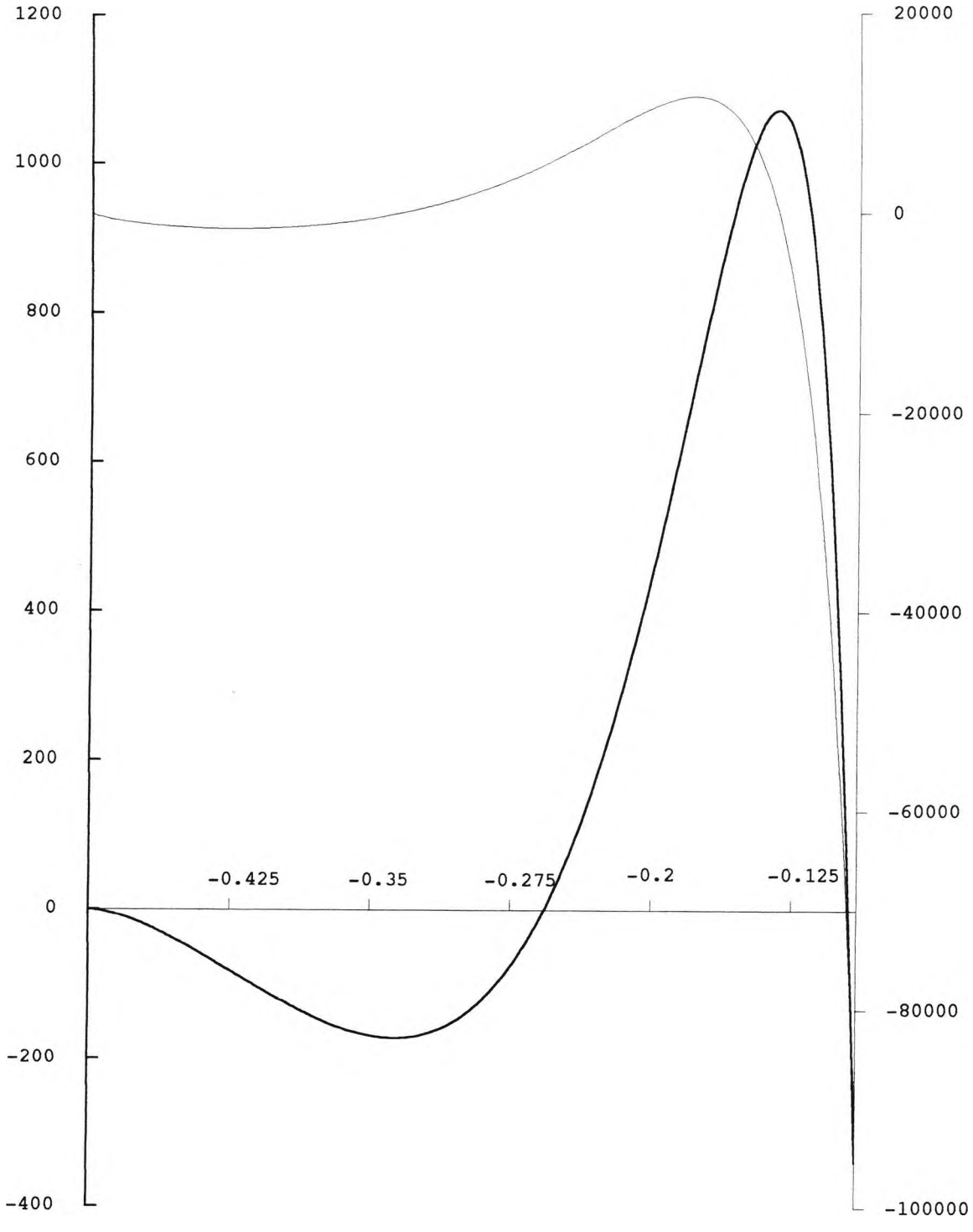

FIGURE 4.7. The outer function f_{13} —— and its derivative f'_{13} —— in the interval [-0.5,0].

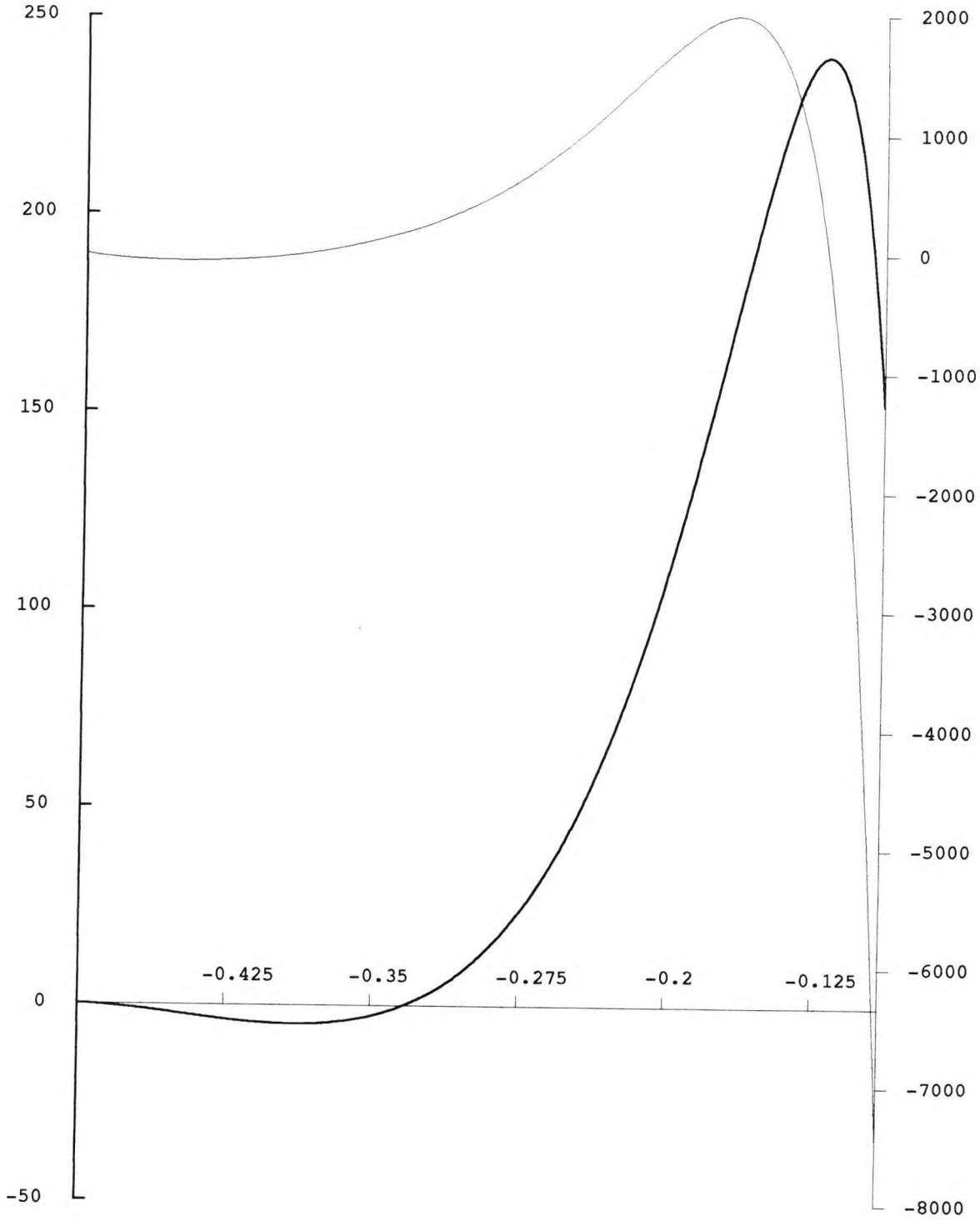

FIGURE 4.8. The outer function f_{23} —— and its derivative f'_{23} —— in the interval [-0.5,0].

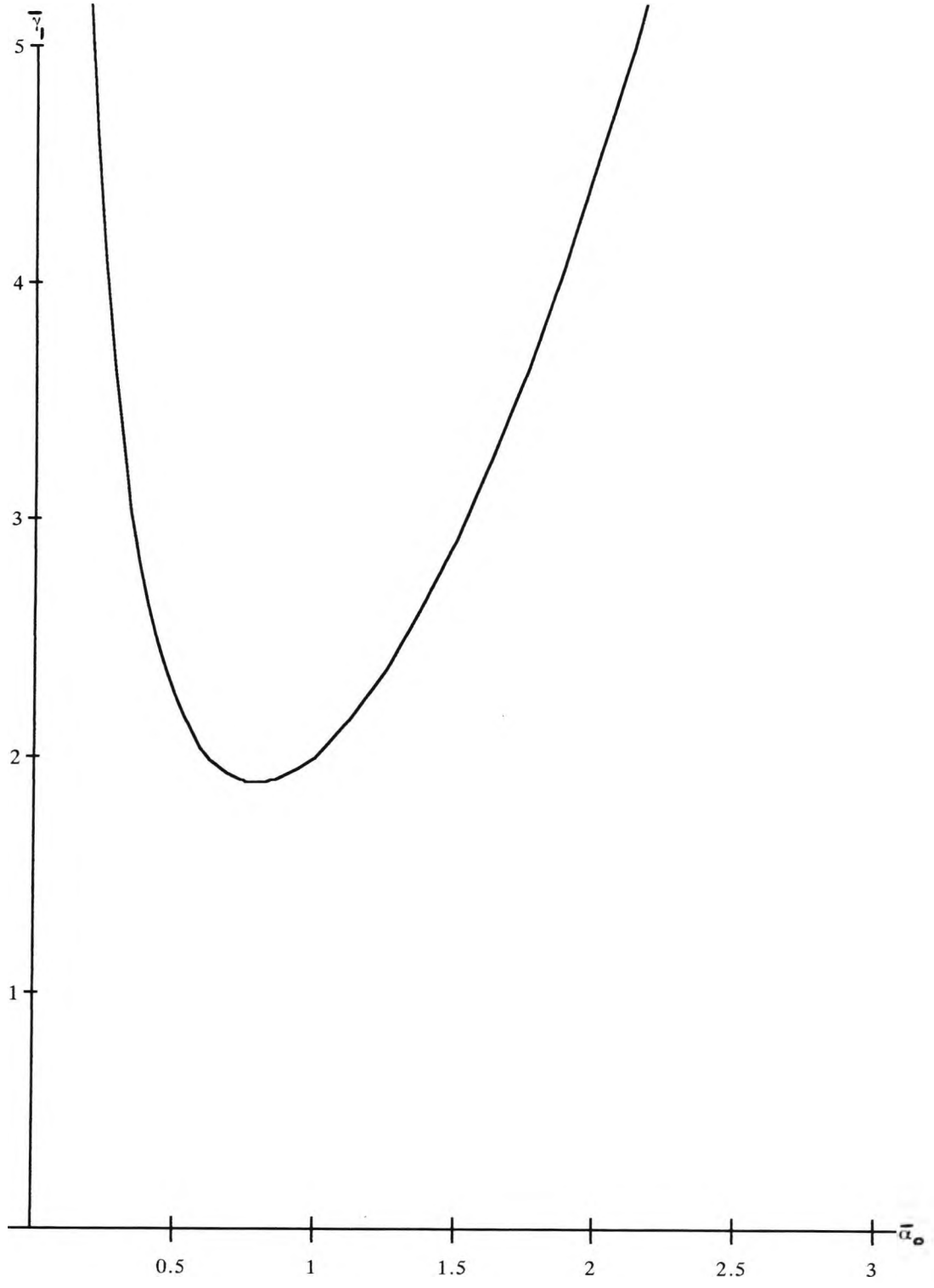

FIGURE 4.9. The scaled convective parameter $\bar{\gamma}_1$ as a function of the scaled wavenumber $\bar{\alpha}_0$.

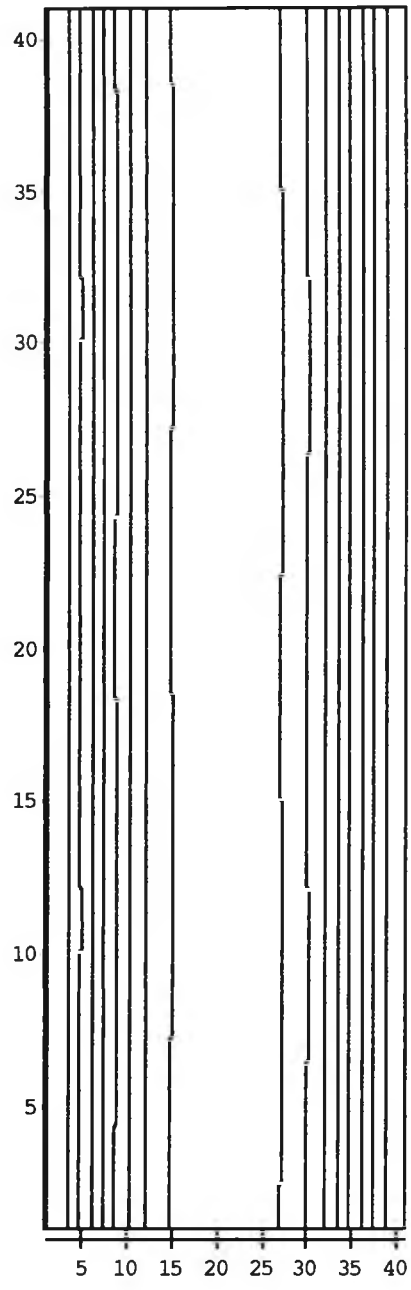

FIGURE 4.10. Streamlines of the overall flow as given by (1.2.26) for $\varepsilon = 0.0001$.

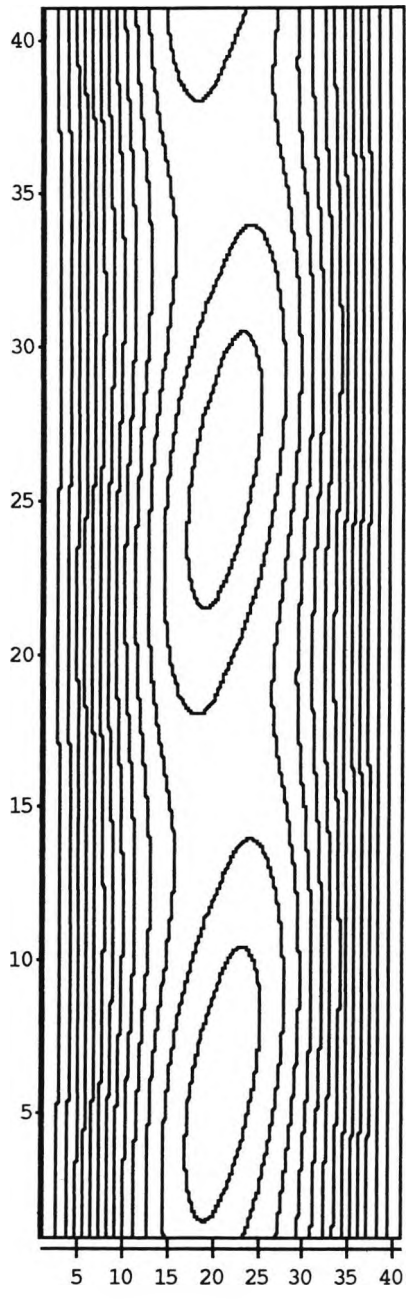

FIGURE 4.11. Streamlines of the overall flow as given by (1.2.26) for $\varepsilon = 0.001$.

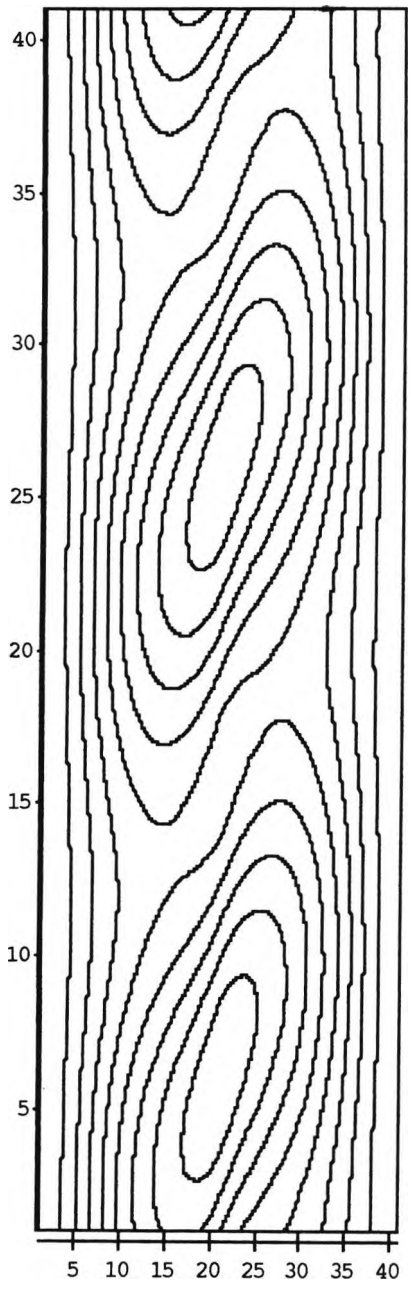

FIGURE 4.12. Streamlines of the overall flow as given by (1.2.26) for $\varepsilon = 0.005$.

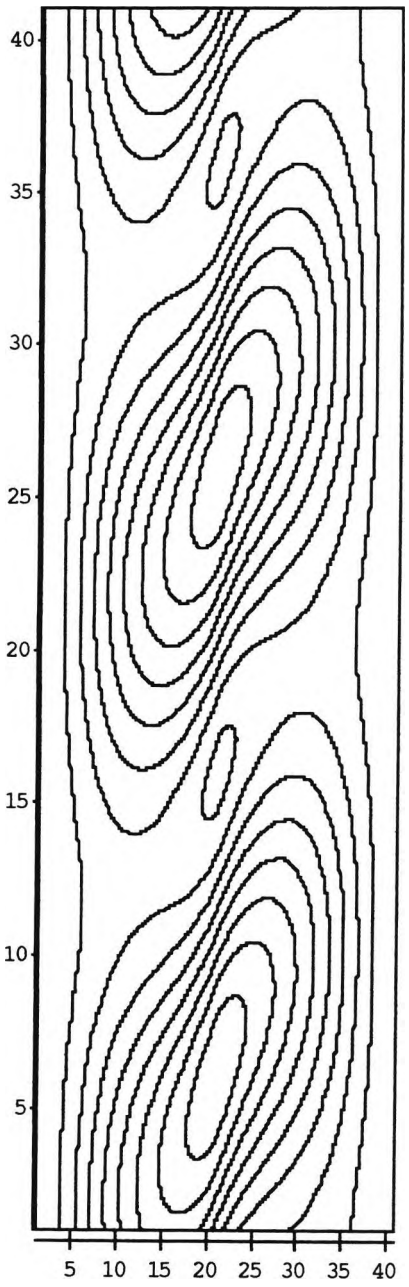

FIGURE 4.13. Streamlines of the overall flow as given by (1.2.26) for $\varepsilon = 0.01$.

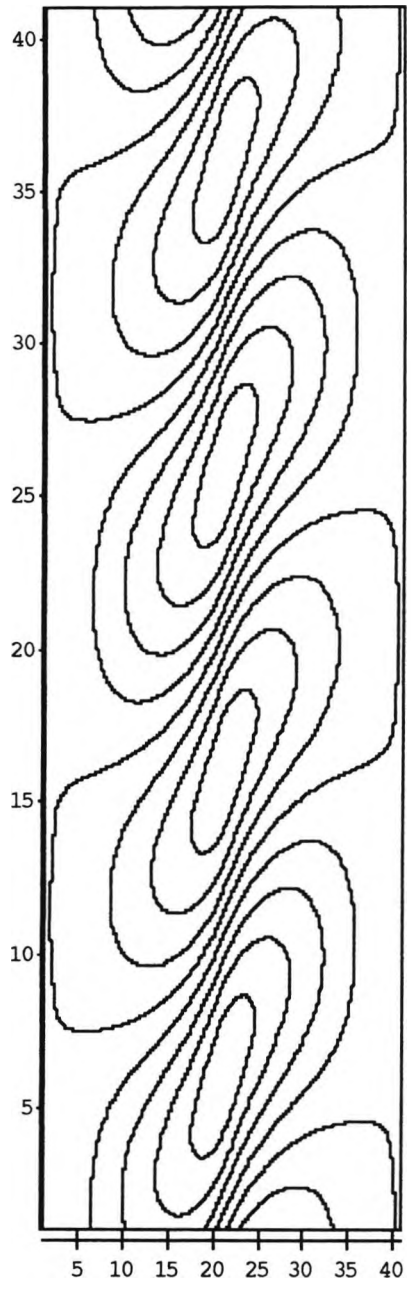

FIGURE 4.14. Streamlines of the overall flow as given by (1.2.26) for $\varepsilon = 0.1$.

CHAPTER FIVE : LARGE RAYLEIGH NUMBER SOLUTION NEAR THE CRITICAL POINT AT LARGE PRANDTL NUMBERS

5.1 Introduction

In this chapter we consider the effect of large but finite Prandtl number on the local form of the neutral stability curve near γ_0. This is done by relaxing the assumption of infinite Prandtl number made in Chapter 2.

The problem is formulated in Section 5.2, and the form of the solution in the limit as $A \to \infty$ is discussed in Section 5.3. This involves choice of an appropriate scaling for the Prandtl number in terms of A that leads to modification of the equation of the neutral stability curve obtained at the end of Chapter 3. The form of the modified neutral stability curve is obtained in Section 5.4 and a discussion of the effect on the critical value of γ_0 is given in Section 5.5.

5.2 Formulation

Consider the non-dimensional Boussinesq system defined in Chapter 1 by equations (1.2.6)-(1.2.9). Investigation of the stability of the exact solution

$$\psi = A\Psi(x), \qquad T = \beta z + \Theta(x), \tag{5.2.1}$$

is carried out by adding perturbations, ϕ and θ, to the stream

function and temperature in (5.2.1). Substitution into the Boussinesq system (1.2.6)-(1.2.9), elimination of the pressure and linearization in the perturbations ϕ and θ, leads to the following system of equations and boundary conditions for finite values of the Prandtl number:

$$\phi'''' - 2\alpha^2\,\phi'' + \alpha^4\phi = \theta' + i\alpha[A\Psi'''\phi - (c + A\Psi')(\phi'' - \alpha^2\phi)]/\sigma, \qquad (5.2.2)$$

$$\theta'' - \alpha^2\theta = i\alpha[A\Theta'\phi - (c + A\Psi')\theta] - 4\gamma^4\phi', \qquad (5.2.3)$$

$$\phi = \phi' = \theta = 0 \qquad (x = \pm 1/2), \qquad (5.2.4)$$

as obtained in (1.2.27)-(1.2.29).

Since we are concerned with stationary disturbances the wave speed, c, is taken to be zero and the linear stability equations become

$$\phi'''' - 2\alpha^2\,\phi'' + \alpha^4\phi - \theta' = i\alpha A[\Psi'''\phi - \Psi'(\phi'' - \alpha^2\phi)]/\sigma, \qquad (5.2.5)$$

$$\theta'' - \alpha^2\theta = i\alpha A[\Theta'\phi - \Psi'\theta] - 4\gamma^4\phi', \qquad (5.2.6)$$

to be solved subject to the boundary conditions

$$\phi = \phi' = \theta = 0 \qquad (x = \pm 1/2). \qquad (5.2.7)$$

This chapter is concerned with large Prandtl numbers such that the right-hand side of (5.2.5) modifies the equation of the neutral stability curve obtained in Chapter 4.

5.3 Solution Structure for $A \to \infty$

In the limit as $A \to \infty$, the scales of the vertical wavenumber and the vertical stratification γ are assumed to be those defined in Chapter 2,

$$\alpha = \alpha_0 A^{-1/3}, \quad \gamma = \gamma_0 + A^{-2/3}\gamma_1 + \ldots, \quad A \to \infty, \tag{5.3.1}$$

and the outer solution for the perturbation functions ϕ and θ is again of the form

$$\phi = \phi_0 + A^{-2/3}\phi_1 + \ldots, \quad A \to \infty, \tag{5.3.2}$$

$$\theta = \theta_0 + A^{-2/3}\theta_1 + \ldots, \quad A \to \infty. \tag{5.3.3}$$

The scale for the Prandtl number σ is chosen to bring the term on the right-hand side of (5.2.5) into play in the solution for the second order function ϕ_1. This requires

$$\sigma = \sigma_0 A^{4/3}, \quad A \to \infty, \tag{5.3.4}$$

with σ_0 assumed to be finite. Substitution of (5.3.1)-(5.3.4) into (5.2.5) and (5.2.6) and equating terms of like powers of A, leads to the following equations and boundary conditions for ϕ_0, θ_0, ϕ_1 and θ_1 :

$$\theta_0 = \frac{\Theta_0'}{\Psi_0'}\phi_0, \tag{5.3.5}$$

$$\phi_0'''' = \theta_0', \tag{5.3.6}$$

$$\theta_1 = \frac{\Theta_0'}{\Psi_0'}\phi_1 + \gamma_1 \frac{\Theta_1'\phi_0 - \Psi_1'\theta_0}{\Psi_0'} - \frac{\theta_0'' + 4\gamma_0^4\phi_0'}{i\alpha_0\Psi_0'}, \qquad (5.3.7)$$

$$\phi_1'''' = \theta_1' + 2\alpha_0^2\phi_0'' + i\alpha_0[\Psi_0'''\phi_0 - \Psi_0'\phi_0'']/\sigma_0, \qquad (5.3.8)$$

$$\phi_0 = \phi_0' = \phi_1 = \phi_1' = 0 \qquad (x = \pm 1/2). \qquad (5.3.9)$$

The leading order outer solutions ϕ_0, θ_0 are precisely those identified in Chapter 2, while the solutions for ϕ_1 and θ_1 are modified by the incorporation of the term involving σ_o in the equation for ϕ_1, which after elimination of θ_1 becomes

$$\phi_1'''' - \frac{d}{dx}\left(\frac{\Theta_0'}{\Psi_0'}\phi_1\right) = \frac{d}{dx}\left(2\alpha_0^2\phi_0' + \gamma_1\frac{\Theta_1'\phi_0 - \Psi_1'\theta_0}{\Psi_0'} - \frac{\theta_0'' + 4\gamma_0^4\phi_0'}{i\alpha_0\Psi_0'}\right) + i\alpha_0[\Psi_0'''\phi_0 - \Psi_0'\phi_0'']/\sigma_0. \qquad (5.3.10)$$

This can be integrated once to give the third order equation

$$\phi_1''' - \frac{\Theta_0'}{\Psi_0'}\phi_1 = 2\alpha_0^2\phi_0' + \gamma_1\frac{\Theta_1'\phi_0 - \Psi_1'\theta_0}{\Psi_0'} - \frac{\theta_0'' + 4\gamma_0^4\phi_0'}{i\alpha_0\Psi_0'} + i\alpha_0[\Psi_0''\phi_0 - \Psi_0'\phi_0']/\sigma_0 + k_1, \qquad (5.3.11)$$

where k_1 is an arbitrary constant. This is to be solved subject to the boundary conditions

$$\phi_1 = \phi_1' = 0 \qquad (x = \pm 1/2). \qquad (5.3.12)$$

The solution for ϕ_1 can be written in the form

$$\phi_1 = \bar{\phi}_1 + 2\alpha_0^2\phi_{11} + \gamma_1\phi_{12} - \phi_{13}/i\alpha_0 + i\alpha_0\phi_{14}/\sigma_0 , \qquad (5.3.13)$$

where the functions $\bar{\phi}_1$, ϕ_{11}, ϕ_{12} and ϕ_{13} are those determined in Section 2.4. In order to complete the general solution for ϕ_1 we now need the particular solution ϕ_{14} associated with σ_0. The equation for ϕ_{14} is

$$\phi_{14}''' - \frac{\Theta_0'}{\Psi_0'}\phi_{14} = \Psi_0''\phi_0 - \Psi_0'\phi_0' , \qquad (5.3.14)$$

and this must be solved subject to the boundary conditions

$$\phi_{14} = \phi_{14}' = 0 \qquad (x = \pm 1/2) . \qquad (5.3.15)$$

The solution for ϕ_{14} in $x<0$ can be written in the form

$$\phi_{14} = \sigma_1^- f_{14}(x) + \sigma_2^- f_{24}(x). \qquad (5.3.16)$$

where f_{i4} (i=1,2) are real functions of x uniquely defined by

$$f_{i4}''' - \frac{\Theta_0'}{\Psi_0'}f_{i4} = \Psi_0''f_i - \Psi_0'f_i' ; \quad (f_{i4}, f_{i4}', f_{i4}'') = (0,0,0) \text{ at } x=-1/2. \qquad (5.3.17)$$

By symmetry, the solution for ϕ_{14} in $x>0$ can be written in the form

$$\phi_{14} = -\sigma_1^- f_{14}(-x) - \sigma_2^- f_{24}(-x). \qquad (5.3.18)$$

The asymptotic forms of the functions f_{i4} (i=1,2) as $x \to 0-$

are given by

$$f_{i4} = a_{i4} + b_{i4}x + c_{i40}x^2\ln|x| + c_{i4}x^2 + d_{i4}x^3 + e_{i40}x^4\ln|x| + e_{i4}x^4 + \ldots \quad . \tag{5.3.19}$$

Here the real constants a_{i4}, b_{i4} and c_{i4} must be determined by a numerical solution and the remaining constants are obtained in terms of these, in the usual way, by substituting (5.3.19), together with the asymptotic forms of the functions f_i (i=1,2) and the appropriate expansions of the base flow functions into equations (5.3.17) and equating terms of like powers in x. This leads to the formulae

$$c_{i40} = a_{i4}s_0/2, \quad d_{i4} = (b_{i4}s_0 + a_i\omega_1)/6,$$

$$e_{i40} = c_{i40}s_0/24, \quad e_{i4} = (s_0c_{i4} + s_1a_{i4} - 26e_{i40})/24 \quad . \tag{5.3.20}$$

The constants a_{i4}, b_{i4} and c_{i4} were determined numerically using the same method as that outlined in Chapter 4. Expansions for the functions f_{i4} about the point X=x+1/2=0 were used to start the Runge-Kutta scheme one step away from the point X=0. These expansions are given by

$$f_{i4} = \sum_{k=3}^{\infty} E_{ik}X^k \quad , \qquad X \to 0 \quad . \tag{5.3.21}$$

Formulae for the real constants E_{ik} (i=1,2; k=3,4,...) are given in Appendix III. Tables 5.1-5.2 give the Runge-Kutta solutions for the functions f_{i4}. The constants a_{i4}, b_{i4} and c_{i4} are determined in the same way used to determine the constants a_{ij}, b_{ij} and c_{ij} (j=1,2,3) in Chapter 4 by solving the following system of equations for i=1,2 :

$$a_{i4}\,\Gamma_{i4} + b_i\,\Lambda_{i4} + c_{i4}\chi_{i4} = f_{i4}(x_s) + K_{i4}\,, \tag{5.3.22}$$

$$a_{i4}\,\Gamma'_{i4} + b_{i4}\,\Lambda'_{i4} + c_{i4}\,\chi'_{i4} = f'_{i4}(x_s) + K'_{i4}\,, \tag{5.3.23}$$

$$a_{i4}\,\Gamma''_{i4} + b_{i4}\,\Lambda''_{i4} + c_{i4}\chi''_{i4} = f''_{i4}(x_s) + K''_{i4}\,, \tag{5.3.24}$$

where the real functions Γ_{i4}, Λ_{i4}, χ_{i4}, K_{i4}, their first derivatives, denoted by Γ'_{i4}, Λ'_{i4}, χ'_{i4}, K'_{i4} and their second derivatives, denoted by Γ''_{i4}, Λ''_{i4}, χ''_{i4}, K''_{i4} are defined explicitly in Appendix III. Values of the real constants a_{i4}, b_{i4} and c_{i4} are given in Table 5.3.

The asymptotic form of ϕ_{14} as $x\to 0\pm$ can now be deduced from (5.3.16) and (5.3.18), so that

$$\phi_{14} = a^{\pm}_{14} + b^{\pm}_{14}\,x + c^{\pm}_{140}\,x^2\ln|x| + c^{\pm}_{14}\,x^2 + d^{\pm}_{14}\,x^3 + e^{\pm}_{140}\,x^4\ln|x| + e^{\pm}_{14}\,x^4 + \ldots, \quad x\to 0\pm\,, \tag{5.3.25}$$

where the constants $a^{\pm}_{14}$, $b^{\pm}_{14}$, ..., are defined in terms of the real constants $a_{14}, b_{14}, \ldots, a_{24}, b_{24}, \ldots$, by the vector equation

$$\underline{v}^{\pm}_{14} = \sigma_1^{\pm}\,\underline{v}_{14} + \sigma_1^{\pm}\,\underline{v}_{24}\,, \tag{5.3.26}$$

where

$\underline{v}^{\pm}_{14} = (\mp a^{\pm}_{14}, b^{\pm}_{14}, \mp c^{\pm}_{140}, \mp c^{\pm}_{14}, d^{\pm}_{14}, \ldots)$, $\underline{v}_{14} = (a_{14}, b_{14}, c_{140}, c_{14}, d_{14}, \ldots)$ and $\underline{v}_{24} = (a_{24}, b_{24}, c_{240}, c_{24}, d_{24}, \ldots)$.

We can now obtain the general form of ϕ_1 as $|x|\to 0$ by combining equations (2,4,10), (2.4.17), (2.4.27), (2.4.36) and (5.3.25) in the overall solution (5.3.13). Thus

$$\phi_1 = \delta_1^{\pm}/x + a_1^{\pm} + b_{10}^{\pm} x\ln|x| + b_1^{\pm} x + c_{10}^{\pm} x^2\ln|x| + c_1^{\pm} x^2 + d_{10}^{\pm} x^3\ln|x| + d_1^{\pm} x^3 + \cdots , \quad x\to 0\pm , \tag{5.3.27}$$

where the constants $\delta_1^{\pm}$, $a_1^{\pm}$,... are defined by the vector relation

$$\underline{v}_1^{\pm} = \bar{\underline{v}}_1^{\pm} + 2\alpha_0^2\, \underline{v}_{11}^{\pm} + \gamma_1 \underline{v}_{12}^{\pm} - \underline{v}_{13}^{\pm}/i\alpha_0 + i\alpha_0 \underline{v}_{14}^{\pm}/\sigma_0 . \tag{5.3.28}$$

Here the vectors $\bar{\underline{v}}_1^{\pm}$, $\underline{v}_{11}^{\pm}$, $\underline{v}_{12}^{\pm}$ and $\underline{v}_{13}^{\pm}$ are those defined in Chapter 2 (see(2.4.41)-(2.4.44)), and

$$\underline{v}_1^{\pm} = (\delta_1^{\pm}, a_1^{\pm}, b_{10}^{\pm}, b_1^{\pm}, c_{10}^{\pm}, c_1^{\pm}, d_{10}^{\pm}, d_1^{\pm},\ldots), \tag{5.3.29}$$

with

$$\underline{v}_{14}^{\pm} = (0, a_{14}^{\pm}, 0, b_{14}^{\pm}, c_{140}^{\pm}, c_{14}^{\pm}, 0, d_{14}^{\pm},\ldots), \tag{5.3.30}$$

the appropriate extension of the vector defined in (5.3.26). Equation (5.3.27) gives the complete asymptotic form for the solution ϕ_1 as $|x|\to 0$. The temperature function θ_1 bears the same relation to ϕ_1 as that given in Chapter 2, so that the asymptotic form for θ_1 is given by (2.4.52)

$$\theta_1 = \Delta_1^{\pm}/x^4 + A_1^{\pm}/x^2 + B_1^{\pm}/x + C_{10}^{\pm}\ln|x| + C_1^{\pm} + \cdots, \tag{5.3.31}$$

where the constants $\Delta_1^{\pm}$, $A_1^{\pm}$,... are as defined in Chapter 2, (2.4.46)-(2.4.50).

Combining the forms of ϕ_0, ϕ_1, θ_0 and θ_1 as $|x|\to 0$, the overall asymptotic forms of the perturbation functions ϕ and θ are as in Chapter 2,

$$\phi = a_0^{\pm} + b_0^{\pm}x + c_{00}^{\pm}x^2\ln|x| + c_0^{\pm}x^2 + d_0^{\pm}x^3 + e_{00}^{\pm}x^4\ln|x| + e_0^{\pm}x^4 + g_0^{\pm}x^5 + h_{00}^{\pm}x^6\ln|x| + h_0^{\pm}x^6 + \cdots + A^{-2/3}(\delta_1^{\pm}/x + a_1^{\pm} + b_{10}^{\pm}x\ln|x| + b_1^{\pm}x + c_{10}^{\pm}x^2\ln|x| + c_1^{\pm}x^2 + d_{10}^{\pm}x^3\ln|x| + d_1^{\pm}x^3 + \ldots), \quad x\to 0\pm , \tag{5.3.32}$$

$$\theta = A_0^{\pm}/x + B_0^{\pm} + C_{00}^{\pm}x\ln|x| + C_0^{\pm}x + D_0^{\pm}x^2 + E_{00}^{\pm}x^3\ln|x| + E_0^{\pm}x^3 + \cdots + A^{-2/3}(\Delta_1^{\pm}/x^4 + A_1^{\pm}/x^2 + B_1^{\pm}/x + C_{10}^{\pm}\ln|x| + C_1^{\pm} + \cdots), \quad x\to 0\pm , \tag{5.3.33}$$

the only difference being the new forms of the constants $a_1^{\pm}, \ldots$ as defined in (5.3.28) and (5.3.29). The next step is to consider the solution in the critical layer and to use the relevant bridging conditions to determine the modified form of the neutral stability curve near γ_0. This is considered in the next section.

5.4 Neutral Stability Curve

The order at which the extra term on the right hand side of (5.2.5) comes into effect in the critical layer solution is higher by order $A^{-2/9}$ than that required to obtain the bridging conditions (3.3.47)-(3.3.50) and (3.4.37)-(3.4.40). Thus the bridging conditions obtained in Chapter 3 are still valid here.

We now consider the effect of the additional outer term ϕ_{14} on the equation of the neutral stability curve which was given in Section 3.7 (equation (3.7.26)). The procedure used in Section 3.7 to obtain the neutral stability curve is repeated here taking into account the additional term. We recall from

Section 3.7, that in $x<0$ the solution for ϕ_0 is given by

$$\phi_0 = \sigma_1^- f_1(x) + \sigma_2^- f_2(x). \tag{5.4.1}$$

and that in $x>0$

$$\phi_1 = \sigma_1^+ f_1(-x) + \sigma_2^+ f_2(-x), \tag{5.4.2}$$

where σ_1^-, σ_2^-, σ_1^+ and σ_2^+ are complex constants and the functions f_i (i=1,2) are uniquely defined by the solutions of (2.3.5) and (2.3.4). Also the forms of f_i as $x\to 0-$ are given by (3.7.3) leading to the general form of ϕ_0 as $x\to 0\pm$:

$$\phi_0 = a_0^{\pm} + b_0^{\pm}x + c_{00}^{\pm} x^2 \ln|x| + c_0^{\pm}x^2 + d_0^{\pm}x^3 + \ldots, \tag{5.4.3}$$

where the constants $a_0^{\pm}$, $b_0^{\pm}$,..., are related to those of f_i (i=1,2) by the vector relation

$$\underline{v}_0^{\pm} = \sigma_1^{\pm}\, \underline{v}_1 + \sigma_2^{\pm}\, \underline{v}_2, \tag{5.4.4}$$

with the vectors $\underline{v}_0^{\pm}$, $\underline{v}_1$ and $\underline{v}_2$ as defined in Chapter 2. Consideration of the leading order bridging conditions (3.3.47)-(3.3.50) then leads to the system of equations given by

$$(\sigma_1^- - \sigma_1^+)a_1 + (\sigma_2^- - \sigma_2^+)a_2 = 0, \tag{5.4.5}$$

$$(\sigma_1^- + \sigma_1^+)b_1 + (\sigma_2^- + \sigma_2^+)b_2 = 0, \tag{5.4.6}$$

$$(\sigma_1^- - \sigma_1^+)c_1 + (\sigma_2^- - \sigma_2^+)c_2 = -i\pi s_0(\sigma_1^- a_1 + \sigma_2^- a_2)/2\ , \tag{5.4.7}$$

$$(\sigma_1^- + \sigma_1^+)d_1 + (\sigma_2^- + \sigma_2^+)d_2 = 0. \tag{5.4.8}$$

Substitution of d_1 and d_2 into (5.4.8) and the fact that b_1 is

zero leads to formulae for the constants σ_1^+, σ_2^-, σ_2^+ in terms of the arbitrary constant σ_1^-, as given by (3.7.11)-(3.7.13). Thus far the analysis is identical to that of Chapter 3.

The solution for ϕ_1 in $x<0$ is given by

$$\phi_1 = \bar{\sigma}_1^- f_1(x) + \bar{\sigma}_2^- f_2(x) + 2\alpha_0^2 [\sigma_1^- f_{11}(x) + \sigma_2^- f_{21}(x)] + \gamma_1 [\sigma_1^- f_{12}(x) + \sigma_2^- f_{22}(x)] - [\sigma_1^- f_{13}(x) + \sigma_2^- f_{23}(x)]/i\alpha_0 + i\alpha_0 [\sigma_1^- f_{14}(x) + \sigma_2^- f_{24}(x)]/\sigma_0, \tag{5.4.9}$$

where the real functions f_{ij} (i=1,2; j=1,2,3) are defined in Chapter 2 and the real functions f_{i4} (i=1,2) are defined in Section 5.3. The corresponding solution for ϕ_1 in $x>0$ is given by

$$\phi_1 = \bar{\sigma}_1^- f_1(-x) + \bar{\sigma}_2^- f_2(-x) + 2\alpha_0^2 [\sigma_1^- f_{11}(-x) + \sigma_2^- f_{21}(-x)] + \gamma_1 [\sigma_1^- f_{12}(-x) + \sigma_2^- f_{22}(-x)] - [\sigma_1^- f_{13}(-x) + \sigma_2^- f_{23}(-x)]/i\alpha_0 - i\alpha_0 [\sigma_1^- f_{14}(-x) + \sigma_2^- f_{24}(-x)]/\sigma_0. \tag{5.4.10}$$

The forms of f_{ij} (i=1,2; j=1,2,3) as $x\to 0-$ are given in Chapter 2, and the forms of f_{i4} (i=1,2) are given by

$$f_{i4} = a_{i4} + b_{i4}x + c_{i40}x^2 \ln|x| + c_{i4}x^2 + d_{i4}x^3 + e_{i40}x^4 \ln|x| + e_{i4}x^4 + \ldots, \quad x\to 0-, \tag{5.4.11}$$

where the constants a_{i4}, b_{i4} and c_{i4} are as determined in Section 5.3 and the remaining constants are known in terms of these from the formulae (5.3.20). Then as $|x|\to 0$, ϕ_1 is given by

$$\phi_1 = \delta_1^\pm/x + a_1^\pm + b_{10}^\pm x\ln|x| + b_1^\pm x + c_{10}^\pm x^2 \ln|x| + c_1^\pm x^2 + d_{10}^\pm x^3 \ln|x| + d_1^\pm x^3 + \ldots, \quad x\to 0\pm, \tag{5.4.12}$$

where the constants $\delta_1^{\pm}$, $a_1^{\pm}$,..., are defined by the relation

$$\underline{v}_1^{\pm} = \bar{\underline{v}}_1^{\pm} + 2\alpha_0^2 \underline{v}_{11}^{\pm} + \gamma_1 \underline{v}_{12}^{\pm} - \underline{v}_{13}^{\pm}/i\alpha_0 + i\alpha_0 \underline{v}_{14}^{\pm}/\sigma_0 , \qquad (5.4.13)$$

with the vectors $\bar{\underline{v}}_1^{\pm}$, $\underline{v}_{11}^{\pm}$, $\underline{v}_{12}^{\pm}$, $\underline{v}_{13}^{\pm}$ as defined in Chapter 2 and $\underline{v}_{14}^{\pm}$ as defined in Section 5.3. Substitution of these into the bridging conditions

$$b_1^+ = b_1^- + \mu_0 \pi (\mu_0 - 12\omega_3) a_0^+/6\alpha_0\omega_1^3 \qquad (5.4.14)$$

and

$$d^+_1 = d^-_1 + \mu_0 \pi a_0^+ [s_0(\mu_0 - 12\omega_3)/6 - (4\gamma_0^4 + 3s_1 + s_0^2/8)\omega_1]/6\omega_1^3\alpha_0 \qquad (5.4.15)$$

and using the fact that b_1 is zero and that $a_0^+ = \sigma_1^- a_1 + \sigma_2^- a_2$ leads, after simplification, to the following equations

$$(\bar{\sigma}_2^- + \bar{\sigma}_2^+)b_2 + (\sigma_1^- + \sigma_1^+)(2\alpha_0^2 b_{11} + \gamma_1 b_{12}) + (\sigma_1^- - \sigma_1^+)[i\alpha_0 b_{14}/\sigma_0 - b_{13}/i\alpha_0] + (\sigma_2^- - \sigma_2^+)[i\alpha_0 b_{24}/\sigma_0 - b_{23}/i\alpha_0] = -\mu_0\pi(\mu_0 - 12\omega_3)(\sigma_1^- a_1 + \sigma_2^- a_2)/6\alpha_0\omega_1^3, \qquad (5.4.16)$$

$$(\bar{\sigma}_2^- + \bar{\sigma}_2^+)d_2 + (\sigma_1^- + \sigma_1^+)(2\alpha_0^2 d_{11} + \gamma_1 d_{12}) + (\sigma_1^- - \sigma_1^+)[i\alpha_0 d_{14}/\sigma_0 - d_{13}/i\alpha_0] + (\sigma_2^- - \sigma_2^+)[i\alpha_0 d_{24}/\sigma_0 - d_{23}/i\alpha_0] = -\mu_0\pi[s_0(-2\omega_3 + \mu_0/6) - (4\gamma_0^4 + 3s_1 + s_0^2/8)\omega_1](\sigma_1^- a_1 + \sigma_2^- a_2)/6\alpha_0\omega_1^3 . \qquad (5.4.17)$$

We recall, from Chapter 3, that

$$\sigma_1^+ = \frac{4a_2c_1 - 4a_1c_2 + i\pi s_0 a_1 a_2}{4a_2c_1 - 4a_1c_2 - i\pi s_0 a_1 a_2}\ \sigma_1^- , \qquad (5.4.18)$$

$$\sigma_2^- = \frac{i\pi s_0 a_1^2}{4a_2c_1 - 4a_1c_2 - i\pi s_0 a_1 a_2}\,\sigma_1^-, \qquad (5.4.19)$$

and

$$\sigma_2^+ = -\sigma_2^-. \qquad (5.4.20)$$

Substitution of (5.4.18)-(5.4.20) into (5.4.16) and (5.4.17), elimination of $(\bar{\sigma}_2^- + \bar{\sigma}_2^+)$ from the resulting equations and simplification then leads to the cubic equation

$$\alpha_0^3 + \bar{c}_0\alpha_0^2/\sigma_0 + \bar{c}_1\alpha_0\gamma_1 + \bar{c}_2 = 0, \qquad (5.4.21)$$

where

$$\bar{c}_0 = \pi a_1 s_0[a_1(b_2d_{24} - d_2b_{24}) - a_2(b_2d_{14} - d_2b_{14})]/3(a_2c_1 - a_1c_2)(d_2b_{11} - b_2d_{11})$$
$$= -0.00108 \qquad (5.4.22)$$

and $\bar{c}_1$ and $\bar{c}_2$ are given by (3.7.27) and (3.7.28) respectively. Equation (5.4.21) represents the modified neutral stability curve. It contains the additional quadratic term $\bar{c}_0\alpha_0^2/\sigma_0$ generated by the large but finite Prandtl number of the fluid. In the next section we consider how this affects the critical wavenumber α_0 and the critical value of γ_1 at the onset of instability.

5.5 Critical Wavenumber

We begin by scaling out the constants $\bar{c}_0$, $\bar{c}_1$ and $\bar{c}_2$ from equation (5.4.21). This is done by use of the transformations

$$\alpha_0 = \bar{\alpha}_0\,\bar{c}_2^{\,1/3}, \qquad (5.5.1)$$

$$\gamma_1 = -\bar{\gamma}_1 \bar{c}_2^{2/3}/\bar{c}_1 \ , \qquad (5.5.2)$$

$$\sigma_0 = -\bar{\sigma}_0 \bar{c}_0/\bar{c}_2^{1/3} \ , \qquad (5.5.3)$$

giving

$$\bar{\alpha}_0^3 - \bar{\alpha}_0^2/\bar{\sigma}_0 - \bar{\alpha}_0\bar{\gamma}_1 + 1 = 0 \ . \qquad (5.5.4)$$

From (5.5.4), $\bar{\gamma}_1$ can be written in terms of $\bar{\alpha}_0$ and $\bar{\sigma}_0$ as

$$\bar{\gamma}_1 = \bar{\alpha}_0^2 - \bar{\alpha}_0/\bar{\sigma}_0 + 1/\bar{\alpha}_0 . \qquad (5.5.5)$$

The minimum value of $\bar{\gamma}_1$ is obtained by setting the derivative of $\bar{\gamma}_1$ with respect to $\bar{\alpha}_0$ equal to zero and, solving for $\bar{\alpha}_0$, we obtain the critical value of the wavenumber $\bar{\alpha}_0$ as

$$\bar{\alpha}_{0\,crit} = [1/4 + (1/16 + 1/432\bar{\sigma}_0^3)^{1/2} + 1/216\bar{\sigma}_0^3]^{1/3} + 1/\bar{\sigma}_0^2[36[1/4 + (1/16 + 1/432\bar{\sigma}_0^3)^{1/2} + 1/216\bar{\sigma}_0^3]^{1/3} + 1/6\bar{\sigma}_0, \qquad (5.5.6)$$

The corresponding critical value of $\bar{\gamma}_1$, $\bar{\gamma}_{1crit}$, is given by substitution of (5.5.6) into (5.5.5).

The behaviour of the critical wavenumber as $\bar{\sigma}_0$ approaches infinity is obtained by considering the limit $\bar{\sigma}_0 \to \infty$ in (5.5.6). This gives the result

$$\bar{\alpha}_{0crit} \to (1/2)^{1/3} \qquad \text{as} \qquad \bar{\sigma}_0 \to \infty \ , \qquad (5.5.7)$$

consistent with the result obtained in Chapter 4. Consideration of the opposite limit shows that as the scaled Prandtl number $\bar{\sigma}_0$ tends to zero, the critical wavenumber has the form

$$\bar{\alpha}_{0\,crit} \sim 1/2\bar{\sigma}_0 \qquad \text{as} \qquad \bar{\sigma}_0 \to 0 \ . \qquad (5.5.8)$$

The corresponding results for the critical value of the convective parameter are

$$\bar{\gamma}_{1\,crit} \to 3 \times 2^{-2/3} \ , \quad \bar{\sigma}_0 \to \infty \ , \tag{5.5.9}$$

$$\bar{\gamma}_{1\,crit} \sim -1/4\,\bar{\sigma}_0^{\,2} \ , \quad \bar{\sigma}_0 \to 0 \ . \tag{5.5.10}$$

Figures 5.3-5.4 show the neutral stability curve for various values of the scaled Prandtl number $\bar{\sigma}_0$ and the critical values $\bar{\alpha}_{0\,crit}$ and $\bar{\gamma}_{1crit}$ are shown as functions of the scaled Prandtl number $\bar{\sigma}_0$ in Figures 5.5-5.6. The graph of the critical vertical wavenumber α as a function of the convective parameter for various values of the scaled Prandtl number $\bar{\sigma}_0$ is shown in Figure 5.7 and is obtained by eliminating the Rayleigh number from the relations in (5.3.1).

x	$10^5 f_{14}$	$10^5 f_{14}'$	$10^5 f_{14}''$
-0.49750	0.00000	0.00000	-0.00001
-0.49000	0.00000	0.00000	-0.00066
-0.47000	-0.00000	-0.00013	-0.01791
-0.45000	-0.00001	-0.00104	-0.08275
-0.43000	-0.00004	-0.00265	-0.15093
-0.41000	-0.00013	-0.00721	-0.31950
-0.39000	-0.00035	-0.01604	-0.58039
-0.37000	-0.00081	-0.03117	-0.95201
-0.35000	-0.00166	-0.05497	-1.45137
-0.33000	-0.00309	-0.09018	-2.09363
-0.31000	-0.00536	-0.13976	-2.89150
-0.29000	-0.00880	-0.20694	-3.85439
-0.27000	-0.01378	-0.29507	-4.98727
-0.25000	-0.02076	-0.40755	-6.28891
-0.23000	-0.03026	-0.54769	-7.74921
-0.21000	-0.04287	-0.71843	-9.34525
-0.19000	-0.05922	-0.92213	-11.03519
-0.17000	-0.07999	-1.16001	-12.74893
-0.15000	-0.10585	-1.43150	-14.37343
-0.13000	-0.13745	-1.73318	-15.72925
-0.11000	-0.17532	-2.05702	-16.53093
-0.09000	-0.21978	-2.38769	-16.31408
-0.07000	-0.27070	-2.69762	-14.28174
-0.05000	-0.32722	-2.93706	-8.90649
-0.03000	-0.38709	-3.00858	3.49510
-0.01000	-0.44490	-2.66021	38.98888
0.00000	-0.46865	-1.91317	8.04E+11

TABLE 5.1. 400-step Runge-Kutta solution for f_{14}

x	$10^6 f_{24}$	$10^6 f_{24}'$	$10^6 f_{24}''$
-0.49750	0.00000	0.00000	0.00000
-0.49000	0.00000	0.00000	-0.00003
-0.47000	0.00000	-0.00002	-0.00249
-0.45000	0.00000	-0.00019	-0.01826
-0.43000	-0.00001	-0.00096	-0.06657
-0.41000	-0.00005	-0.00323	-0.17250
-0.39000	-0.00016	-0.00844	-0.36477
-0.37000	-0.00042	-0.01860	-0.67380
-0.35000	-0.00095	-0.03637	-1.12995
-0.33000	-0.00195	-0.06497	-1.76205
-0.31000	-0.00365	-0.10820	-2.59588
-0.29000	-0.00640	-0.17030	-3.65274
-0.27000	-0.01062	-0.25590	-4.94771
-0.25000	-0.01683	-0.36984	-6.48757
-0.23000	-0.02563	-0.51701	-8.26785
-0.21000	-0.03776	-0.70203	-10.26850
-0.19000	-0.05400	-0.92894	-12.44741
-0.17000	-0.07521	-1.20063	-14.73026
-0.15000	-0.10233	-1.51804	-16.99455
-0.13000	-0.13623	-1.87900	-19.04367
-0.11000	-0.17773	-2.27630	-20.56271
-0.09000	-0.22742	-2.69462	-21.03687
-0.07000	-0.28547	-3.10505	-19.57901
-0.05000	-0.35123	-3.45396	-14.48360
-0.03000	-0.42253	-3.63441	-1.63012
-0.01000	-0.49377	-3.36648	36.96396
0.00000	-0.52458	-2.60009	8.99E+11

TABLE 5.2. 400-step Runge-Kutta solution for f_{24}

i	$x_s=-ih$	$a_{14}\times10^5$	$b_{14}\times10^5$	$c_{14}\times10^4$
1	-0.00125	-0.46866	-1.90535	-4.03094
2	-0.00250	-0.46866	-1.90543	-4.03511
3	-0.00375	-0.46865	-1.90545	-4.03685
4	-0.00500	-0.46865	-1.90567	-4.03860
5	-0.00625	-0.46866	-1.90587	-4.04033
6	-0.00750	-0.46865	-1.90603	-4.04200
7	-0.00875	-0.46866	-1.90634	-4.04379

i	$x_s=-ih$	$a_{24}\times10^6$	$b_{24}\times10^6$	$c_{24}\times10^5$
1	-0.00125	-0.52458	-2.59128	-4.87413
2	-0.00250	-0.52458	-2.59128	-4.87690
3	-0.00375	-0.52458	-2.59128	-4.87708
4	-0.00500	-0.52458	-2.59128	-4.87712
5	-0.00625	-0.52458	-2.59128	-4.87715
6	-0.00750	-0.52458	-2.59128	-4.87718
7	-0.00875	-0.52458	-2.59128	-4.87721

TABLE 5.3. Values of the constants a_{i4}, b_{i4} and c_{i4} (i=1,2).

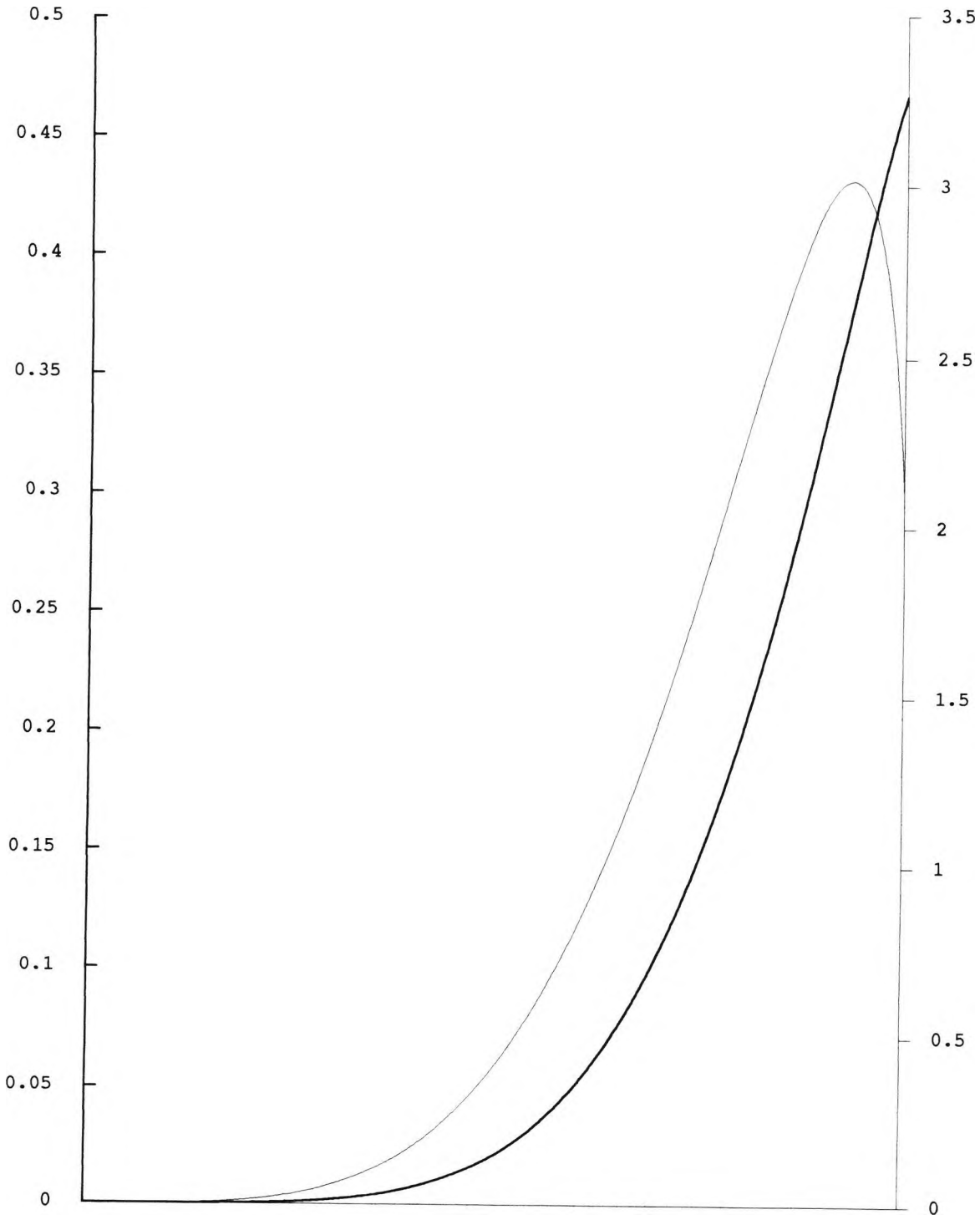

FIGURE 5.1. The outer function $-10^5 f_{14}$ —— and its derivative $-10^5 f'_{14}$ —— in the interval [-0.5,0].

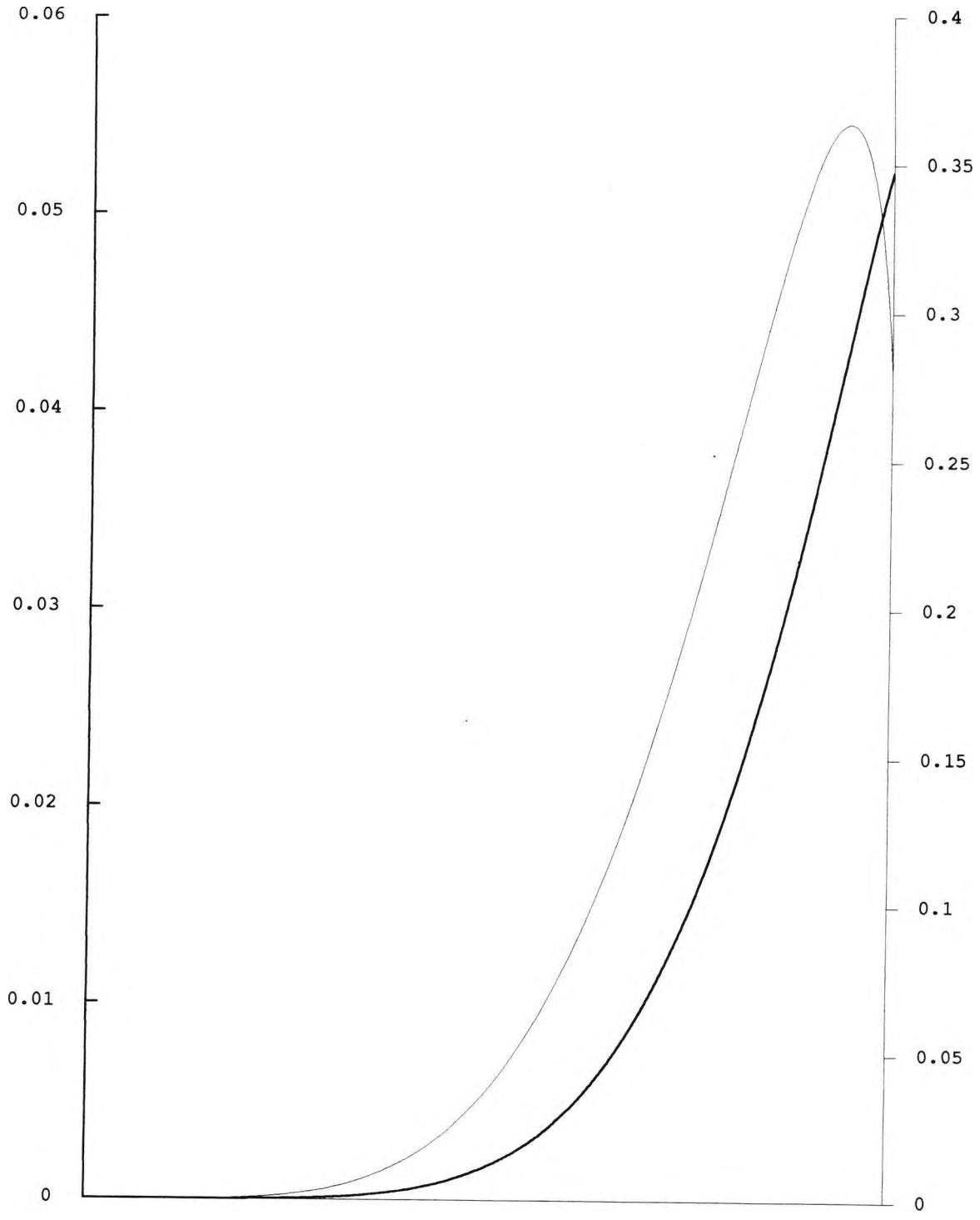

FIGURE 5.2. The outer function $-10^5 f_{24}$ —— and its derivative $-10^5 f'_{24}$ —— in the interval [-0.5,0].

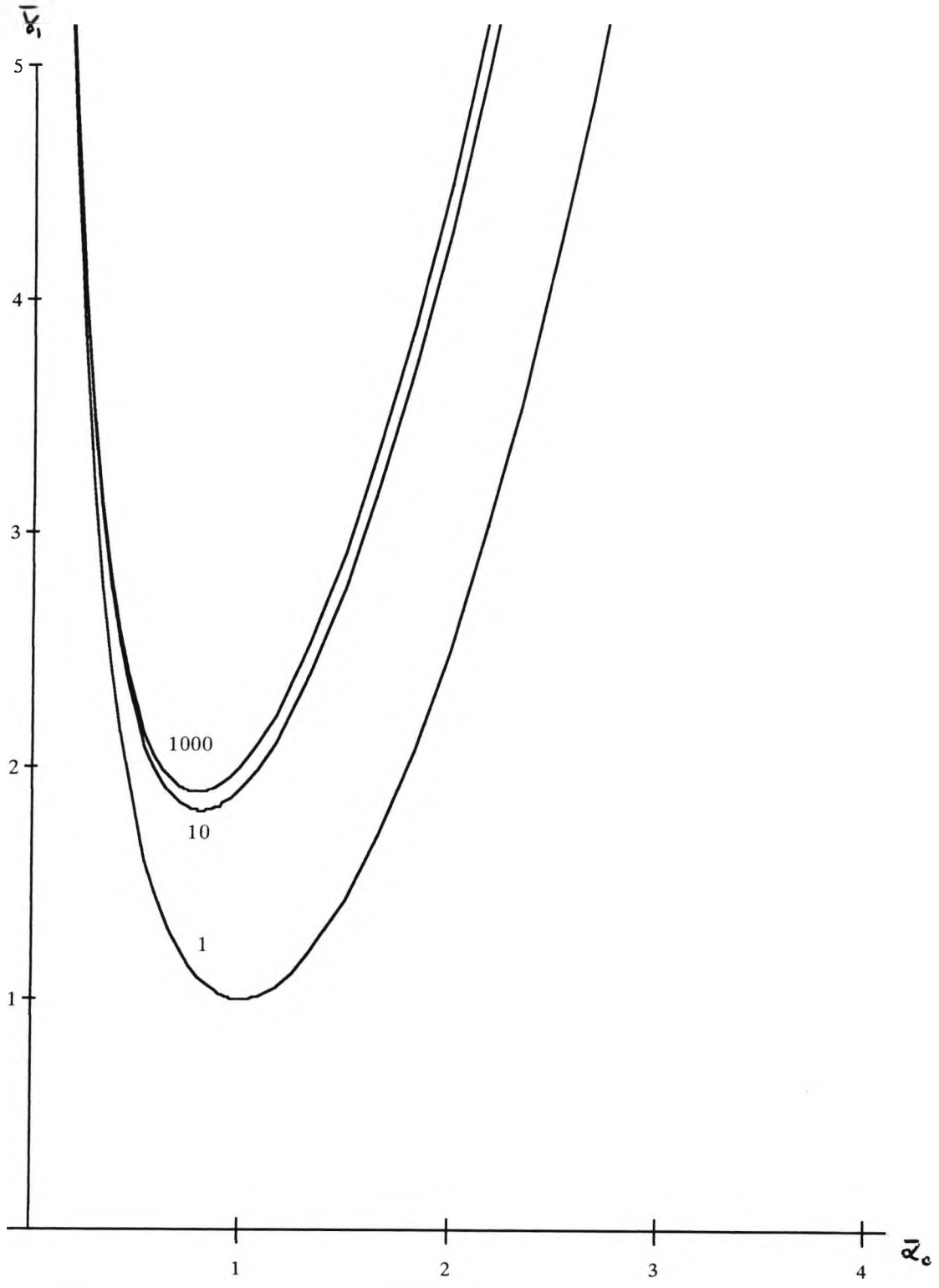

FIGURE 5.3. The neutral stability curve for various values of the scaled Prandtl number $\bar{\sigma}_0$.

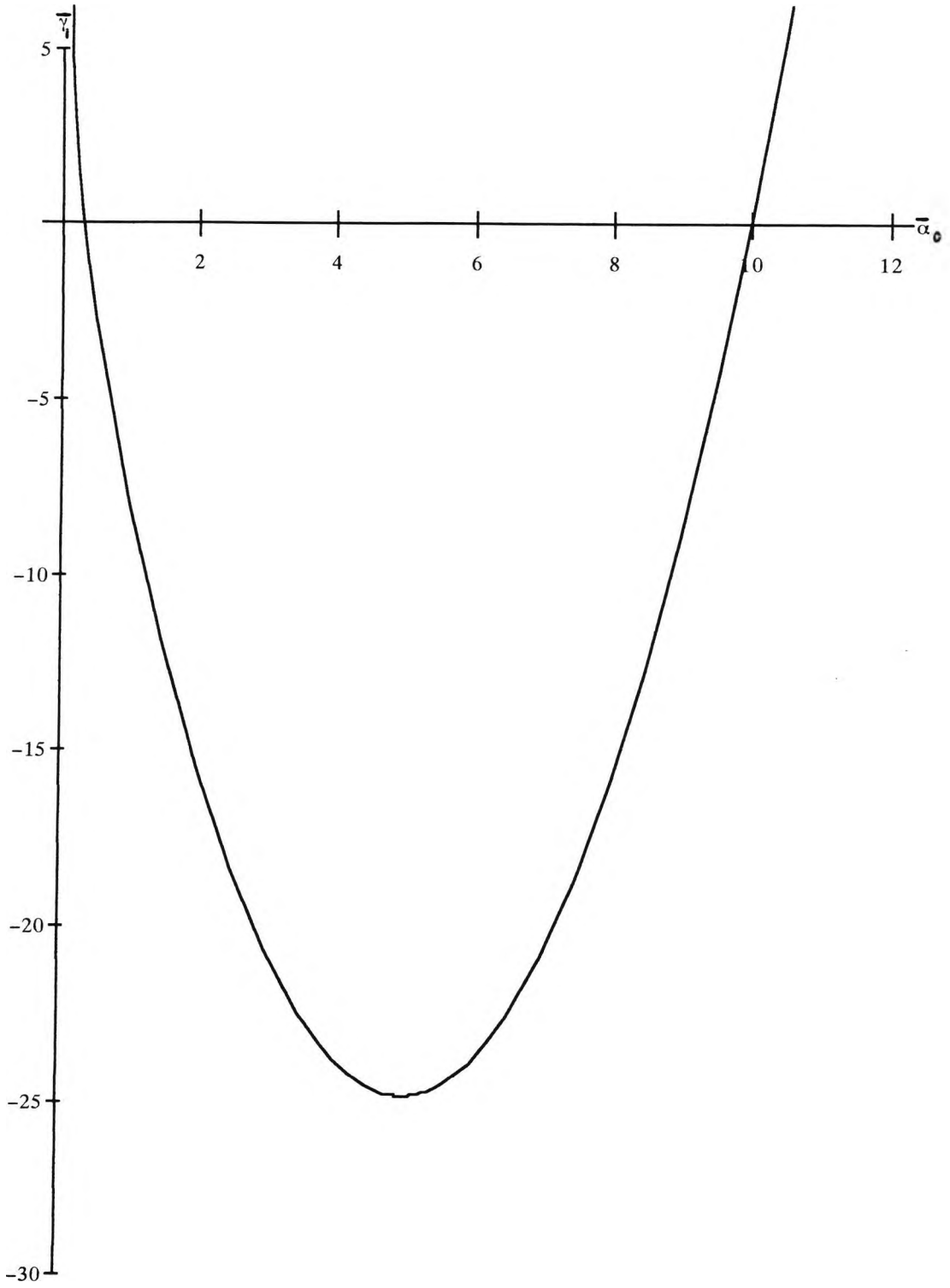

FIGURE 5.4. The neutral stability curve for the scaled Prandtl number $\overline{\sigma}_0=0.1$.

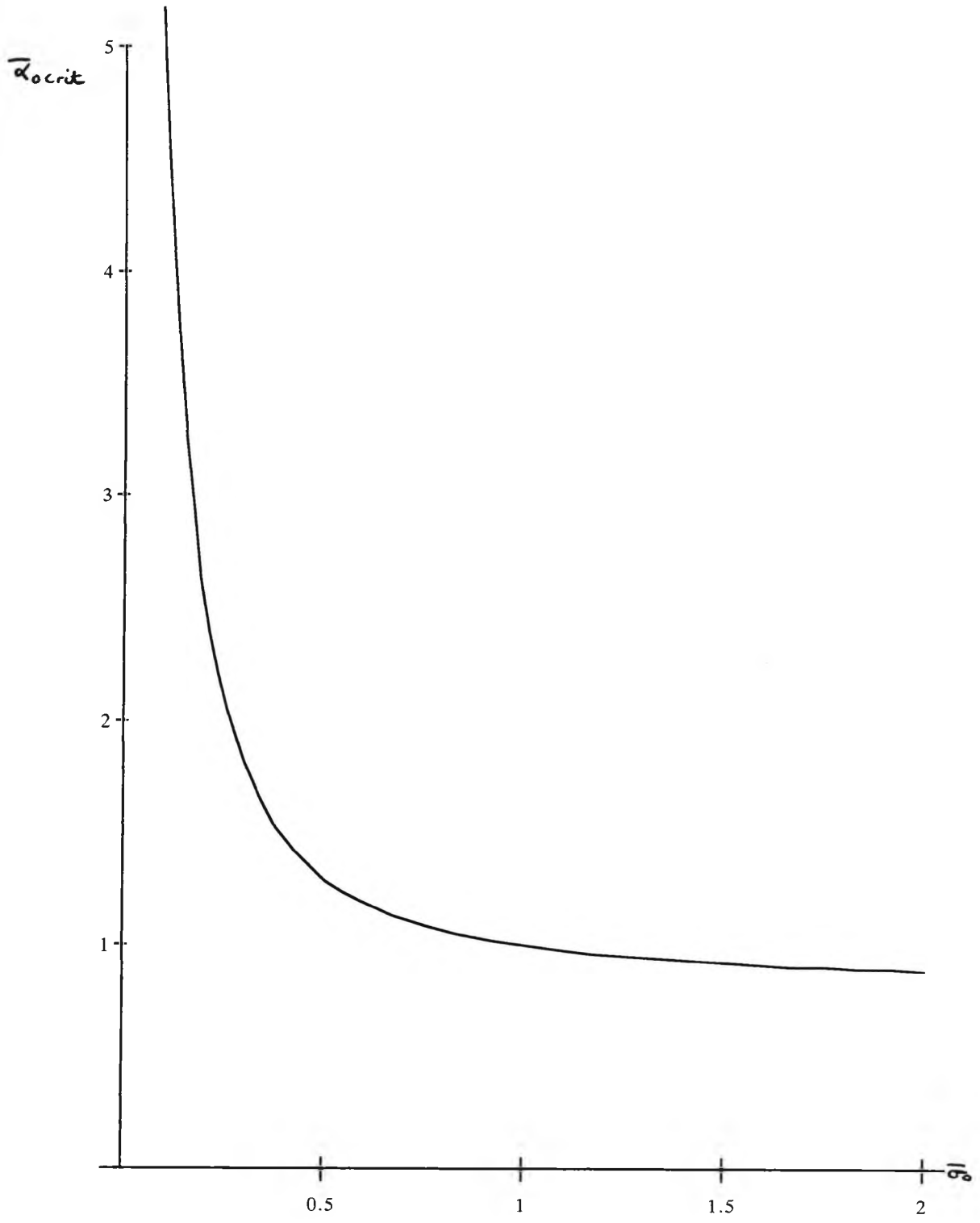

FIGURE 5.5. The critical wavenumber $\bar{\alpha}_{0crit}$ as a function of the scaled Prandtl number $\bar{\sigma}_0$.

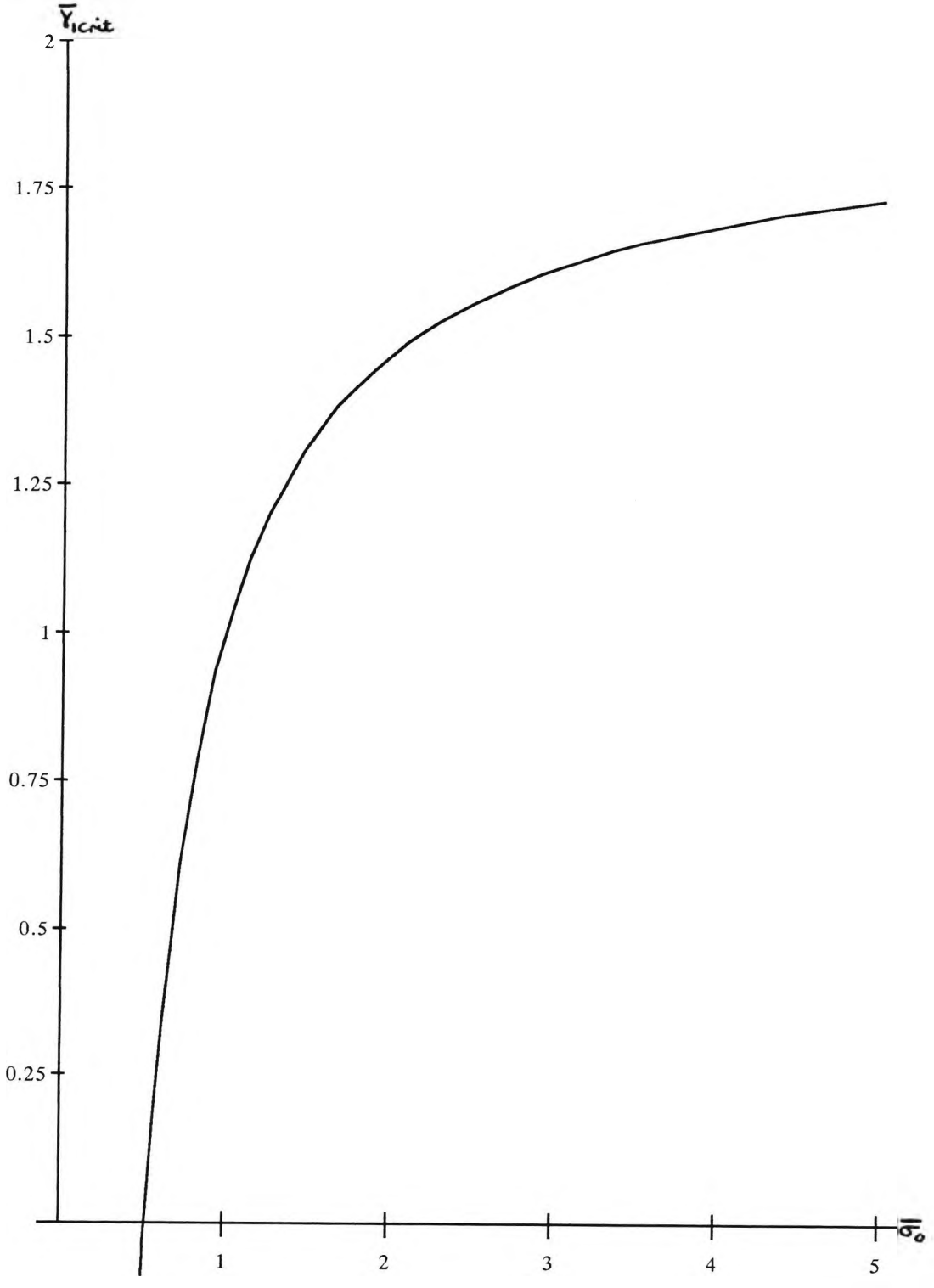

FIGURE 5.6. The critical convective parameter $\bar{\gamma}_{1crit}$ as a function of the scaled Prandtl number $\bar{\sigma}_0$.

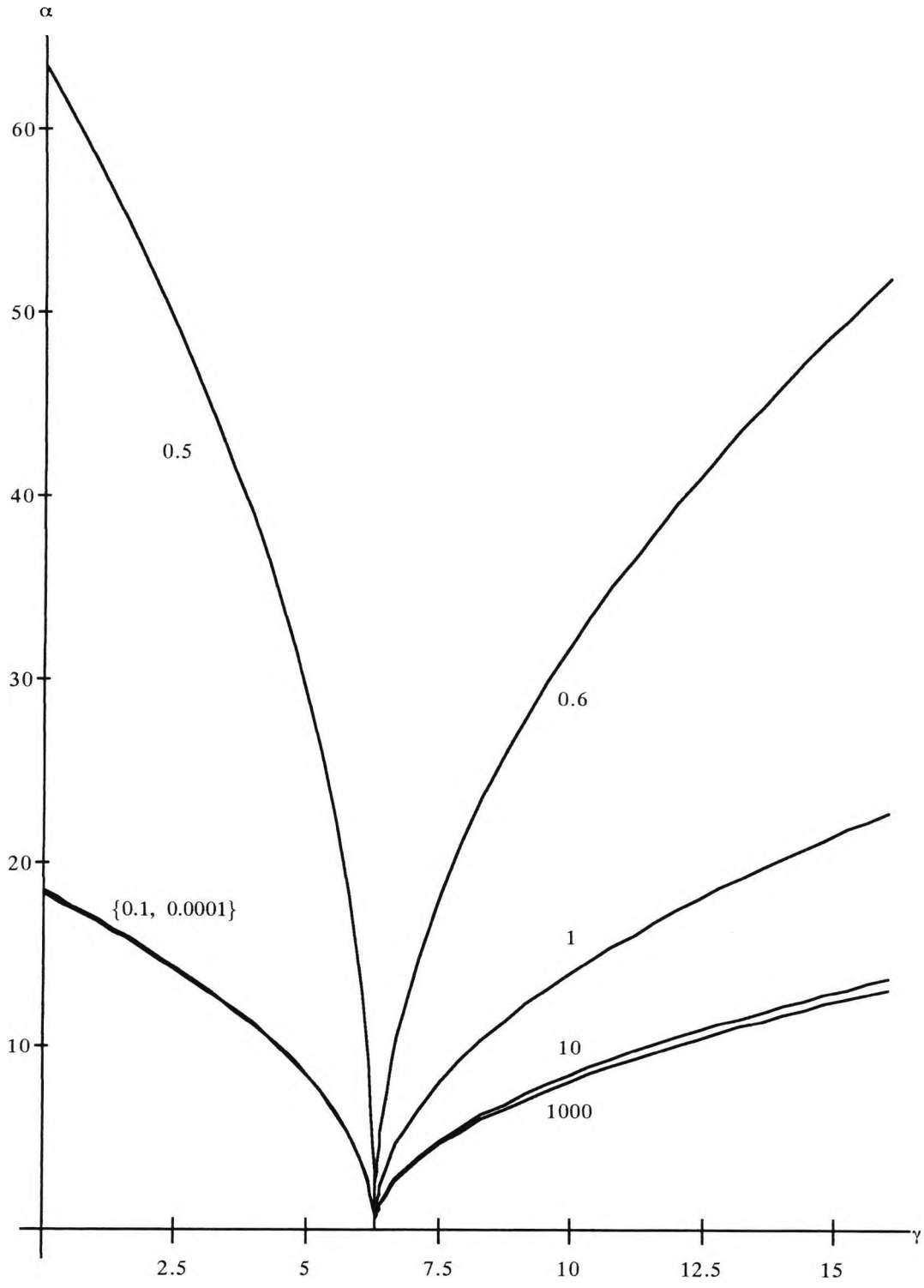

FIGURE 5.7. The critical wavenumber α versus convective parameter γ for various values of the scaled Prandtl number $\bar{\sigma}_0$.

CHAPTER SIX : LOWER BRANCH OF THE NEUTRAL STABILITY CURVE

6.1 Introduction

This chapter is concerned with identifying the asymptotic structure of the lower branch of the neutral stability curve for large values of the Rayleigh number, A. Solutions are found for Prandtl numbers in the range $\sigma \geq 50$, including the limit structure for $\sigma \to \infty$. The relevant lower branch stability equations and boundary conditions are derived in Section 6.2 and solutions are found for various values of the Prandtl number and general values of γ in Section 6.3 using a numerical method based on a fourth order Runge Kutta scheme. The limiting form of the neutral stability curve as $\sigma \to \infty$ is considered in Section 6.4 where it is shown that for $\gamma < \gamma_0 = 6.30$ the scaled wavenumber assumes a form proportional to the Prandtl number, while for $\gamma > \gamma_0$ the scaled wavenumber is finite as $\sigma \to \infty$. A numerical solution of the appropriate limiting problem in $\gamma < \gamma_0$ is undertaken in Section 6.5. The results are discussed in Section 6.6 and are placed in context with those obtained in Chapters 2-5 for the neighbourhood of γ_0. This enables a general picture to be constructed of the form of the neutral stability curve for large Rayleigh numbers and Prandtl numbers.

6.2 Formulation

The linear stability equations for the lower branch of the neutral stability curve are obtained, by assuming a low wavenumber limit in the full stability equations

$$\phi'''' - 2\alpha^2 \phi'' + \alpha^4\phi = \theta' + i\alpha A[\Psi'\phi'' - \alpha^2\phi\Psi' - \Psi'''\phi]/\sigma, \qquad (6.2.1)$$

$$\theta'' - \alpha^2\theta = i\alpha A[\Theta'\phi - \Psi'\theta] - 4\gamma^4\phi', \qquad (6.2.2)$$

previously derived in Chapter 1. Here the base flow functions Θ and Ψ are defined by

$$\Theta = 2(D_- - D_+)\sinh\gamma x\cos\gamma x - 2(D_- + D_+)\cosh\gamma x\sin\gamma x, \qquad (6.2.3)$$

$$\Psi = \gamma^{-3}(D + D_+\cosh\gamma x\cos\gamma x + D_-\sinh\gamma x\sin\gamma x), \qquad (6.2.4)$$

where the constants D, D_+ and D_- are given by (1.2.21)-(1.2.22) and the appropriate boundary conditions are

$$\phi = \phi' = 0 \qquad (x = \pm 1/2), \qquad (6.2.5)$$

$$\theta = 0 \qquad (x = \pm 1/2). \qquad (6.2.6)$$

The lower branch system corresponds to small wavenumbers α of order A^{-1} as $A\to\infty$ and is obtained from the system (6.2.1)-(6.2.6) by assuming

$$\alpha \sim \bar{\alpha}A^{-1}, \qquad A\to\infty. \qquad (6.2.7)$$

Substitution into (6.2.1)-(6.2.6) then shows that the leading approximations to the perturbation functions ϕ and θ satisfy the reduced system

$$\phi'''' + i\tilde{\alpha}[\Psi'\phi'' - \Psi'''\phi]/\sigma = \theta', \tag{6.2.8}$$

$$\theta'' = i\tilde{\alpha}[\Theta'\phi - \Psi'\theta] - 4\gamma^4\phi', \tag{6.2.9}$$

to be solved subject to the boundary conditions

$$\phi = \phi' = 0 \qquad (x = \pm 1/2), \tag{6.2.10}$$

$$\theta = 0 \qquad (x = \pm 1/2). \tag{6.2.11}$$

In the next section we consider the computation of solutions of the above system for general values of the Prandtl number and general values of the convective parameter γ. A solution for infinite Prandtl number in the region $\gamma > \gamma_0 = 6.30$ was previously found by Daniels (1987).

6.3 Lower Branch Solution

It is clear from equations (6.2.8)-(6.2.9) that the functions ϕ and θ are of complex form. Thus we need to write ϕ and θ as

$$\phi = \phi_r + i\,\phi_i, \tag{6.3.1}$$

$$\theta = \theta_r + i\,\theta_i, \tag{6.3.2}$$

where ϕ_r, ϕ_i, θ_r and θ_i are real functions of x. Substitution of (6.3.1) and (6.3.2) into (6.2.8) and (6.2.9) and balancing of the real and imaginary parts leads to the following system for the real functions ϕ_r, ϕ_i, θ_r and θ_i :

$$\phi_r'''' + \tilde{\alpha}(\Psi'''\phi_i - \Psi'\phi_i'')/\sigma = \theta_r', \tag{6.3.3}$$

$$\phi_i'''' - \bar{\alpha}\,(\Psi'''\phi_r - \Psi'\phi_r'')/\sigma = \theta_i', \tag{6.3.4}$$

$$\theta_r'' + \bar{\alpha}\,(\Theta'\phi_i - \Psi'\theta_i) = 4\gamma^4\phi_r', \tag{6.3.5}$$

$$\theta_i'' - \bar{\alpha}\,(\Theta'\phi_r - \Psi'\theta_r) = 4\gamma^4\phi_i' \ . \tag{6.3.6}$$

The boundary conditions (6.2.10)-(6.2.11) now become

$$\phi_r = \phi_i = \phi_r' = \phi_i' = 0 \qquad (x = \pm 1/2), \tag{6.3.7}$$

$$\theta_r = \theta_i = 0 \qquad (x = \pm 1/2). \tag{6.3.8}$$

Equations (6.3.3)-(6.3.6) are to be solved subject to (6.3.7) and (6.3.8) for specific values of σ, γ and $\bar{\alpha}$. The solution is obtained by converting (6.3.3)-(6.3.6) into a system of twelve first order equations by introducing the vector form $\underline{y}=(y_1,y_2,\ldots,y_{12})$, where

$$(y_1,y_2,\ldots,y_{12}) = (\phi_r,\ldots,\phi_r''',\phi_i,\ldots,\phi_i''',\theta_r,\theta_r',\theta_i,\theta_i'). \tag{6.3.9}$$

The required solution can then be written in the form

$$\underline{y} = \bar{A}\,\underline{y}^{(1)} + \bar{B}\,\underline{y}^{(2)} + \bar{C}\,\underline{y}^{(3)}\ , \tag{6.3.10}$$

where $\bar{A}$, $\bar{B}$ and $\bar{C}$ are complex constants and the vectors $\underline{y}^{(k)}$ $(k=1,2,3)$ denote the particular solutions of the system (6.3.3)-(6.3.6) subject to the initial conditions

$$(\phi_r,\ldots,\phi_r''',\phi_i,\ldots,\phi_i''',\theta_r,\theta_r',\theta_i,\theta_i')=(0,0,1,0,\ldots,0), \tag{6.3.11}$$

$$(\phi_r,\ldots,\phi_r''',\phi_i,\ldots,\phi_i''',\theta_r,\theta_r',\theta_i,\theta_i')=(0,0,0,1,0..,0), \tag{6.3.12}$$

$$(\phi_r,\ldots,\phi_r''',\phi_i,\ldots,\phi_i''',\theta_r,\theta_r',\theta_i,\theta_i')=(0,0,\ldots,1,0,0), \tag{6.3.13}$$

at x=-1/2 respectively. Application of the boundary conditions at x=1/2 then leads to the following homogeneous system

$$\bar{A}(y_1^{(1)}+ y_5^{(1)}) + \bar{B}(y_1^{(2)}+ y_5^{(2)}) + \bar{C}(y_1^{(3)}+ y_5^{(3)})=0, \qquad (6.3.14)$$

$$\bar{A}(y_2^{(1)}+ y_6^{(1)}) + \bar{B}(y_2^{(2)}+ y_6^{(2)}) + \bar{C}(y_2^{(3)}+ y_6^{(3)})=0, \qquad (6.3.15)$$

$$\bar{A}(y_9^{(1)}+ y_{11}^{(1)}) + \bar{B}(y_9^{(2)}+ y_{11}^{(2)}) + \bar{C}(y_9^{(3)}+ y_{11}^{(3)})=0, \qquad (6.3.16)$$

where each of the functions is evaluated at x=1/2. A non-trivial solution for the constants $\bar{A}$, $\bar{B}$ and $\bar{C}$ then exists provided that the determinant

$$\begin{vmatrix} y_1^{(1)} + iy_5^{(1)} & y_1^{(2)} + iy_5^{(2)} & y_1^{(3)} + iy_5^{(3)} \\ y_2^{(1)} + iy_6^{(1)} & y_2^{(2)} + iy_6^{(2)} & y_2^{(3)} + iy_6^{(3)} \\ y_9^{(1)} + iy_{11}^{(1)} & y_9^{(2)} + iy_{11}^{(2)} & y_9^{(3)} + iy_{11}^{(3)} \end{vmatrix} = D_r + iD_i \qquad (6.3.17)$$

vanishes at x=1/2. In order to compute the determinant in (6.3.17), a fourth order Runge-Kutta scheme was used with 400 steps across the interval [-1/2,0]. The eigenvalues $\bar{\alpha}$ were located for fixed values of the Prandtl number σ and the convective parameter γ by varying $\bar{\alpha}$ until the real and imaginary parts of the determinant, D_r and D_i, change sign simultaneously. The required value of $\bar{\alpha}$ is then obtained by the bisection method. Tables 6.1-6.3 show bounds $[\alpha_1, \alpha_2]$ on the relevant values of $\bar{\alpha}$ and the corresponding values of γ for values of the Prandtl number σ = 50,100 and 1000. This

determines the lower branch of the neutral stability curve in each case in the range $0 \leq \gamma \leq 10$. Graphical results are presented following consideration now of the limiting form of the solution for $\sigma \to \infty$.

6.4 Large Prandtl Number Limit

For infinite Prandtl number, σ, solutions for α in the range $\gamma > \gamma_0 = 6.30$ were obtained by Daniels (1987) by solving the lower branch system (6.2.8)-(6.2.11) with $\sigma = \infty$. In the range $\gamma < \gamma_0 = 6.30$ it is necessary to consider solutions with $\tilde{\alpha}$ of order σ as $\sigma \to \infty$.

Consider the equations (6.2.8) and (6.2.9) for the lower branch of the neutral stability curve obtained in Section 6.2:

$$\phi'''' + i\tilde{\alpha}[\Psi'\phi'' - \Psi''\phi]/\sigma = \theta', \qquad (6.4.1)$$

$$\theta'' = i\tilde{\alpha}[\Theta'\phi - \Psi'\theta] - 4\gamma^4\phi', \qquad (6.4.2)$$

with boundary conditions

$$\phi = \phi' = 0 \qquad (x = \pm 1/2), \qquad (6.4.3)$$

$$\theta = 0 \qquad (x = \pm 1/2). \qquad (6.4.4)$$

In order to determine the limiting form of the solution as $\sigma \to \infty$ in the region $\gamma < \gamma_0 = 6.30$ it is necessary to write

$$\tilde{\alpha} = \lambda\sigma \qquad (6.4.5)$$

and assume that λ is of order one as $\sigma \to \infty$. Substitution of (6.4.5) into (6.4.1) gives

$$\phi'''' + i\lambda(\Psi'\phi'' - \Psi'''\phi) = \theta', \tag{6.4.6}$$

and substitution of (6.4.5) into (6.4.2) gives

$$\theta'' + i\lambda\sigma(\Psi'\theta - \Theta'\phi) = 4\gamma^4\phi', \tag{6.4.7}$$

which at leading order as $\sigma \to \infty$ reduces to the convection-dominated form

$$\Psi'\theta - \Theta'\phi = 0 . \tag{6.4.8}$$

Thus to a first approximation,

$$\theta = \frac{\Theta'}{\Psi'}\phi \tag{6.4.9}$$

and substitution of this result into (6.4.6) leads to the equation

$$\phi'''' + i\lambda(\Psi'\phi'' - \Psi'''\phi) - \frac{d}{dx}\left(\frac{\Theta'}{\Psi'}\phi\right) = 0 . \tag{6.4.10}$$

The solution for ϕ subject to (6.4.3) in $x<0$ can be written in the form

$$\phi_0 = \nu_1^- \bar{f}_1(x) + \nu_2^- \bar{f}_2(x) , \tag{6.4.11}$$

where ν_1^- and ν_2^- are complex constants and the functions $\bar{f}_1$ and $\bar{f}_2$ are complex and uniquely defined by the solutions of the third-order systems

$$\bar{f}_1''' - \frac{\Theta'}{\Psi'}\bar{f}_1 = i\lambda(\Psi''\bar{f}_1 - \Psi'\bar{f}_1'); \quad (\bar{f}_1, \bar{f}_1', \bar{f}_1'') = (0,0,1) \text{ at } x = -\frac{1}{2}, \tag{6.4.12}$$

$$\bar{f}_2''' - \frac{\Theta'}{\Psi'}\bar{f}_2 = i\lambda(\Psi''\bar{f}_2 - \Psi'\bar{f}_2') + 1; \quad (\bar{f}_2, \bar{f}_2', \bar{f}_2'') = (0,0,0) \text{ at } x = -\frac{1}{2}, \tag{6.4.13}$$

The appropriate solution for ϕ in $x>0$ follows from the fact that the base flow functions Θ' and Ψ' are odd and even functions of x respectively, and can be written as

$$\phi = \nu_1^+ \bar{f}_1^*(-x) + \nu_2^+ \bar{f}_2^*(-x), \tag{6.4.14}$$

where $\bar{f}_j^*$ denotes the complex conjugate of $\bar{f}_j$ and ν_1^+ and ν_2^+ are complex constants.

The general form of $\bar{f}_j(x)$ as $x \to 0-$ is given by

$$\bar{f}_j = \bar{a}_j + \bar{b}_j x + \bar{c}_{j0} x^2 \ln|x| + \bar{c}_j x^2 + \bar{d}_j x^3 + \bar{e}_{j0} x^4 \ln|x| + \bar{e}_j x^4 + \bar{g}_{j0} x^5 \ln|x| + \bar{g}_j x^5 + \ldots, \quad x \to 0-, \tag{6.4.15}$$

where the constants $\bar{a}_j$, $\bar{b}_j$ and $\bar{c}_j$ $(j=1,2)$ are determined from a numerical solution which is to be undertaken in the next section and the remaining constants are expressed in terms of these by substituting the forms of $\bar{f}_j$ $(j=1,2)$ into equations (6.4.12) and (6.4.13) respectively and equating like terms in x. Thus

$$\bar{c}_{j0} = s_0\bar{a}_j/2, \quad \bar{d}_j = (s_0\bar{b}_j + i\lambda\omega_1\bar{a}_j + j-1)/6, \quad \bar{e}_{j0} = s_0\bar{c}_{j0}/24,$$

$$\bar{e}_j = (s_0\bar{c}_j + s_1\bar{a}_j - 26\bar{e}_{jj})/24, \quad \bar{g}_{j0} = -i\lambda\omega_1\bar{c}_{j0}/60,$$

$$\bar{g}_j = [s_0\bar{d}_j + s_1\bar{b}_j - 47\bar{g}_{j0} + i\lambda(3\omega_3\bar{a}_j - \omega_1\bar{c}_j - \omega_1\bar{c}_{j0})]/60 \quad (6.4.16)$$

where s_0, s_1, ω_1, ω_3 are defined by (2.3.11) but where the expansions (2.3.7) and (2.3.8) are viewed as the expansions of Θ' and Ψ' at general values of γ.

We now have the outer solution for ϕ and the outer solution for θ can be deduced from equation (6.4.9). At the centre-line $x=0$ the singular form of the outer solution is smoothed out within a critical layer. This has thickness $x = O(\sigma^{-1/3})$ which can be seen by considering the correspondence $\alpha A \leftrightarrow \lambda\sigma$, equivalent to $\alpha_0 A^{2/3} \leftrightarrow \lambda\sigma$ in the context of Chapters 2-5. Hence the critical layer expansions here are like those of Chapter 3 but with $\sigma \sim A^{2/3}$. Therefore expansions for the critical layer will proceed as in Chapter 3 provided that the term $i\lambda(\Psi'\phi'' - \Psi'''\phi)$ does not contribute to the bridging conditions obtained in Chapter 3. To show that this is the case we consider the size of the term $i\lambda(\Psi'\phi'' - \Psi'''\phi)$ relative to the term ϕ'''' used to obtain the fourth leading order bridging condition. The latter is of order $A^{2/9}$ whereas the magnitude of $\Psi'\phi''$ and $\Psi'''\phi$ are order $A^{-2/9}\ln A$ and $A^{-2/9}$ respectively. Thus the bridging conditions are precisely those determined in equations (3.3.47)-(3.3.50) and substitution from (6.4.15) leads to the following system:

$$\nu_1^+\bar{a}_1^* - \nu_1^-\bar{a}_1 + \nu_2^+\bar{a}_2^* - \nu_2^-\bar{a}_2 = 0, \quad (6.4.17)$$

$$\nu_1^+\bar{b}_1^* + \nu_1^-\bar{b}_1 + \nu_2^+\bar{b}_2^* + \nu_2^-\bar{b}_2 = 0, \quad (6.4.18)$$

$$\nu_1^+(\bar{c}_1^* - is_0\pi\bar{a}_1^*/2) - \nu_1^-\bar{c}_1 + \nu_2^+(\bar{c}_2^* - is_0\pi\bar{a}_2^*/2) - \nu_2^-\bar{c}_2 = 0, \quad (6.4.19)$$

$$\nu_1^+ \bar{d}_1^* + \nu_1^- \bar{d}_1 + \nu_2^+ \bar{d}_2^* + \nu_2^- \bar{d}_2 = 0, \qquad (6.4.20)$$

where $\bar{a}_1^*,\ldots,\bar{d}_2^*$ denote the complex conjugates of $\bar{a}_1,\ldots,\bar{d}_2$ respectively. Substitution of $\bar{d}_1$, $\bar{d}_1^*$, $\bar{d}_2$ and $\bar{d}_2^*$, into (6.4.20) yields

$$(-i\lambda\omega_1\bar{a}_1^* + s_0\bar{b}_1^*)\nu_1^+ + (i\lambda\omega_1\bar{a}_1 + s_0\bar{b}_1)\nu_1^- + (1-i\lambda\omega_1\bar{a}_2^* + s_0\bar{b}_2^*)\nu_2^+$$
$$+ (1+i\lambda\omega_1\bar{a}_2 + s_0\bar{b}_2)\nu_2^- = 0 . \qquad (6.4.21)$$

Adding (6.4.17) multiplied by $i\lambda\omega_1$ and subtracting (6.4.18) multiplied by s_0 from equation (6.4.21) leads to the result

$$\nu_2^+ = -\nu_2^- \qquad (6.4.22)$$

and using this result in (6.4.17)-(6.4.19) gives the reduced system

$$\nu_1^+ \bar{a}_1^* - \nu_1^- \bar{a}_1 + \nu_2^+ (\bar{a}_2^* + \bar{a}_2) = 0, \qquad (6.4.23)$$

$$\nu_1^+ \bar{b}_1^* + \nu_1^- \bar{b}_1 + \nu_2^+ (\bar{b}_2^* - \bar{b}_2) = 0 , \qquad (6.4.24)$$

$$\nu_1^+ (\bar{c}_1^* - is_0\pi\bar{a}_1^*/2) - \nu_1^-\bar{c}_1 + \nu_2^+ (\bar{c}_2^* - is_0\pi\bar{a}_2^*/2 + \bar{c}_2) = 0, \qquad (6.4.25)$$

for ν_1^+, ν_1^- and ν_2^+. The above system has a non-trivial solution provided that the determinant

$$\begin{vmatrix} \bar{a}_1^* & -\bar{a}_1 & \bar{a}_2^* + \bar{a}_2 \\ \bar{b}_1^* & \bar{b}_1 & \bar{b}_2^* - \bar{b}_2 \\ \bar{c}_1^* - is_0\pi\bar{a}_1^*/2 & -\bar{c}_1 & \bar{c}_2^* - is_0\pi\bar{a}_2^*/2 + \bar{c}_2 \end{vmatrix} = 0 \qquad (6.4.26)$$

Evaluation of this determinant leads to the requirement

$$\bar{a}_1^*[\bar{b}_1(\bar{c}_2^* - is_0\pi\bar{a}_2^*/2 + \bar{c}_2) + (\bar{b}_2^* - \bar{b}_2)\bar{c}_1] + \bar{a}_1[\bar{b}_1^*(\bar{c}_2^* - is_0\pi\bar{a}_2^*/2 + \bar{c}_2) - (\bar{b}_2^* - \bar{b}_2)(\bar{c}_1^* - is_0\pi\bar{a}_1^*/2)] + (\bar{a}_2^* + \bar{a}_2)[-\bar{b}_1^*\bar{c}_1 - \bar{b}_1(\bar{c}_1^* - is_0\pi\bar{a}_1^*/2)] = 0. \tag{6.4.27}$$

The left hand side of (6.4.27) is real. This can be seen by writing (6.4.27) in the form

$$(\bar{a}_1^*\bar{b}_1 + \bar{a}_1\bar{b}_1^*)(\bar{c}_2^* + \bar{c}_2) + (\bar{a}_1^*\bar{c}_1 - \bar{a}_1\bar{c}_1^*)(\bar{b}_2^* - \bar{b}_2) - (\bar{b}_1^*\bar{c}_1 + \bar{b}_1\bar{c}_1^*)(\bar{a}_2^* + \bar{a}_2) - is_0\pi[(\bar{a}_1\bar{a}_2^*\bar{b}_1^* - \bar{a}_1^*\bar{a}_2\bar{b}_1) - (\bar{b}_2^* - \bar{b}_2)\bar{a}_1\bar{a}_1^*]/2 = 0. \tag{6.4.28}$$

Since $\bar{a}_j$, $\bar{b}_j$ and $\bar{c}_j$ are functions of λ and γ, this equation expresses a functional relation between these two parameters which determines the location of the neutral stability curve in the limit of infinite Prandtl number.

6.5 Numerical Solution for the Large Prandtl Number Limit

In order to determine the limiting form of the neutral stability curve, the complex constants $\bar{a}_j$, $\bar{b}_j$ and $\bar{c}_j$ must be found and the parameters λ and γ chosen to ensure that (6.4.28) is satisfied. The numerical method used to solve equations (6.4.12) and (6.4.13) for the constants $\bar{a}_j$, $\bar{b}_j$ and $\bar{c}_j$ (j=1,2) is described in this section.

Since the solutions for $\bar{f}_j$ (j=1,2) are complex we write $\bar{f}_j$ in the form

$$\bar{f}_j = f_{jr} + if_{ji} \qquad (j=1,2) \tag{6.5.1}$$

where f_{jr} and f_{ji} are real functions of x. Substitution of (6.5.1) into (6.4.12) and collecting real and imaginary terms yields the following equations:

$$f_{1r}''' - \frac{\Theta'}{\Psi'} f_{1r} = \lambda(\Psi' f_{1i}' - \Psi'' f_{1i}), \tag{6.5.2}$$

$$f_{1i}''' - \frac{\Theta'}{\Psi'} f_{1i} = -\lambda(\Psi' f_{1r}' - \Psi'' f_{1r}), \tag{6.5.3}$$

$$f_{2r}''' - \frac{\Theta'}{\Psi'} f_{2r} = 1 + \lambda(\Psi' f_{2i}' - \Psi'' f_{2i}), \tag{6.5.4}$$

$$f_{2i}''' - \frac{\Theta'}{\Psi'} f_{2i} = -\lambda(\Psi' f_{2r}' - \Psi'' f_{2r}), \tag{6.5.5}$$

which, from (6.4.12) and (6.4.13), must be solved subject to the initial conditions

$$(f_{1r}, f_{1r}', f_{1r}'') = (0,0,1) \quad , \quad (x=-1/2), \tag{6.5.6}$$

$$(f_{1i}, f_{1i}', f_{1i}'') = (0,0,0) \quad , \quad (x=-1/2), \tag{6.5.7}$$

$$(f_{2r}, f_{2r}', f_{2r}'') = (0,0,0) \quad , \quad (x=-1/2), \tag{6.5.8}$$

$$(f_{2i}, f_{2i}', f_{2i}'') = (0,0,0) \quad , \quad (x=-1/2). \tag{6.5.9}$$

The system (6.5.2)-(6.5.9) is equivalent to twelve first order differential equations which were solved by use of a fourth

order Runge-Kutta scheme with 400 steps across the interval [-1/2,0]. A series expansion was used to start off the computation near x=-1/2. The Taylor expansions for the base flow functions are equivalent to (4.3.1) and (4.3.2) viewed as expansions for general values of γ:

$$\Theta' = \sum_{k=0} \bar{\mu}_k X^k \quad , \; X \to 0 \; , \tag{6.5.10}$$

$$\Theta' = \sum_{k=0} \bar{\omega}_k X^k \quad , \; X \to 0 \; , \tag{6.5.11}$$

where X=x+1/2. Corresponding expansions for the functions $\bar{f}_j$ (j=1,2) are given by

$$\bar{f}_1 = X^2/2 + \sum_{k=3}^{\infty} \bar{A}_k X^k \; , \tag{6.5.12}$$

$$\bar{f}_2 = \sum_{k=3}^{\infty} \bar{B}_k X^k \; , \tag{6.5.13}$$

where the coefficients $\bar{A}_k$, $\bar{B}_k$ can be found by substitution of (6.5.10)-(6.5.12) into (6.4.12) and equating like terms in x. This gives

$$\bar{A}_3 = 0, \qquad \bar{A}_4 = \bar{\mu}_0/48\bar{\omega}_1 \; , \qquad \bar{A}_5 = -(i\bar{\omega}_1 + \bar{\mu}_0\bar{\omega}_2/\bar{\omega}_1^2)/120$$

$$\bar{A}_6 = \bar{\mu}_0/5760\bar{\omega}_1^2 + (\bar{\mu}_0\bar{\omega}_2^2 - \bar{\mu}_0\bar{\omega}_1\bar{\omega}_3 + \bar{\mu}_2\bar{\omega}_1^2)/\bar{\omega}_1^3 \; , \tag{6.5.14}$$

and

$$\bar{B}_3 = 1/6, \qquad \bar{B}_4 = 0 \; , \qquad \bar{B}_5 = \bar{\mu}_0/360\bar{\omega}_1 \; ,$$

$$\bar{B}_6 = -\bar{\mu}_0\bar{\omega}_2/720\bar{\omega}_1^2 - i\lambda\bar{\omega}_1/360 \; . \tag{6.5.15}$$

The real and imaginary parts of $\bar{f}_1$ and $\bar{f}_2$ in (6.5.1) can now be used to initiate the Runga-Kutta computation just beyond x = -1/2. Values of the convective parameter γ and the scaled

wavenumber λ are fixed and the computation proceeds to the neighbourhood of $x = 0$ where the complex constant $\bar{a}_j$, $\bar{b}_j$ and $\bar{c}_j$ must be determined. This is done by use of the expansions for $\bar{f}_j$ (j=1,2) derived in Section 6.4:

$$\bar{f}_j = \bar{a}_j + \bar{b}_j x + \bar{c}_{j0}\, x^2 \ln|x| + \bar{c}_j x^2 + \bar{d}_j\, x^3 + \bar{e}_{j0}\, x^4 \ln|x| + \bar{e}_j\, x^4 + \bar{g}_{j0}\, x^5 \ln|x| + \bar{g}_j x^5 + \ldots,\ x \to 0-, \tag{6.5.16}$$

The Runge-Kutta values of $\bar{f}_1$, $\bar{f}_1'$, $\bar{f}_1''$ and $\bar{f}_2$, $\bar{f}_2'$, $\bar{f}_2''$ at $x=x_s$, where x_s is small and negative, are equated to the corresponding formulae given by the series expansions (6.5.16). This leads to the following pair of complex non-homogeneous systems of equations for $\bar{a}_j$, $\bar{b}_j$ and $\bar{c}_j$ (j=1,2). These systems are given by

$$\bar{a}_j \bar{\Gamma}_j + \bar{b}_j \bar{\Lambda}_j + \bar{c}_j \bar{\chi}_j = \bar{f}_j(x_s) + \bar{K}_j \tag{6.5.17}$$

$$\bar{a}_j \bar{\Gamma}'_j + \bar{b}_j \bar{\Lambda}'_j + \bar{c}_j \bar{\chi}'_j = \bar{f}'_j(x_s) + \bar{K}'_j \tag{6.5.18}$$

$$\bar{a}_j \bar{\Gamma}''_j + \bar{b}_j \bar{\Lambda}''_j + \bar{c}_j \bar{\chi}''_j = \bar{f}''_j(x_s) + \bar{K}''_j \tag{6.5.19}$$

The complex functions $\bar{\Gamma}_j$, $\bar{\Lambda}_j$ and $\bar{\chi}_j$, $\bar{K}_j$ and their first and second derivatives are defined explicitly in Appendix III. The solution of the systems of equations (6.5.17)-(6.5.19) were tested for accuracy and consistency by solving them at several points $x_s=-kh$ (k = 0,1,2,...) where h = 0.00125 is the step length in the Runge-Kutta solution. Results are shown in Table 6.4.

The neutral stability curve was obtained by fixing the convective parameter γ and adjusting the value of λ until equation (6.4.28) was satisfied. This led to solutions in the region $0 \le \gamma \le 6.30$, as shown in Table 6.4 and Figure 6.1. These

results are consistent with the numerical solution for finite, large values of σ found in Section 6.3, as shown in Figure 6.2. As $\sigma \to \infty$ the lower branch of the neutral stability curve adopts two distinct forms in the regions $\gamma < \gamma_0$ and $\gamma > \gamma_0$. For $\gamma < \gamma_0$ the wavenumber is proportional to the Prandtl number $\bar{\alpha} \sim \lambda\sigma$ with λ finite, whereas for $\gamma > \gamma_0$ the wavenumber $\bar{\alpha}$ is finite as $\sigma \to \infty$.

6.6 Discussion

This thesis has considered instability in the form of neutrally stable stationary convection in the flow between two vertical planes. Results have been obtained which determine the form of the neutral stability curve in the limit as $A \to \infty$ for general values of the convective parameter γ and for large (and infinite) Prandtl numbers.

The results of the present chapter demonstrate that the lower branch of the neutral stability curve experiences a dramatic transition as the Prandtl number becomes large. For finite Prandtl number the lower branch extends all the way to $\gamma=0$, so that long wavelength stationary convection can occur with $\alpha = O(A^{-1})$ for any value of the convective parameter. As the Prandtl number increases the wavenumber of the section of the lower branch in the range $0 \leq \gamma < 6.3$ increases in proportion to the size of the Prandtl number, so that when $\sigma \sim A^{2/3}$ the wavenumber α will be of order $A^{-1/3}$, comparable with the critical wavenumber for infinite Prandtl number determined in Chapter 4. When the Prandtl number reaches values of order A, the theory outlined in this chapter is no longer formally valid

in the range $0 \leq \gamma < 6.3$ because the wavenumber α there is then of order one, contradicting the approximations used to obtain the lower branch equation in Section 6.2. However, it seems reasonable to conjecture that as the Prandtl number increases through values of order A the finite wavelength disturbances corresponding to the section of the lower branch in $0 \leq \gamma < 6.3$ transform into the upper branch of the neutral stability curve for $\sigma = \infty$ identified by Daniels (1989) and described in Chapter 1. A schematic diagram of this process is shown in Figure 6.3.

In order to verify this conjecture it would be necessary to undertake computations of the upper branch solution for values of an appropriately scaled Prandtl number σ, of order A, which is beyond the scope of the present thesis. However, it is possible to relate the lower branch computations of this chapter near $\gamma = \gamma_0 = 6.30$ to the results of Chapter 5 where the form of the neutral stability curve was obtained for Prandtl numbers in the range $\sigma = O(A^{4/3})$. There it was shown that with $\sigma = A^{4/3}\sigma_0$ the neutral stability curve has the form

$$\alpha_0^3 + \frac{\bar{c}_0}{\bar{\sigma}_0}\alpha_0^2 + \bar{c}_1\alpha_0\gamma_1 + \bar{c}_2 = 0, \qquad (6.6.1)$$

where $\alpha = A^{-1/3}\alpha_0$ and $\gamma \approx \gamma_0 + A^{-2/3}\gamma_1$. As $\sigma_0 \to 0$ this curve is dominated by the balance between the second and third terms, equivalent to

$$\alpha_0 \sim -\bar{c}_1\sigma_0\gamma_1/\bar{c}_0 \qquad (6.6.2)$$

provided that γ_1 is large and σ_0 lies in the range

$$\gamma_1^{-2} << \sigma_0 << \gamma_1^{-1/2} . \qquad (6.6.3)$$

For fixed σ_0, equation (6.6.2) expresses a linear relation between the wavenumber and the convective parameter precisely equivalent to the finite slope in the limit curve of λ versus γ near γ_0 in Figure 6.1. This slope has been accurately evaluated from the numerical results shown in Figure 6.4 as

$$-m = -50653 \qquad (6.6.4)$$

so that

$$\lambda \sim m(\gamma_0 - \gamma), \quad \gamma \to \gamma_0 - . \qquad (6.6.5)$$

Recalling that

$$\alpha = A^{-1/3} \alpha_0 \approx \bar{\alpha}/A = \lambda\sigma/A \qquad (6.6.6)$$

and $\sigma = A^{4/3}\sigma_0$, $\gamma \approx \gamma_0 + A^{-2/3}\gamma_1$, the result (6.6.5) can be expressed in the form

$$\alpha_0 \sim -m\,\gamma_1\,\sigma_0 \qquad (6.6.7)$$

so that m is identified with the ratio $\bar{c}_1/\bar{c}_0$ in (6.6.2). From the results of Chapter 5, the value of this ratio is 49194, in good agreement with the value of m quoted in (6.6.4).

Thus the lower branch evolution with increasing Prandtl number ties in with the analysis of Chapter 5 describing the form of the neutral stability curve in the neighbourhood of the critical point γ_0; at this stage the lower and upper branches have assumed the infinite-Prandtl number limit forms in $\gamma > 6.30$ previously found by Daniels (1987,1989) and disturbances of

finite wavenumber are confined to the range $\gamma > \gamma_0$.

Various extensions to the present results are needed in order to investigate further features of the convective instability. First, an investigation of the precise form of the upper branch of the neutral stability curve for large (but finite) Prandtl number is needed in order to complete the analysis of order one wavenumber disturbances. This will require computations of the upper branch solution for an appropriately scaled Prandtl number of order A. Second, the incorporation of weakly non-linear effects in the stability analysis would allow the amplitude, ε, of the disturbance (that leads to the form of the cells shown in Figure 4.11) to be determined. However, this analysis may well involve very complex calculations as suggested by the results obtained here for the linear system. Finally, it would be instructive to consider ways in which the basic state assumed here for infinite vertical planes could be improved to provide a better approximation to the actual basic flow in a vertical slot, perhaps making use of a boundary-layer approximation to the latter flow of the type developed by Daniels (1987). This might lead to a more realistic comparison with experimental results.

$\sigma = 1000$		
γ	α_1	α_2
0.1	15000000	15500000
1	16000000	17000000
2	18500000	19500000
3	20500000	21000000
4	26000000	26500000
5	29500000	30000000
5.5	27500000	28500000
6	21500000	22000000
7	500000	550000
8	200000	300000
9	800000	1000000
10	1200000	1500000

TABLE 6.1. Bounds $[\alpha_1,\alpha_2]$ on the eigenvalue $\tilde{\alpha}$ and the corresponding values of the convective parameter γ for σ=1000.

$\sigma = 100$		
γ	α_1	α_2
0.1	1600000	1700000
1	1750000	1800000
2	2000000	2100000
3	2450000	2550000
4	3950000	4000000
5	6620000	6670000
5.5	6900000	6950000
6	5050000	5100000
7	65000	70000
8	55000	60000
9	922500	924000
10	1450000	1500000

TABLE 6.2. Bounds $[\alpha_1,\alpha_2]$ on the eigenvalue $\tilde{\alpha}$ and the corresponding values of the convective parameter γ for σ=100.

σ =50		
γ	α_1	α_2
0.1	1200000	1250000
1	1300000	1350000
2	1450000	1500000
3	1700000	1750000
4	4150000	4200000
5	6100000	6050000
5.5	6250000	6300000
6	4550000	4600000
7	605000	610000
8	640000	650000
9	960000	965000
10	1540000	1560000

TABLE 6.3. Bounds $[\alpha_1,\alpha_2]$ on the eigenvalue $\tilde{\alpha}$ and the corresponding values of the convective parameter γ for σ=50.

γ	λ_1	λ_2
0.1	13800	14400
1	14600	14900
2	15200	15600
3	16400	16900
4	19300	20100
5	22600	23400
6	7390	7380

TABLE 6.4. Bounds $[\lambda_1,\lambda_2]$ on the eigenvalue λ and the corresponding values of the convective parameter γ.

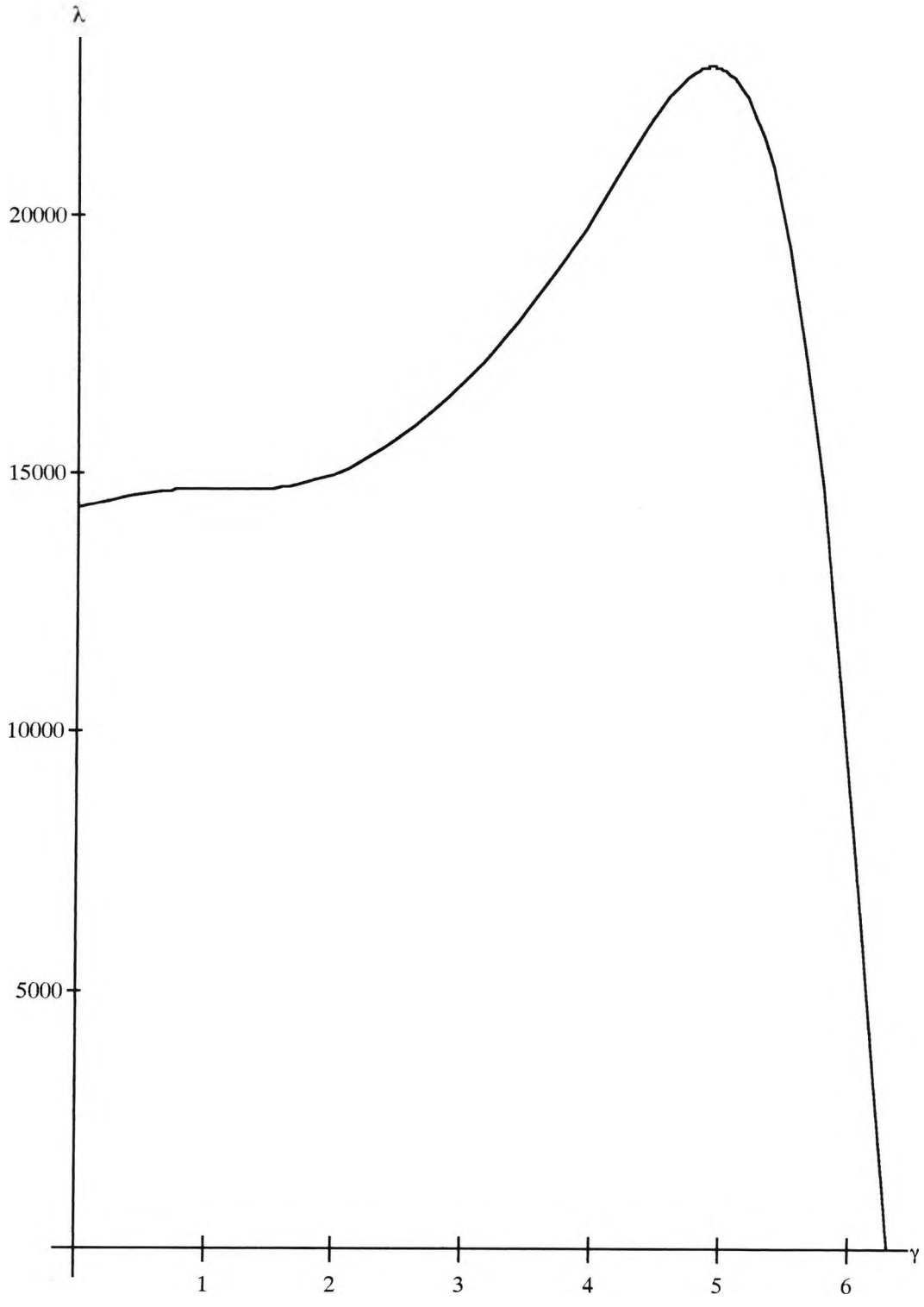

FIGURE 6.1. The lower branch limit for infinite Prandtl number in the range $0 \leq \gamma \leq \gamma_0$.

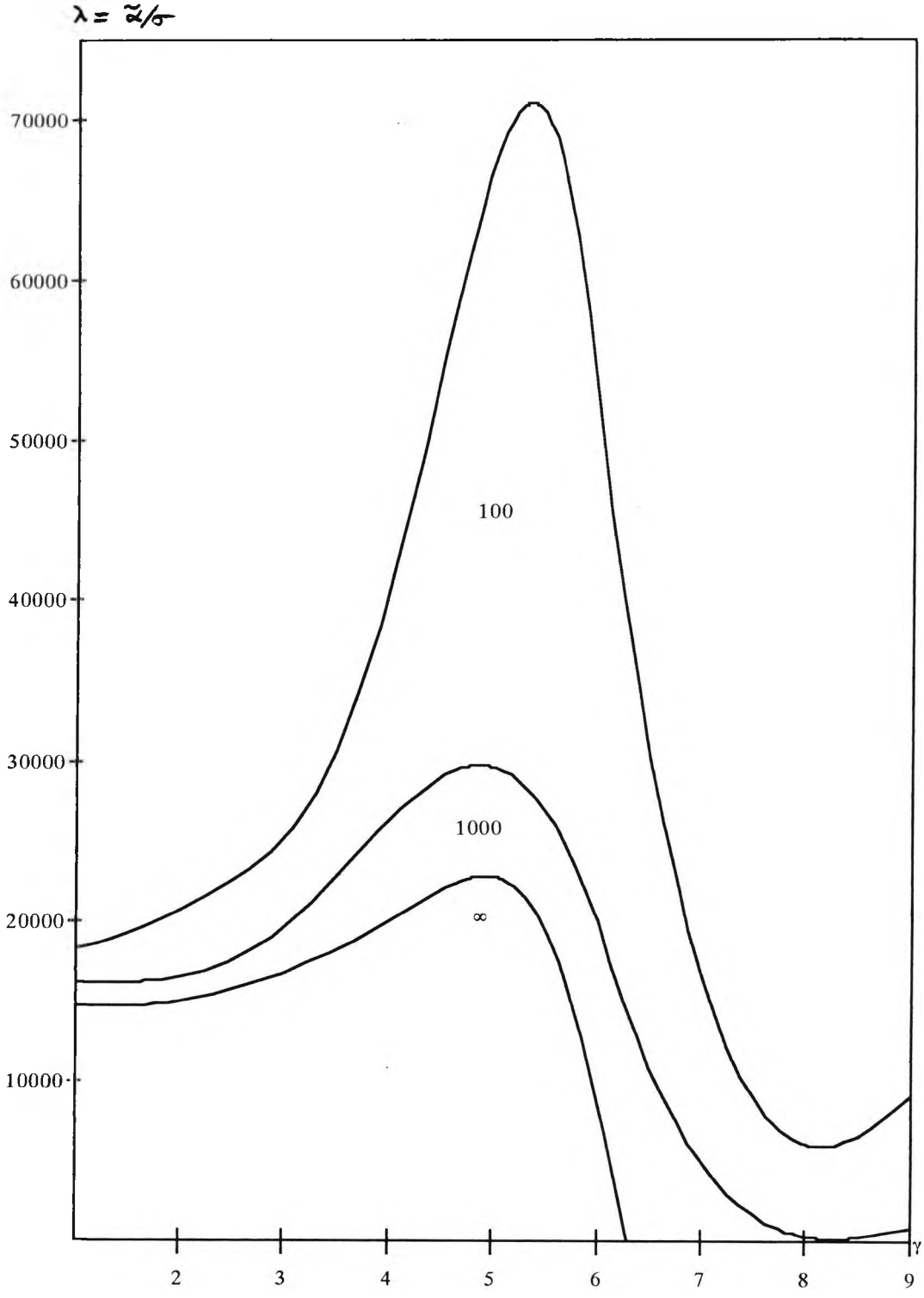

FIGURE 6.2. The lower branch for various values of the Prandtl number σ in the range $0 \leq \gamma \leq 9$.

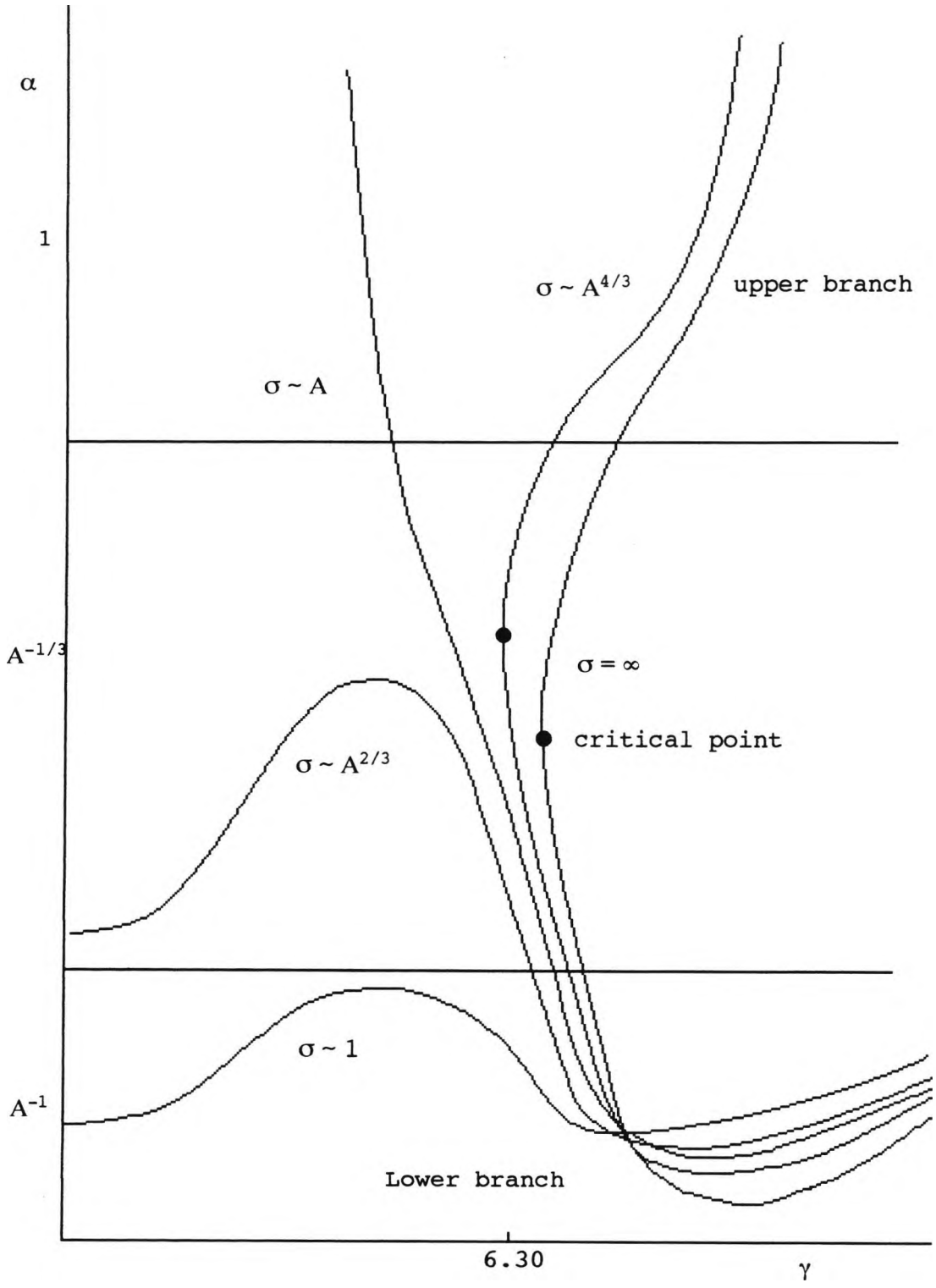

FIGURE 6.3. Schematic diagram of the variation of the neutral stability curve in the limit $A \to \infty$ for large and infinite Prandtl numbers.

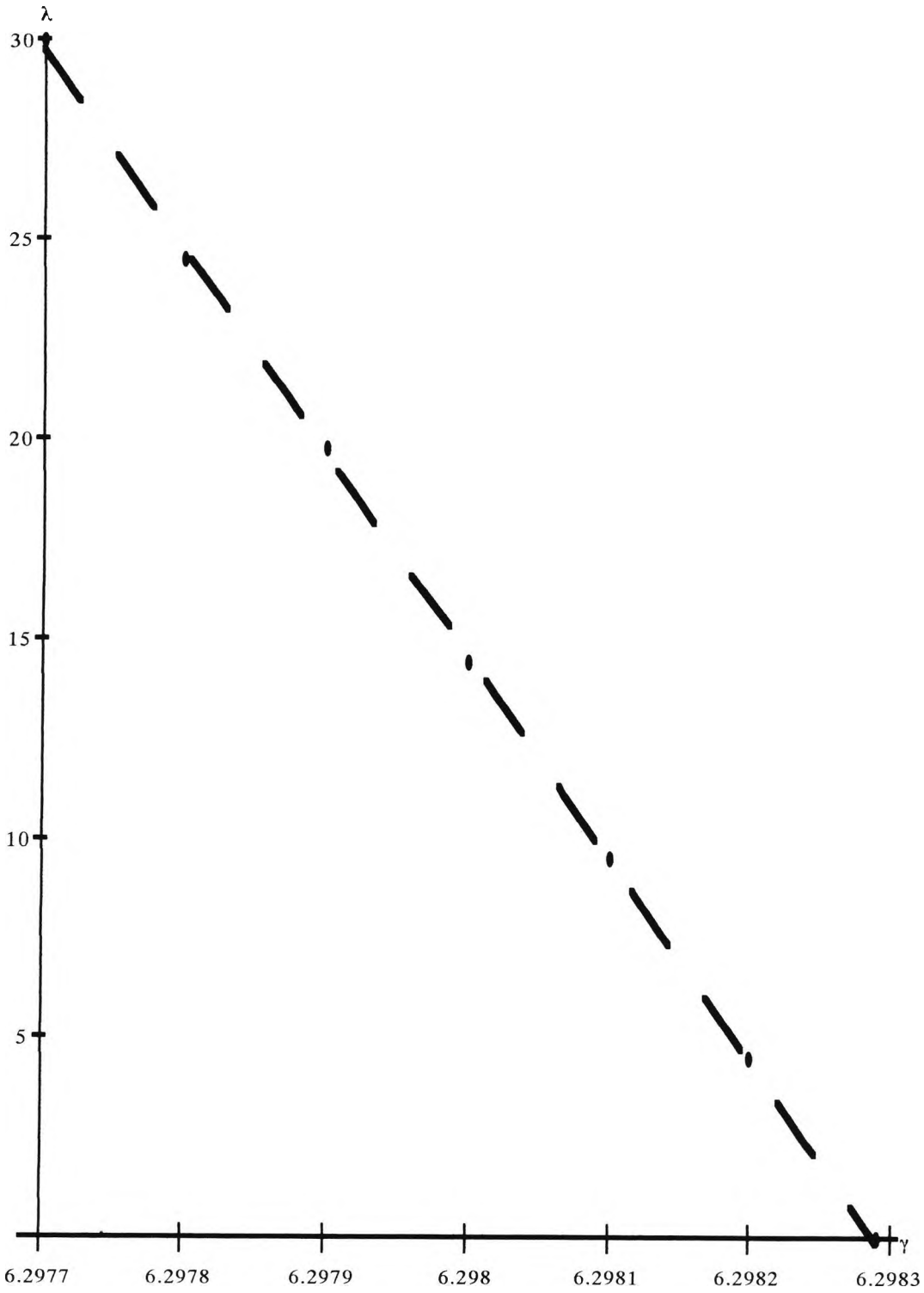

FIGURE 6.4. The slope of the large Prandtl number limit curve near γ_0.

APPENDIX ONE

In equation (3.5.11) the coefficients A_{j1} are given by

$A_{13} = 0,$

$A_{14} = \bar{\mu}_0/48\bar{\omega}_1,$

$A_{15} = -(\bar{\omega}_2\bar{\mu}_0 - \bar{\omega}_1\bar{\mu}_1)/120\bar{\omega}_1^2,$

$A_{16} = (24\bar{\omega}_2^2\bar{\mu}_0 - 24\bar{\omega}_1\bar{\omega}_3\bar{\mu}_0 + \bar{\omega}_1\bar{\mu}_0^2 - 24\bar{\omega}_1\bar{\omega}_2\bar{\mu}_1 + 24\bar{\omega}_1^2\bar{\mu}_2)/5760\bar{\omega}_1^3.$

In equation (3.5.12) the coefficients A_{j2} are given by

$A_{23} = 1/6,$

$A_{24} = 0,$

$A_{25} = \bar{\mu}_0/360\bar{\omega}_1,$

$A_{26} = (-\bar{\omega}_2\bar{\mu}_0 + \bar{\omega}_1\bar{\mu}_1)/720\bar{\omega}_1^3 .$

In equations (3.5.16) the coefficients B_{j1} are given by

$B_{13} = 0,$

$B_{14} = 1/24,$

$B_{15} = 0,$

$B_{16} = (96A_{14}\bar{\omega}_1 + \bar{\mu}_0)/2880\,\bar{\omega}_1 .$

In equation (3.5.17) the coefficients B_{j2} are given by

$$B_{23} = 0,$$

$$B_{24} = 0,$$

$$B_{25} = A_{23}/20,$$

$$B_{26} = 0$$

In equation (3.5.18) the coefficients C_{j1} are given by

$$C_{13} = 0,$$

$$C_{14} = -(-\hat{\mu}_0\bar{\omega}_1 + \bar{\omega}_1\bar{\mu}_0)/48\bar{\omega}_1^2,$$

$$C_{15} = -(-\hat{\mu}_1\bar{\omega}_1^2 + \hat{\mu}_0\bar{\omega}_1\bar{\omega}_2 + \bar{\omega}_2\bar{\omega}_1\bar{\mu}_0 - 2\bar{\omega}_1\bar{\omega}_2\bar{\mu}_0 + \bar{\omega}_1\bar{\omega}_1\bar{\mu}_1)/120\bar{\omega}_1^3,$$

$$\begin{aligned} C_{16} = -(\bar{\mu}_0 - \hat{\mu}_0\bar{\omega}_1 + \bar{\omega}_1\bar{\mu}_0)/5760\bar{\omega}_1^3 - (-2A_{14}\hat{\mu}_0\bar{\omega}_1^3 - \hat{\mu}_2\bar{\omega}_1^3 + \hat{\mu}_1\bar{\omega}_1^2\bar{\omega}_2 \\ -\hat{\mu}_0\bar{\omega}_1\bar{\omega}_2^2 + \hat{\mu}_0\bar{\omega}_1^2\bar{\omega}_3 + 2A_{14}\bar{\omega}_1\bar{\omega}_1^2\bar{\mu}_0 + \bar{\omega}_3\bar{\omega}_1^2\bar{\mu}_0 - 2\bar{\omega}_2\bar{\omega}_1\bar{\omega}_2\bar{\mu}_0 \\ + 3\bar{\omega}_1\bar{\omega}_2^2\bar{\mu}_0 - 2\omega_1\bar{\omega}_1\bar{\omega}_3\bar{\mu}_0 + \bar{\omega}_2\bar{\omega}_1^2\bar{\mu}_1 - 2\bar{\omega}_1\bar{\omega}_1\bar{\omega}_2\bar{\mu}_1 \\ + \bar{\omega}_1\bar{\omega}_1^2\bar{\mu}_2)/240\bar{\omega}_1^4 \ . \end{aligned}$$

In equation (3.5.19) the coefficients C_{j2} are given by

$$C_{23} = 0,$$

$$C_{24} = 0,$$

$$C_{25} = A_{23}(\hat{\mu}_0\bar{\omega}_1 - \bar{\omega}_1\bar{\mu}_0)/60\bar{\omega}_1^2,$$

$$C_{26} = A_{23}(\hat{\mu}_1\bar{\omega}_1^2 - \hat{\mu}_0\bar{\omega}_1\bar{\omega}_2 - \bar{\omega}_2\bar{\omega}_1\bar{\mu}_0 + 2\bar{\omega}_1\bar{\omega}_2\bar{\mu}_0 - \bar{\omega}_1\bar{\omega}_1\bar{\mu}_1)/120\bar{\omega}_1^3$$

In equation (3.5.20) the coefficients D_{j1}, D_{j10} are given by

$$D_{120} = \Omega_{-1}/2,$$

$$D_{13} = \Omega_0/6,$$

$$D_{140} = \delta_{-1}\Omega_{-1}/48,$$

$$D_{14} = \Omega_1/24 - 13\delta_{-1}\Omega_{-1}/576,$$

$$D_{150} = \delta_0\Omega_{-1}/120,$$

$$D_{15} = \Omega_2/60 - \delta_{-1}\Omega_0/360 - 47\delta_0\Omega_{-1}/7200,$$

$$D_{16} = [\delta_0 D_{13} - \delta_{-1}D_{14} + \Omega_3]/120,$$

where the constants δ_{-1}, δ_0 and δ_1 are given by

$$\delta_{-1} = \bar{\mu}_0/48\bar{\omega}_1,$$

$$\delta_0 = -\bar{\mu}_0\bar{\omega}_2/\bar{\omega}_1^2,$$

$$\delta_1 = (\bar{\mu}_0\bar{\omega}_2^2 - \bar{\mu}_0\bar{\omega}_1\bar{\omega}_3 + \bar{\mu}_2\bar{\omega}_1^2)/\bar{\omega}_1^3,$$

and Ω_{-1}, Ω_0, Ω_1, Ω_2 and Ω_3 are defined by

$$\Omega_{-1} = \delta_0/\bar{\omega}_1,$$

$$\Omega_0 = (4\gamma_0^4\bar{\omega}_1 + 6A_{14}\bar{\omega}_1\delta_{-1} - \bar{\omega}_2\delta_0 + 3\bar{\omega}_1\delta_1)/\bar{\omega}_1^2,$$

$$\Omega_1 = (-4\gamma_0^4\bar{\omega}_1\bar{\omega}_2 + 12A_{15}\bar{\omega}_1^2\delta_{-1} - 6A_{14}\bar{\omega}_1\bar{\omega}_2\delta_{-1} + 12A_{14}\bar{\omega}_1^2\delta_0 + \bar{\omega}_2^2\delta_0 - \bar{\omega}_1\bar{\omega}_3\delta_0 - 3\bar{\omega}_1\bar{\omega}_2\delta_1)/\bar{\omega}_1^3,$$

$$\Omega_2 = (16A_{14}\gamma_0^4\bar{\omega}_1^3 + 4\gamma_0^4\bar{\omega}_1\bar{\omega}_2^2 - 4\gamma_0^4\bar{\omega}_1^2\bar{\omega}_3 + 20A_{16}\bar{\omega}_1^3\delta_{-1} - 12A_{15}\bar{\omega}_1^2\bar{\omega}_2\delta_{-1} + 6A_{14}\bar{\omega}_1\bar{\omega}_2^2\delta_{-1} - 6A_{14}\bar{\omega}_1^2\bar{\omega}_3\delta_{-1} + 20A_{15}\bar{\omega}_1^3\delta_0 - 12A_{14}\bar{\omega}_1^2\bar{\omega}_2\delta_0 - \bar{\omega}_2^3\delta_0 + 2\bar{\omega}_1\bar{\omega}_2\bar{\omega}_3\delta_0 - \bar{\omega}_1^2\bar{\omega}_4\delta_0 + 20A_{14}\bar{\omega}_1^3\delta_1 + 3\bar{\omega}_1\bar{\omega}_2^2\delta_1 - 3\bar{\omega}_1^2\bar{\omega}_3\delta_1)/\bar{\omega}_1^4,$$

$$\Omega_3 = (20A_{15}\gamma_0^4\overline{\omega}_1^4 - 16A_{14}\gamma_0^4\overline{\omega}_1^3\overline{\omega}_2 - 4\gamma_0^4\overline{\omega}_1\overline{\omega}_2^3 + 8\gamma_0^4\overline{\omega}_1^2\overline{\omega}_2\overline{\omega}_3 - 4\gamma_0^4\overline{\omega}_1^3\overline{\omega}_4$$
$$- 20A_{16}\overline{\omega}_1^3\overline{\omega}_2\delta_{-1} + 12A_{15}\overline{\omega}_1^2\overline{\omega}_2^2\delta_{-1} - 6A_{14}\overline{\omega}_1\overline{\omega}_2^3\delta_{-1} - 12A_{15}\overline{\omega}_1^3\overline{\omega}_3\delta_{-1}$$
$$+ 12A_{14}\overline{\omega}_1^2\overline{\omega}_2\overline{\omega}_3\delta_{-1} - 6A_{14}\overline{\omega}_1^3\overline{\omega}_4\delta_{-1} + 30A_{16}\overline{\omega}_1^4\delta_0 - 20A_{15}\overline{\omega}_1^3\overline{\omega}_2\delta_0$$
$$+ 12A_{14}\overline{\omega}_1\overline{\omega}_2^2\delta_0 + \overline{\omega}_2^4\delta_0 - 12A_{14}\overline{\omega}_1^3\overline{\omega}_3\delta_0 - 3\overline{\omega}_1\overline{\omega}_2^2\overline{\omega}_3\delta_0 + \overline{\omega}_1^2\overline{\omega}_3^2\delta_0$$
$$+ 2\overline{\omega}_1^2\overline{\omega}_2\overline{\omega}_4\delta_0 - \overline{\omega}_1^3\overline{\omega}_5\delta_0 + 30A_{15}\overline{\omega}_1^4\delta_1 - 20A_{14}\overline{\omega}_1^3\overline{\omega}_2\delta_1 - 3\overline{\omega}_1\overline{\omega}_2^3\delta_1$$
$$+ 6\overline{\omega}_1^2\overline{\omega}_2\overline{\omega}_3\delta_1 - 3\overline{\omega}_1^3\overline{\omega}_4\delta_1)/\overline{\omega}_1^5 .$$

Similarly in equation (3.5.21) the coefficients D_{j2}, D_{j20} are given by

$$D_{22} = \Omega_{-1}/2,$$

$$D_{32} = \Omega_0/6,$$

$$D_{420} = \delta_{-1}\Omega_{-1}/48,$$

$$D_{42} = \Omega_1/24 - 13\delta_{-1}\Omega_{-1}/576,$$

$$D_{520} = \delta_0\Omega_{-1}/120,$$

$$D_{52} = \Omega_2/60 - \delta_{-1}\Omega_0/360 - 47\delta_0\Omega_{-1}/7200,$$

$$D_{62} = [\delta_0 D_{32} - \delta_{-1}D_{42} + \Omega_3]/120,$$

where Ω_{-1}, Ω_0, Ω_1, Ω_2 and Ω_3 are defined as follows:

$$\Omega_{-1} = (2A_{23}\delta_{-1})/\overline{\omega}_1 ,$$

$$\Omega_0 = (-2A_{23}\overline{\omega}_2\delta_{-1} + 6A_{23}\overline{\omega}_1\delta_0)/\overline{\omega}_1^2 ,$$

$$\Omega_1 = (12A_{23}\gamma_0^4\overline{\omega}_1^2 + 12A_{25}\overline{\omega}_1^2\delta_{-1} + 2A_{23}\overline{\omega}_2^2\delta_{-1} - 2A_{23}\overline{\omega}_1\overline{\omega}_3\delta_{-1}$$
$$- 6A_{23}\overline{\omega}_1\overline{\omega}_2\delta_0 + 12A_{23}\overline{\omega}_1^2\delta_1)/\overline{\omega}_1^3 ,$$

$$\Omega_2 = (-12A_{23}\gamma_0^4\bar{\omega}_1^2\bar{\omega}_2 + 20A_{26}\bar{\omega}_1^3\delta_{-1} - 12A_{25}\bar{\omega}_1^2\bar{\omega}_2\delta_{-1} - 2A_{23}\bar{\omega}_2^3\delta_{-1} + 4A_{23}\bar{\omega}_1\bar{\omega}_2\bar{\omega}_3\delta_{-1} - 2A_{23}\bar{\omega}_1^2\bar{\omega}_4\delta_{-1} + 20A_{25}\bar{\omega}_1^3\delta_0 + 6A_{23}\bar{\omega}_1\bar{\omega}_2^2\delta_0 - 6A_{23}\bar{\omega}_1^2\bar{\omega}_3\delta_0 - 12A_{23}\bar{\omega}_1^2\bar{\omega}_2\delta_1)/\bar{\omega}_1^4 ,$$

$$\Omega_3 = (20A_{25}\gamma_0^4\bar{\omega}_1^4 + 12A_{23}\gamma_0^4\bar{\omega}_1^2\bar{\omega}_2^2 - 12A_{23}\gamma_0^4\bar{\omega}_1^3\bar{\omega}_3 - 20A_{26}\bar{\omega}_1^3\bar{\omega}_2\delta_{-1} + 12A_{25}\bar{\omega}_1^2\bar{\omega}_2^2\delta_{-1} + 2A_{23}\bar{\omega}_2^4\delta_{-1} - 12A_{25}\bar{\omega}_1^3\bar{\omega}_3\delta_{-1} - 6A_{23}\bar{\omega}_1\bar{\omega}_2^2\bar{\omega}_3\delta_{-1} + 2A_{23}\bar{\omega}_1^2\bar{\omega}_3^2\delta_{-1} + 4A_{23}\bar{\omega}_1^2\bar{\omega}_2\bar{\omega}_4\delta_{-1} - 2A_{23}\bar{\omega}_1^3\bar{\omega}_5\delta_{-1} + 30A_{26}\bar{\omega}_1^4\delta_0 - 20A_{25}\bar{\omega}_1^3\bar{\omega}_2\delta_0 - 6A_{23}\bar{\omega}_1\bar{\omega}_2^3\delta_0 + 12A_{23}\bar{\omega}_1^2\bar{\omega}_2\bar{\omega}_3\delta_0 - 6A_{23}\bar{\omega}_1^3\bar{\omega}_4\delta_0 + 30A_{25}\bar{\omega}_1^4\delta_1 + 12A_{23}\bar{\omega}_1^2\bar{\omega}_2^2\delta_1 - 12A_{23}\bar{\omega}_1^3\bar{\omega}_3\delta_1)/\bar{\omega}_1^5 .$$

APPENDIX TWO

The functions Γ_i, Λ_i, χ_i and K_i in equation (4.4.14) are defined as follows:

$$\Gamma_i = 1 - 13s_0^2x^4/576 + s_1x^4/24 - 17s_0^3x^6/57600 - s_0s_1x^6/450 + s_2x^6/120 + (s_0x^2/2 + s_0^2x^4/48)\ln|x| + s_0^3x^6\ln|x|/5760 + s_0s_1x^6\ln|x|/240 ,$$

$$\Lambda_i = x + s_0x^3/6 + s_0^2x^5/360 + s_1x^5/60 ,$$

$$\chi_i = x^2 + s_0x^4/24 + s_0^2x^6/2880 + s_1x^6/120 ,$$

$$K_i = (i-1)(x^3/6 + s_0x^5)/360 ,$$

The functions Γ_{ij}, Λ_{ij}, χ_{ij} and K_{ij} in equations (4.3.17) are defined as follows:

$$\Gamma_{i1} = 1 - 13s_0^2x^4/576 + s_1x^4/24 + s_0x^2\ln|x|/2 + s_0^2x^4\ln|x|/48 ,$$

$$\Lambda_{i1} = x + s_0x^3/6 ,$$

$$\chi_{i1} = x^2 + s_0x^4/24 + a_is_0x^4\ln|x|/24 ,$$

$$K_{i1} = b_ix^3/6 + c_ix^4/12 - 7a_is_0x^4/288 ,$$

$$\Gamma_{i2} = (576 - 13s_0^2x^4 + 24s_1x^4 + 288s_0x^2\ln|x| + 12s_0^2x^4\ln|x|)/576$$

$$\Lambda_{i2} = x + s_0x^3/6 ,$$

$$\chi_{i2} = x^2 + s_0x^4/24 ,$$

$$K_{i2} = a_i(r_1/24 - q_1 s_0/24 - 13r_0 s_0/576 + 13q_0 s_0^2/576 - q_0 s_1)x^4/24 + (r_0/2 - q_0 s_0/2)x^2 \ln|x| + (r_0 s_0/48 - q_0 s_0^2/48)x^4 \ln|x| + b_i x^3/6 + c_{i0}(-13r_0 + 13q_0 s_0)x^4/288 + (r_0/24 - q_0 s_0/24)x^4 \ln|x| + c_i(r_0 - q_0 s_0)x^4/24 ,$$

where q_i and s_i $(i=0,1,2)$ are defined by

$$q_0 = \bar{\omega}_1/\omega_1 ,$$

$$q_1 = (\omega_1 \bar{\omega}_3 - \bar{\omega}_1 \omega_3)/\omega_1^2 ,$$

$$q_2 = (\bar{\omega}_5 \omega_1^2 - \bar{\omega}_3 \omega_3 \omega_1 + \bar{\omega}_1(\omega_3^2 - \omega_1 \omega_5))/\omega_1^3 ,$$

$$s_0 = \mu_0/\omega_1 ,$$

$$s_1 = (\mu_2 \omega_1 - \mu_0 \omega_3)/\omega_1^2 ,$$

$$s_2 = (\mu_4 \omega_1^2 - \mu_2 \omega_1 \omega_3 + \mu_0(\omega_3^2 - \omega_1 \omega_5))/\omega_1^3 .$$

$$\Gamma_{i3} = 1 + (s_0 x^2 \ln|x|)/2$$

$$\Lambda_{i3} = (x + (s_0 x^3)/6)$$

$$\chi_{i3} = x^2$$

$$K_{i3} = -a_i s_0 x/3\omega_1 + 4c_i \gamma_0^4/3\omega_1 - 16c_{i0}\gamma_0^4/9\omega_1 + e_i s_0/\omega_1 - e_{i0} s_0/\omega_1 + 11c_{i0} s_0^2/36\omega_1 - 11a_i s_0^3/108\omega_1 + c_i s_1/\omega_1 - c_{i0} s_1/\omega_1 + a_i s_0 s_1/18\omega_1 + a_i s_2/\omega_1 - c_{i0} s_0 \omega_3/6\omega_1^2 - 11a_i s_0^2 \omega_3/18\omega_1^2 + a_i s_0 \omega_3^2/3\omega_1^3 - a_i s_0 \omega_5 x^3/3\omega_1^2 + -c_{i0} s_0/\omega_1 + a_i s_0^2/3\omega_1 + 2a_i s_0 \omega_3 x \ln|x|/\omega_1^2 + 2b_i \gamma_0^4/\omega_1 + d_i s_0/\omega_1 + b_i s_1 x^2 \ln|x|/\omega_1 + 4c_{i0}\gamma_0^4/3\omega_1 + e_{i0} s_0/\omega_1 - c_{i0} s_0^2/6\omega_1 + a_i s_0^3/18\omega_1 + c_{i0} s_1/\omega_1 + a_i s_0^2 \omega_3 x^3 \ln|x|/3\omega_1^2 .$$

APPENDIX THREE

The coefficients E_{1j} in equation (5.3.21) are given by

$$E_{13} = 0,$$

$$E_{14} = 0,$$

$$E_{15} = -\bar{\omega}_1/120,$$

$$E_{16} = -A_{13}\,\bar{\omega}_1/60,$$

The coefficients E_{2j} in equation (5.3.21) are given by

$$E_{23} = 0,$$

$$E_{24} = 0,$$

$$E_{25} = 0,$$

$$E_{26} = -A_{23}\,\bar{\omega}_1/60.$$

The functions Γ_{i4}, Λ_{i4}, χ_{i4} and K_{i4} in equation (5.3.22) are given by

$$\Gamma_{i4} = 1 - 13s_0^2x^4/576 + s_1x^4/24 + \ln|x|(s_0x^2/2 + s_0^2x^4/48),$$

$$\Lambda_{i4} = (x + s_0x^3/6),$$

$$\chi_{i4} = (x^2 + s_0x^4/24),$$

$$K_{i4} = -ai\omega_1 x^3/6 \ .$$

In Chapter 6 the functions Γ_i, Λ_i, $\bar{\chi}_i$ and $\bar{K}_{i4}$ in (6.5.17) are given by

$$\begin{aligned}\Gamma_i = 1 &+ i\lambda\omega_1 x^3/6 - 13s_0^2x^4/576 + s_1x^4/24 + 7i\lambda s_0\omega_1 x^5/7200 + \\ &i\lambda\omega_3 x^5/20 - 17s_0^3x^6/57600 - s_0s_1x^6/450 + s_2x^6/120 + \\ &\lambda^2\omega_1^2x^6/360 + (s_0x^2/2 + s_0^2x^4/48 + -i\lambda s_0\omega_1 x^5/120 + \\ &s_0^3x^6/5760 + s_0s_1x^6/240)\ln|x| \ ,\end{aligned}$$

$$\begin{aligned}\Lambda_i = x &+ s_0x^3/6 + s_0^2x^5/360 + s_1x^5/60 \ - i\lambda s_0\omega_1 x^6/360 + \\ &i\lambda\omega_3 x^6/60 \ ,\end{aligned}$$

$$\bar{\chi}_i = x^2 + s_0x^4/24 \ - i\lambda\omega_1 x^5/60 + s_0^2x^6/2880 \ + s_1x^6/120 \ ,$$

$$\bar{K}_{i4} = x^3/6 + s_0x^5/360 \ - i\lambda\omega_1 x^6/360 \ .$$

REFERENCES

ABRAMOWITZ, M. & STEGUN, I.A. (1970).
Handbook of mathematical functions.
(New York: Dover Publication, INC.,)

BATCHELOR, G.K. (1954)
Heat transfer by free convection across a closed cavity between vertical boundaries at different temperatures.
Q. Appl. Maths. **12**, 209.

BERGHOLZ, R.F. (1978)
Instability of steady natural convection in a vertical fluid layer.
J. Fluid Mech. **84**, 743.

BIRIKH, R.V., GERSHUNI, G.Z.,ZHUKHOVITSKII, E.M. & RUDAKOV, R.N. (1969)
Stability of the steady convective motion of a fluid with a longitudinal temperature gradient.
Prikl.Mat.Mekh. **33**, 958.

BLYTHE, P.A., DANIELS, P.G. & SIMPKINS, P.G. (1983)
Thermal convection in a cavity: the core structure near the horizontal boundaries
Proc. R. Soc. Lond. A **387**, 367.

DANIELS, P.G. (1985)
Stationary instability of the buoyancy-layer flow between heated vertical planes.
Proc. R. Soc. Lond. A **401**, 145.

DANIELS, P.G. (1987)
Convection in a vertical slot.
J. Fluid Mech. **176**, 419.

DANIELS, P.G. (1989)
Stationary instability of the convective flow between differentially heated vertical planes.
J. Fluid Mech. **203**, 525.

DANIELS, P.G. & WEINSTEIN (1992)
A note on the solution of a third-order eigenvalue problem arising in convective instability.
J. Franklin Institute. **329** , 77.

DE VAHL DAVIS, G. & MALLINSON, G.D. (1975)
A note on natural convection in a vertical slot.
J. Fluid Mech. **72**, 87.

ECKERT, E.R.G & CARLSON, W.O. (1961)
Natural convection in an air layer enclosed between two vertical plates with different temperature.
Intl. J. Heat Mass Transfer. **2**, 106.

ELDER, J.W. (1965)
Laminar free convection in a vertical slot.
J. Fluid Mech. **23**, 77.

ELDER, J.W. (1966)
Numerical experiments with free convection in a vertical slot.
J. Fluid Mech. **24**, 823.

GILL, A.E. (1966)
The boundary layer regime for convection in a rectangular cavity.
J. Fluid Mech. **26**, 515.

GILL, A.E. & DAVEY, A. (1969)
Instabilities of a buoyancy-driven system.
J. Fluid Mech. **35**, 775.

GILL, A.E. & KIRKHAM, C.C. (1970)
A note on the stability of convection in a vertical slot.
J. Fluid Mech. **42**, 125.

HART, J.E. (1971)
Stability of the flow in a differentially heated inclined box.
J. Fluid Mech. **47**, 547.

KORPELA, S.A., GÖZÜM, D. & BAXI, C.B. (1973)
On the stability of the conduction regime of natural convection in a vertical slot.
Intl. J. Heat Mass Transfer. **16**, 1683.

LEE, Y. & KORPELA, S.A. (1983)
Multicellular natural convection in a vertical slot.
J. Fluid Mech. **126**, 91.

MIZUSHIMA, J. & GOTOH, K. (1976)
The stability of natural convection in a vertical fluid layer.
J. Fluid Mech. **73**, 65.

MORDCHELLES-REGNIER, G. & KAPLAN, C. (1963)
Visualization of natural convection on a plane wall and in a vertical gap by differential interferometry. Transitional and turbulent regimes.
Heat Transfer Fluid Mech. Inst., p. 94.

NUSSELT, W. (1909)
V.D.I. Forsch. Arb. Nor. **63**, 78.

SEKI, N., FUKUSAKO, S. & INABA, H.J. (1978)
Visual observation of natural convective flow in a narrow vertical cavity.
J. Fluid Mech. **84**, 695.

SIMPKINS, P.G. & DUDDERAR, T.D. (1981)
Convection in rectangular cavities with differentially heated end walls.
J. Fluid Mech. **110**, 433.

VEST, C.M. & ARPACI, V. S. (1969)
Stability of natural convection in a vertical slot.
J. Fluid Mech. **36**, 1.